Carbon Capture Efficiency in Natural Gas Combined Cycle Power Plants: Analyzing the Effects of Variable Load Operations

by

Caleb M. Knight

B.S. Petroleum Engineering, West Virginia University, 2014

Submitted to the System Design and Management Program
in partial fulfillment of the requirements for the degree of

MASTER OF SCIENCE IN ENGINEERING AND MANAGEMENT

at the

MASSACHUSETTS INSTITUTE OF TECHNOLOGY

September 2024

Authored by:	Caleb M. Knight System Design and Management Program August 16, 2024
Certified by:	Dr. Donna H. Rhodes Principal Research Scientist, Sociotechnical Systems Research Center Thesis Supervisor
Certified by:	Dr. Ruaridh MacDonald Research Scientist, MIT Energy Initiative Thesis Supervisor
Accepted by:	Joan S. Rubin Executive Director, System Design and Management Program

Carbon Capture Efficiency in Natural Gas Combined Cycle Power Plants: Analyzing the Effects of Variable Load Operations

by

Caleb M. Knight

Submitted to the System Design and Management Program
on August 16, 2024 in partial fulfillment of the requirements for the degree of

MASTER OF SCIENCE IN ENGINEERING AND MANAGEMENT

ABSTRACT

Natural gas power generation retrofitted with carbon capture technology is poised to play a crucial role in ensuring energy reliability amidst the transition to variable renewable energy resources. While natural gas generation is used primarily for baseload power, it is expected to transition towards an intermittent power generator, serving as a load-following resource during periods of low renewable energy availability. It will be critical to understand how start-up, shutdown, and load-following behavior may impact system performance and influence future grid design.

This thesis performs a comprehensive literature review to establish context on various techniques of carbon capture technology. Post-combustion carbon capture, specifically absorption-based technology, remains the preferred candidate for retrofitting natural gas plants due to its technical maturity, scalability, relatively high capture efficiencies, and ease of retrofitting. The literature highlights that absorption-based carbon capture units exhibit degraded performance during non-steady-state operating conditions. Specifically, cold start-ups result in lower capture efficiencies and higher heat rates, although hot start-ups incur significantly less performance reduction.

The literature review findings are integrated into GenX, a grid optimization tool, to evaluate natural gas combined cycle power plants equipped with carbon capture technology. The modified optimization models are run using the ISO New England grid system, and results suggest that incorporating advanced start-up penalties for natural gas plants reduces operational flexibility in an emissions-constrained environment. As capture efficiencies decrease and heat rates increase during start-ups, utilizing natural gas plants becomes more expensive due to the additional emissions and reduced thermal efficiency. Comparing models with different levels of performance degradation during start-up suggests that installing less gas capacity could be optimal, with those units operating at higher capacity factors to mitigate start-up penalties. Under modest emissions constraints, natural gas units may be operated continuously even during periods of renewable energy surplus. Harsher start-up penalties applied to natural gas plants likely increase the incremental value of alternative energy technologies, although natural gas retains a critical role in the energy mix.

Thesis supervisor: Dr. Donna H. Rhodes
Title: Principal Research Scientist, Sociotechnical Systems Research Center

Thesis supervisor: Dr. Ruaridh MacDonald
Title: Research Scientist, MIT Energy Initiative

Acknowledgments

This past year has been one of the most enriching, challenging, and rewarding years of my life. I want to express my deepest gratitude to everyone who has supported and guided me throughout the course of my studies at MIT. The journey has been transformative, and I am profoundly grateful for the experiences and knowledge gained.

First and foremost, I would like to thank my advisor, Dr. Donna Rhodes, for her continued support, insightful guidance, and encouragement. Thank you for your flexibility and willingness to advise a student on a topic that falls beyond the scope of your primary research areas. I would also like to extend my sincere gratitude to Dr. Ruaridh MacDonald, without whom this thesis would not be possible. His mentorship and insights were invaluable in shaping and enriching my work.

I am also grateful to the MIT Energy Initiative for providing a platform that fosters interdisciplinary collaboration and innovation in energy research. My experience at MIT has been dramatically enhanced by the support and intellectual engagement of my fellow students and professors, whose discussions and shared knowledge have been instrumental in my academic journey. The vibrant academic community at MIT is unlike any other, and I am blessed to be considered a part of it.

I would also like to acknowledge my family's immense support and encouragement, particularly my father, Terry, and my mother, Patricia. Their belief in my potential has been a source of strength and motivation throughout my studies. Their unwavering support has been the foundation upon which I have built my academic and personal successes, and for that, I am eternally grateful.

Finally, I would like to express my sincere gratitude to Chevron, whose sponsorship has made this experience possible. Their commitment to empowering individuals to grow their capabilities and fostering research and development in energy technology is greatly appreciated. Chevron's support has allowed me to focus on my studies and pursue my research with the resources necessary to make meaningful contributions to the field.

Thank you all for your invaluable contributions to this work.

Contents

Acknowledgments **3**

List of Figures 6

List of Tables 8

List of Acronyms **9**

1 Introduction **11**
1.1 Motivation . . . 11
1.2 Background . . . 12
1.2.1 Gas Turbines for Power Generation . . . 14
1.2.2 The Role of Natural Gas Power Plants . . . 15
1.3 Research Objective . . . 17
1.4 Research Approach . . . 17
1.5 Outline . . . 18

2 Literature Review **19**
2.1 Literature Search Process . . . 19
2.2 Carbon Capture Technologies . . . 24
2.2.1 Post-Combustion Carbon Capture . . . 26
2.2.2 Pre-Combustion Carbon Capture . . . 27
2.2.3 Oxyfuel Combustion Capture . . . 29
2.3 Post-Combustion Carbon Capture Separation Methods . . . 31
2.3.1 Absorption . . . 31
2.3.2 Adsorption . . . 33
2.3.3 Membranes . . . 35
2.3.4 Cryogenic Separation . . . 37
2.3.5 Calcium Looping . . . 38
2.3.6 Summary Comparison . . . 40
2.3.7 Non-Steady State Carbon Capture . . . 40

3 GenX Model Overview and Validation **45**
3.1 GenX Overview . . . 45
3.2 Default GenX Start-up Calculations . . . 48
3.3 Advanced Start-up Capture & Heat Rate Penalties . . . 50
3.4 Carbon Capture Penalty Simplified Case . . . 54

3.4.1 Simple Solar and Natural Gas Model 54
3.4.2 Simple Onshore Wind and Natural Gas Model 58
3.4.3 Modified One-Hour Penalty 61

4 GenX Optimization Modeling on the ISO New England Grid System 66
4.1 ISO New England Model Overview 66
4.2 ISO New England Model Results 72
4.2.1 Impact of Start-Up Penalties on System Operational and Behavioral Decisions 72
4.2.2 Impact of Start-Up Penalties on Resource Capacity 74
4.2.3 Impact of Start-Up Penalties on Value of Alternative Energy Generation 79

5 Conclusion and Future Studies 84

References 86

A Model Repository 100

List of Figures

1.1 U.S. Greenhouse Gas Emissions by Sector [4] . . . 12
1.2 U.S. Electricity Generation by Source. Source: U.S. Energy Information Administration . . . 13
1.3 World Electricity Demand Forecast. Source: U.S. Energy Information Administration (2023) . . . 14
1.4 Combined Cycle Gas Turbine Process Flow [13] . . . 16

2.1 NGCC Power System Representation with System Boundary . . . 21
2.2 Network of Literature Papers. Circles sized by number of connections . . . 23
2.3 Decomposition of Common Carbon Capture Technologies. Note ionic liquids can absorb CO_2 by both physical and chemical processes . . . 25
2.4 Map of Current Post-Combustion Carbon Capture Projects . . . 27
2.5 Pre-Combustion Carbon Capture Process flow [46] . . . 28
2.6 Oxyfuel Block Diagram Process Flow [55] . . . 30
2.7 Flow Diagram of Absorption-Desorption CO_2 Capture Process [61] . . . 32
2.8 Membrane Separation Process [89] . . . 36
2.9 Calcium Looping Process Diagram [110] . . . 39
2.10 Pilot Plant Data for Cold Start-up Operations [72] . . . 42
2.11 Comparison of Observed Data with Linear Approximation Used in Model - Instantaneous Capture Rate . . . 43
2.12 Comparison of Observed Data with Linear Approximation Used in Model - Cumulative Capture Rate . . . 44

3.1 Potential GenX Configuration Options [20] . . . 46
3.2 Graphical View of GenX Inputs, Constraints, and Outputs. Inputs used in this analysis are highlighted in green. . . . 47
3.3 Installed Solar Capacity per Emissions Limit Constraint . . . 55
3.4 Hot Start-Ups vs Cold Start-Up Capture Rate Drop (25, 30 g/kWh emissions limit) . . . 56
3.5 Heat Map of Heat Rate Penalty, Capture Rate Penalty, and Mean Total System Cost Under Each Emissions Intensity Limit. . . . 57
3.6 Comparison of Advanced Penalties, No Penalties, and One-Hour Penalties - Solar . . . 57
3.7 Percent Difference in Total Cost for Integer vs Linearized Clustering . . . 58
3.8 Onshore Wind and Natural Gas Capacity Under Each Emissions Intensity Limit 59

3.9 Tornado Plot for Simple Wind Model 60
3.10 Heat Map of Heat Rate Penalty, Capture Rate Penalty, and Mean Total System Cost Under Each Emissions Intensity Limit - Wind 60
3.11 Heat Map of Heat Rate Penalty, Cooldown Period, and Mean Total System Cost Under Each Emissions Intensity Limit - Wind 61
3.12 Comparison of Hot Start Percentage Under Varying Parameters 62
3.13 Comparison of Advanced Penalties, No Penalties, and One-Hour Penalties - Wind 62
3.14 Advanced Penalties (All Starts) vs Modified One-Hour Penalties - Total Cost 65
3.15 Advanced Penalties (Cold Starts Only) vs Modified One-Hour Penalties - Total Cost 65

4.1 Two Week View of VRE Availability, Summer 67
4.2 Two Week View of VRE Availability, Winter 67
4.3 Demand Data 68
4.4 Power Output by Resource - High Solar Availability (12g/kWh emissions limit) 75
4.5 Power Output by Resource - Low Solar Availability (12g/kWh emissions limit) 76
4.6 Total System Cost for Optimized Solution 77
4.7 Capacity Factors for NGCC and NGCC with CCS 77
4.8 12-Hour Capacity Factor Distributions for NGCC with CCS, Excluding Periods of Gas Utilization $< 1.0\%$. Bins and CDF truncated at 1.0% 78
4.9 Maximum Capex per kW vs Maximum Installed Fission Capacity 79
4.10 Maximum Capex per kW vs Maximum Installed NGCC Plant Capacity . . . 80
4.11 Maximum Capex per kW vs Maximum Installed Solar Capacity 80
4.12 Maximum Capex per kW vs Maximum Installed Battery Capacity 81

List of Tables

1.1 2023 U.S. Share of Electricity Generation by Resource Type [7] 13

2.1 Initial Research Papers for Network Creation 22
2.2 Summary of Pre-Combustion Carbon Capture Related Projects [43] 29
2.3 Comparison of Carbon Capture Technologies for NGCC Power Plants 40
2.4 Impact of Operating Modes on Capture Rate and Heat Rate 42

3.1 Operational Parameters and Changes 54

4.1 Resource Allocation for ISO-NE and Quebec with Expansion Capacities . . . 69
4.2 VRE Annual Availability 70
4.3 Generator Data for Baseline Model 71
4.4 Initial GenX Settings 72
4.5 Advanced Start-Up Penalties Parameters 73

List of Acronyms

CCS carbon capture and storage

NGCC natural gas combined cycle

MEA monoethanolamine

DEA diethanolamine

MDEA methyl diethanolamine

CCE carbon capture efficiency

EIA Energy Information Administration

IEA International Energy Agency

IRA Inflation Reduction Act

solar PV solar photovoltaic

SCGT simple-cycle gas turbine

CCGT combined-cycle gas turbine

EPA Environmental Protection Agency

HRSG heat recovery steam generator

IGCC integrated gasification combined cycle

DGA diglycolamine

DIPA di-isopropanolamine

AMP 2-amino-2-methyl-l-propanol

PZ Piperazine

PSA pressure swing adsorption

TSA temperature swing adsorption

VSA vacuum swing adsorption

CCC Cryogenic-based carbon capture

CaL Calcium looping

TRL technology readiness level

NETL National Energy Technology Laboratory

IEAGHG International Energy Agency Greenhouse Gas

VRE variable renewable energy

PHS pumped hydro storage

ROR run-of-the-river

ISO-NE ISO New England

NREL National Energy Research Laboratory

Chapter 1

Introduction

1.1 Motivation

Despite the extensive research applied to climate science, the planet continues to warm. According to the 2023 Intergovernmental Panel on Climate Change report, global warming will likely exceed the 1.5 °C target outlined in the Paris Agreement [1]. As a response, more countries are pledging net-zero emissions by various years, with many targeting 2050. Multiple scenarios have been created, leveraging integrated assessment models, to develop potential pathways to achieve those climate goals. In virtually every model, coal is rapidly phased out and replaced by renewable energy sources, and natural gas use for power plants peaks by 2030 [2]. However, in many of these scenarios, natural gas-fired power generation equipped with carbon capture still significantly contributes to the energy supply [3]. Despite rapid expansion, renewable energy sources are subject to inherent variability associated with resource availability. Flexible, low-emissions power generation offers a cost-effective solution to ensure seasonal and hourly electricity demand can be adequately met. Fossil-fuel-generated electricity equipped with carbon capture and storage (CCS) technology will be a key enabler towards smoothing the energy transition as it can be quickly dispatched to meet demand during periods of insufficient renewable energy supply.

While many publications incorporate elements of CCS into analyzing pathways to reduced emissions, much of the work includes broad assumptions surrounding the CCS technology itself. It is widely recognized that natural gas-fired power plants with CCS equipment may likely be operated under load-following conditions, increasing or decreasing output depending on demand and available supply from renewable energy sources and energy storage systems. Limited studies have been conducted, however, on the carbon capture efficiency (CCE) of this technology under variable operating conditions. Much of the existing work focuses exclusively on chemical absorption gas separation via amine scrubbing. This thesis seeks to contribute to the under-explored area of the impact of variable operating conditions on CCE and thermal efficiency across multiple carbon capture methods.

1.2 Background

The United States has been experiencing a declining trend in CO_2 emissions since 2007, as seen in Figure 1.1. The electric power industry is the largest source of emissions reductions among all sectors, demonstrating a 36% reduction over that time period. [4]. Multiple factors

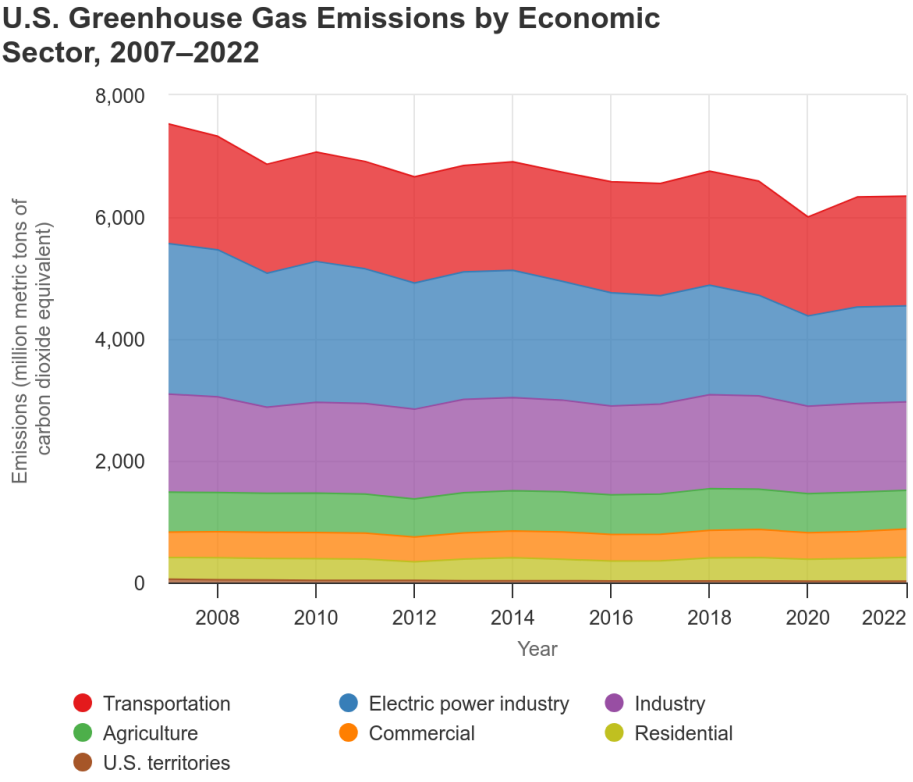

Figure 1.1: U.S. Greenhouse Gas Emissions by Sector [4]

have contributed to this decreasing emissions trend. First, natural gas has largely displaced coal as the primary fuel for electricity generation. Coal has been the dominant energy source for most of the last century, yet its electricity market share has decreased since 2007. This corresponds with the associated emissions drop since 2007, mainly due to the expansion of natural gas due to the shale boom. In 2016, natural gas displaced coal as the dominant fuel for electricity generation in the United States. Electricity generation by source is illustrated in Figure 1.2.

Natural gas has a lower carbon intensity than coal, generating 0.97 pounds of CO_2 per kilowatt-hour compared to 2.30 pounds of CO_2 per kilowatt-hour for coal. Natural gas plants also generate fewer pollutants, such as sulfur dioxide and particulate matter, than coal [5]. Finally, natural gas-fired power plants are cheaper to build and operate than coal-fired plants and generally operate with a higher thermal efficiency [6]. These factors contributed to the rapid expansion of gas-fired electricity generation and the subsequent decrease in coal-fired electricity and overall emissions. The breakdown of electricity generation by resource type

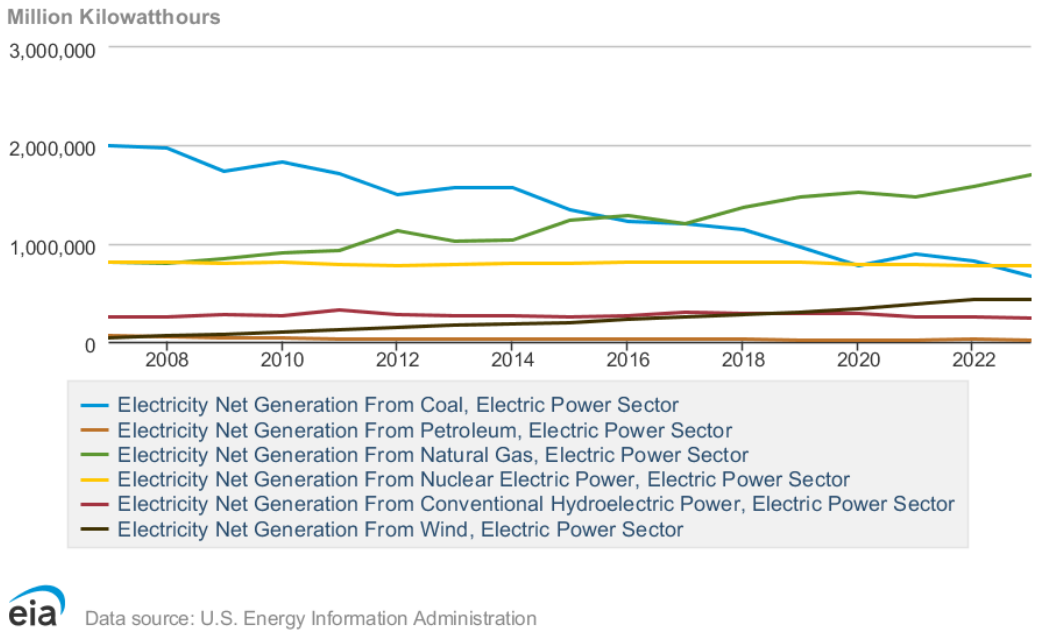

Figure 1.2: U.S. Electricity Generation by Source. Source: U.S. Energy Information Administration

for 2023 is shown in Table 1.1

The energy landscape is shifting once more, however, as renewable energy sources are positioning to replace natural gas as the primary source for generating electricity. Advances in technology are likely to play a pivotal role in combating climate change, and significant progress has been made in renewable energy. The Energy Information Administration (EIA)'s 2023 Annual Energy Outlook indicates significant expansion in renewable electricity generation, rapidly surpassing natural gas [6]. The expansion of renewable energy is largely driven by technological advances in conversion efficiency and cost reductions made in solar photovoltaic (solar PV) and wind energy [8],[9]. Solar PV is projected to become the primary energy source for electricity generation across the U.S., supported by wind energy and natural gas. Energy storage technologies, such as pumped storage hydroelectric or batteries, are essential components in facilitating the energy transition to renewable energy sources. These technologies will enable the integration of intermittent energy sources such

Table 1.1: 2023 U.S. Share of Electricity Generation by Resource Type [7]

Resource Type	**Percent of Total Electricity Generated**
Natural Gas	43%
Nuclear	18%
Coal	16%
Wind	10%
All Other	8%
Solar	4%

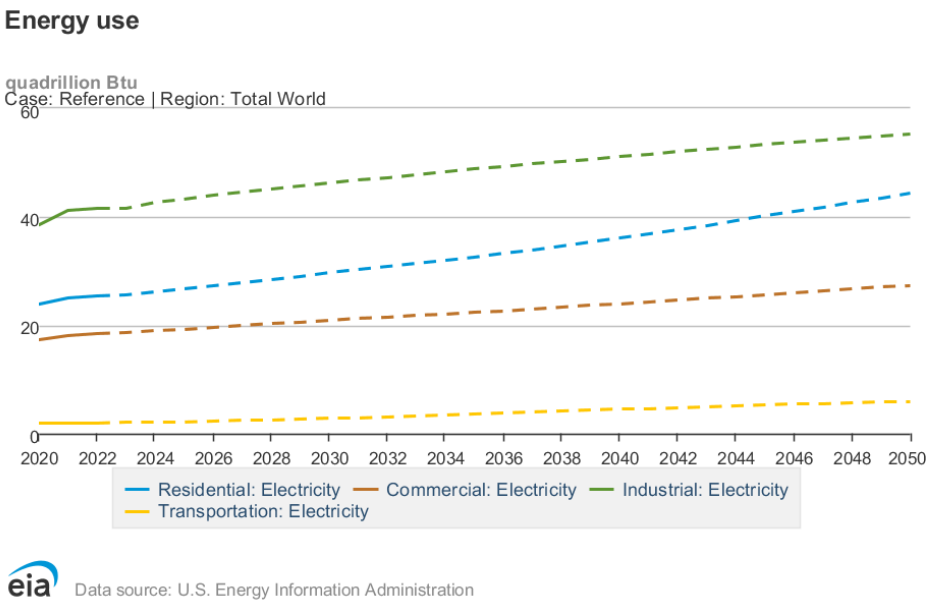

Figure 1.3: World Electricity Demand Forecast. Source: U.S. Energy Information Administration (2023)

as wind and solar PV. Rapid progress is being made in developing and expanding energy storage, but storage capacity still needs significant expansion to be able to adequately meet demand. The EIA projects a steady increase in energy demand in all sectors, as seen in Figure 1.3, necessitating a joint approach to providing a low-emissions energy solution. One approach is to leverage existing power generation, equipped with CCS technology, combined with renewable energy growth and grid enhancements. Gas-fired power plants are especially viable in meeting energy demand due to their ability to be rapidly dispatched, and they are able to bridge the gap during periods of intermittent renewable energy supply and fluctuating energy demand.

1.2.1 Gas Turbines for Power Generation

There are two main categories of technology that are used in natural gas-fired power plants: simple-cycle gas turbine (SCGT) and combined-cycle gas turbine (CCGT). Both systems generate electricity by burning natural gas, but they vary in their operation, cost, and efficiency. SCGT power plants utilize the Brayton Cycle to generate electricity by first injecting natural gas into a combustion chamber. Air is then drawn through a compressor and mixed with the natural gas. The air and natural gas mixture is then ignited, generating a high-temperature, high-pressure gas. The gas undergoes rapid expansion as it passes through the turbine, spinning the turbine blades. The rotating turbine blades provide energy to the compressor and propel a generator that converts mechanical energy into electrical energy. A key advantage of SCGT power plants is that they are able to be quickly ramped up and down in response to electricity demand due to their simple single cycle operation. They are often used as peaker plants today, with the annual average capacity factor median value

being less than 10% [10]. However, the low capacity factors and the lost energy from waste heat result in SCGT power plants having a relatively poor thermal efficiency, ranging from 33%-43% under full load but dropping significantly operating under partial loads [11].

CCGT power plants initially generate electricity in the same manner as SCGT power plants. They burn a natural gas and compressed air mixture to produce gas that spins a turbine, powering a generator to create electricity. The key difference in CCGT operation is in the utilization of the waste heat produced. CCGT power plants combine the Brayton Cycle with the Rankine Cycle, capturing the hot exhaust gases from the turbine that would otherwise be lost and routing them through a heat recovery steam generator (HRSG). The HRSG is essentially a heat exchanger that uses the hot exhaust gas to convert water into steam, which is then used to rotate a steam turbine and generate additional electricity. The steam is then condensed back into liquid water and recycled for reuse. This results in CCGT power plants being able to produce nearly 50% more electricity than SCGT plants, measured in kilowatt-hours of electricity converted per btu of natural gas [12]. This is often referred to as heat rate, which is defined as the quantity of fuel (Btu or MMBtu) required to generate a single unit of electricity (kWh). These CCGT plants have a thermal efficiency ranging from 50%-60% [13]. The superior thermal efficiency and fuel usage makes CCGT power plants the dominant type of natural gas power plan in the U.S., accounting for 58% of all gas-fired generating capacity [7]. The process flow for a CCGT power plant is shown in Figure 1.4. Due to their higher thermal efficiency, CCGT power plants generate less CO_2 emissions than SCGT power plants [14]. In a carbon-constrained environment, this makes them the preferred candidates for future retrofitting with CCS technology.

Significant progress has been made in developing CCGT power plants that can quickly ramp up production under both hot start and cold start conditions. Hot start refers to restarting the plant after a relatively brief shutdown period, typically less than eight hours. A cold start refers to restarting the plant after a longer shutdown period greater than 48 hours. Warm starts are generally any start-up that falls between the hot and cold thresholds. Older CCGT power plants can take approximately one hour to reach full plant load under hot start conditions and up to four hours for cold start conditions [15]. The National Energy Technology Laboratory published cold, warm, and hot start-up times for a variety of different class turbines. Their findings show that the cold start to full load duration is around two hours for most turbine systems. This decreases to approximately one hour for a warm start and 30 minutes for a hot start[16]. New research on flexible combined cycle plants suggests that they can start up even faster, within 15 minutes for gas turbine full load and 30 minutes for combined cycle full load [17]. This indicates that CCGT power plants can also be operated as load-following electricity generation sources, responding extremely quickly to changing demand from steady-state operating conditions without completely shutting down. As improvements continue to reduce start-up and dispatch response time, CCGT power plants are likely to replace SSGT power plants for delivering intermediate and peaking load generation.

1.2.2 The Role of Natural Gas Power Plants

As highlighted earlier, natural gas-fired power plants are expected to provide energy security and stability during the transition to renewable energy sources. As solar PV and wind

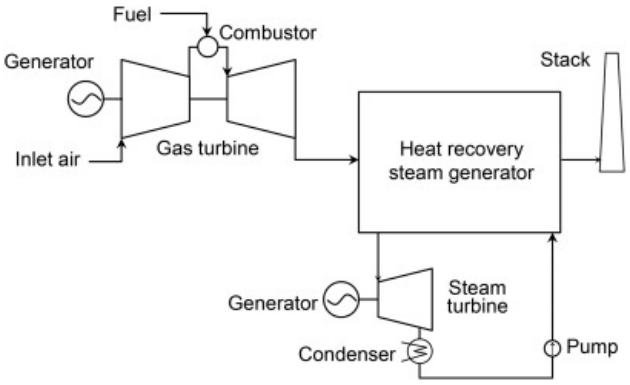

Figure 1.4: Combined Cycle Gas Turbine Process Flow [13]

energy are not dispatchable energy sources, one approach to mitigating the intermittency of the renewable energy supply is to utilize natural gas-fired power plants to generate electricity when energy demand exceeds available supply from renewable sources and shutting down when there is a surplus of renewable energy available. In the NetZero America study, researchers at Princeton University define five pathways to net zero emissions by 2050, each making different assumptions around energy demand and energy supply technology options. In all five pathways, natural gas-fired power generation plays a significant role, maintaining 500-1,000 GW of generating capacity to ensure firm reliability. Carbon capture and storage is also required in all five pathways modeled, requiring at least 0.7 Gt/y of CO_2 stored in the most optimistic scenario and over 1.0 Gt/y of CO_2 stored in all other pathways [3]. To meet climate goals, these gas-fired power plants would be required to be retrofitted with CCS equipment. The Department of Energy requirements for CCS are to capture at least 90% of the CO_2 emissions with at least a 95% CO_2 purity [18].

The primary barrier to implementing CCS in the electricity sector is the prohibitive cost of the gas separation equipment and process. Recently, CCS has gained greater prominence in the energy field with the passing of the Inflation Reduction Act (IRA) in 2022. The IRA is a comprehensive bill that updated the Internal Revenue Service Section 45Q incentives for carbon oxide sequestration. It increased the tax credit incentives from \$35/mt to \$60/mt for CO_2 captured and used in enhanced oil recovery and other industrial operations and from \$50/mt to \$85/mt for permanent sequestration of CO_2 [19]. In order to be eligible to claim the Section 45Q tax credit for carbon sequestration, power plants must capture at least 75% of the baseline CO_2 emissions of the unit. This bill has ignited renewed interest in pursuing the idea of retrofitting natural gas combined cycle (NGCC) power plants with carbon capture equipment, and it appears policy is positioned to continue supporting carbon credits and offsets. It will be vital to understand the relationship between carbon capture efficiency, the specific carbon capture methods used, and the power plant operating conditions as the industry moves forward under these new guidelines.

1.3 Research Objective

Multiple studies suggest that natural gas-fired power plants will retain a role in ensuring energy reliability even amidst the transition towards more renewable energy sources. It is also understood that carbon capture and storage technology is essential in keeping the average increase in global temperature below 2 °C relative to the pre-industrial levels, and ideally below 1.5 °C. This thesis endeavors to answer the following questions:

- Multiple methods of carbon capture currently exist. How do they compare on cost, carbon capture efficiency, and impact on plant heat rate? Which carbon capture technique appears to be most applicable for retrofitting NGCC power plants?
- NGCC power plants are expected to be retrofitted with CCS technology and serve to operate as load-following or intermediate sources of electricity generation when renewable energy supply is limited.
  - How does NGCC carbon capture efficiency vary under steady-state operating conditions compared to load-following, start-up, and shutdown conditions?
  - How does carbon capture impact heat rate / thermal efficiency during these variable operating conditions?
- How does the performance of non-steady-state carbon capture influence NGCC plant operational strategy?
- How does the performance of non-steady-state carbon capture influence the optimal future grid design?

1.4 Research Approach

The research approach for this thesis begins by conducting a thorough literature review examining the current methods of carbon capture. The review initially outlines the three main categories of separating carbon dioxide from other gases as applied to the power sector. Post-combustion capture, pre-combustion capture, and oxyfuel combustion capture are reviewed at a high level. The literature review then zooms into a more detailed analysis of post-combustion capture, evaluating the different post-combustion carbon capture technologies currently available. Increased focus is given to each technology's applicability for CCS on NGCC power plants, focusing on their capture efficiency, energy penalty, and retrofit applicability. Next, the results of the literature review are synthesized, and an optimization model is constructed. The model incorporates findings from the literature review relating to capture efficiency and energy penalty to evaluate different energy supply and demand scenarios using the ISO New England grid network. The optimization model seeks to understand how flexible carbon capture power generation impacts the optimum grid design and behavior under different constraints and scenarios.

1.5 Outline

The following thesis structure is utilized to address the research questions in Section 1.3

- **Chapter 1 - Introduction:** This chapter introduces the topic and briefly reviews the current status of climate change. It describes the motivation for this thesis and provides background information on electricity supply and demand. Emphasis is placed on gas-fired power plants, including its emissions and its role in the changing energy landscape.

- **Chapter 2 - Literature Review**: The literature review provided in Chapter 2 examines the current methods of carbon capture. Topics covered include post-combustion capture, pre-combustion capture, and oxyfuel combustion capture. Specific post-combustion capture techniques, such as absorption, adsorption, membranes, cryogenic, and calcium looping are reviewed in further detail. Finally, a comparative summary of all technologies is provided.

- **Chapter 3 - GenX Model Overview and Validation**: This chapter provides a comprehensive overview of the GenX electricity capacity expansion model. Modifications made to the default GenX configuration are explained, incorporating the findings from the literature review. The modified model is validated using simple models while varying key input parameters. A modified model is created using fuel consumption as a proxy for advanced penalties, and the performance of all models is compared.

- **Chapter 4 - GenX Optimization Modeling on the ISO New England Grid System**: This chapter describes The ISO-NE model, explaining the overall system and any important resource values, constraints, and assumptions. Multiple modeling runs are executed using the ISO-NE grid as a baseline. All model results are compared across a variety of metrics to understand the behavioral and operational changes observed. The chapter concludes by discussing the broader impacts of flexible natural gas on the overall grid design and valuation of alternate energy generation.

- **Chapter 5 - Conclusion and Future Studies**: The conclusion summarizes the overall findings explored in this thesis. It highlights the limitations of the current research and provides recommendations for future work.

Chapter 2

Literature Review

A preliminary literature review was conducted to understand the current carbon capture technologies applicable to the electricity sector. This focuses on the CO_2 separation and capture processes, and the transportation, utilization, and storage of CO_2 will not be addressed in detail. The literature review focuses on three primary categories. First, the various types of carbon capture are reviewed, including post-combustion carbon capture, pre-combustion carbon capture, and oxyfuel combustion capture. Next, the detailed capture processes and methods of post-combustion capture, such as absorption, adsorption, and membranes, are analyzed. Finally, the performance of these post-combustion technologies is evaluated under various operating conditions.

2.1 Literature Search Process

This thesis employs a two-phase approach to address the research questions outlined in Section 1.3. The first phase includes a comprehensive literature review that evaluates the current status of various carbon capture technologies, including absorption-based capture, adsorption-based, membrane capture, cryogenic capture, and calcium looping capture. To better set the scope of the thesis, a system problem statement and associated system boundary must be defined. The objective of this work is to determine the impact of carbon capture penalties on the optimal electricity generation portfolio by modeling start-up operations under varying assumptions using the GenX constrained mixed integer and linear optimization model. Accordingly, a system representation of the NGCC power plant to be analyzed and the system boundary is displayed in Figure 2.1. This thesis focuses on the electricity generation and carbon capture efficiency penalty within the NGCC plant. Thus, energy and financial requirements for compressing, transporting, and storing the captured CO_2 are not considered. Second, an electricity resource capacity expansion model, GenX [20], incorporates findings from the literature review and evaluates multiple electricity generation portfolios under various assumptions. This is presented in detail in Chapter 3. The literature review process seeks to address the first research question by performing a comparative analysis of existing carbon capture technologies across an array of key metrics, shown below.

- Carbon capture efficiency

- Energy penalty/plant heat rate reduction
- Retrofitting complexity
- Cost ($/ton CO_2)
- Technical maturity level
- Operational challenges

To obtain information to address the above metrics, the literature search utilized the following academic and industry databases:

- Google Scholar
- Sciencedirect
- Web of Science
- CORE
- Springer Link
- IEEE Xplore
- MIT Libraries

Beyond academic databases, this review also included government-sponsored literature provided by the EIA, International Energy Agency (IEA), Environmental Protection Agency (EPA), and National Energy Technology Laboratory (NETL). To more fully explore the research space, an artificial intelligence tool, researchrabbit.ai, was used in conjunction with traditional databases[21]. It uses machine learning algorithms to suggest related research papers based on input papers provided by the user. Ten papers found through academic databases were selected as the starting point for generating the initial network. These papers were selected as they each address a key metric as outlined above or provide a comprehensive overview of a specific technology. In an attempt to establish unique search results that cover a broad range of possible papers, a single author or publication was only permitted to be included twice in the original set of ten papers. Adding additional papers to the search criteria resulted in an overwhelming number of related papers and reduced the overall quality of the matches, returning fringe papers that were not entirely relevant. Narrowing the selection down to only a few papers yielded focused results but did not adequately address all of the target metrics or technologies. No date filters were explicitly set within the tool, but the search did begin exploring by exclusively showing papers published after the source material to obtain the most recent publications possible. Older publications were included in instances where they remained relevant. Leveraging artificial intelligence tools to assist in gathering focused literature is a relatively novel technique. Yet, it is a rapidly expanding and useful method for compiling research [22], [23], [24]. Other generative artificial intelligence technologies, including OpenAI's ChatGPT, were utilized for code debugging and troubleshooting in Chapter 3 and Chapter 4. The initial selection of papers to build the network is shown in Table 2.1.

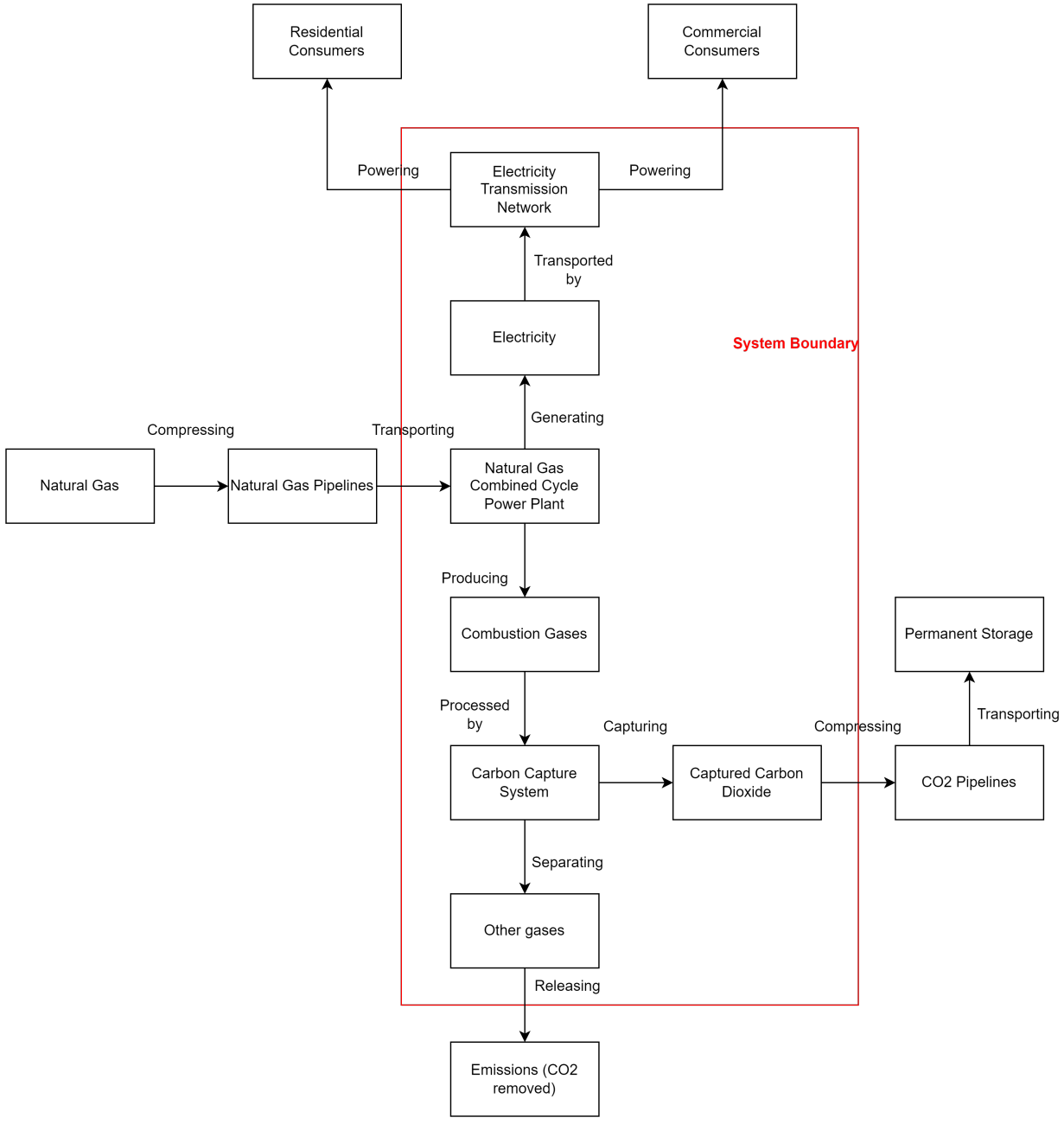

Figure 2.1: NGCC Power System Representation with System Boundary

Table 2.1: Initial Research Papers for Network Creation

Title	**Author(s)**	**Year**	**Publication**
Flexible CO_2 capture for open-cycle gas turbines via vacuum-pressure swing adsorption: A model-based assessment [25]	Wilkes et al.	2022	Energy
Dynamic operation and modeling of amine-based CO_2 capture at pilot scale [26]	Bui et al.	2018	International Journal of Greenhouse Gas Control
Post-combustion CO_2 capture from a natural gas combined cycle power plant using activated carbon adsorption [27]	Jiang et al.	2019	Applied Energy
Thermal integration of a flexible calcium looping CO_2 capture system in an existing back-up coal power plant [28]	Arias et al.	2020	ACS Omega
A pilot-scale study of dynamic response scenarios for the flexible operation of post-combustion CO_2 capture [29]	Tait et al.	2016	International Journal of Greenhouse Gas Control
Flexible carbon capture using MOF fixed bed adsorbers at an NGCC plant [30]	Habib et al.	2024	Carbon Capture Science and Technology
A review of material development in the field of carbon capture and the application of membrane-based processes in power plants and energy-intensive industries [31]	He	2018	Energy, Sustainability, and Society
Carbon capture and storage (CCS): the way forward [32]	Bui et al.	2018	Energy and Environmental Science
A Comparison of Post-combustion Capture Technologies for the NGCC [33]	Subramanian et al.	2017	Energy Procedia
Assessing absorption-based CO2 capture: Research progress and techno-economic assessment overview [34]	Khan et al.	2023	Carbon Capture Science and Technology

A network of research papers was created, showing the connections between papers, authors, cross-references, and themes. This network generated over 3,000 similar papers, with the top 50 displayed in Figure 2.2.

After acquiring an extensive collection of literature from the aforementioned academic databases supplemented with AI-assisted recommendations, inclusion and exclusion criteria were developed to pare the results down to a more concentrated subset of information. The titles and abstracts were screened to bring the total number of evaluated papers down to 200 for detailed analysis. Papers that studied NGCC plants were preferred to those that analyzed coal-fired power plants, and literature on commercial-scale or pilot-scale studies

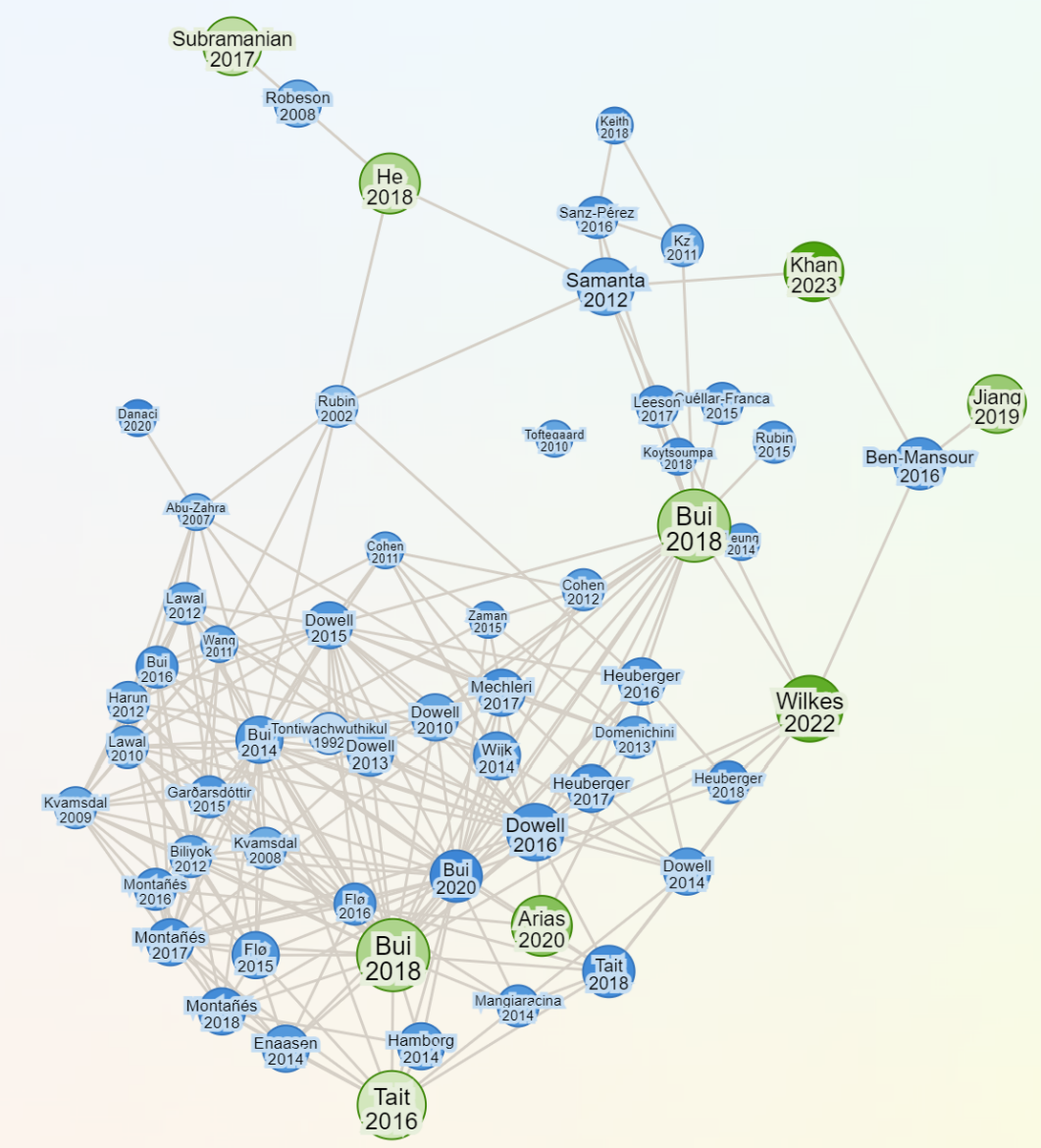

Figure 2.2: Network of Literature Papers. Circles sized by number of connections

was prioritized over model-based results. However, coal-based and model-based literature was included for technologies and metrics where NGCC field trial data was not available. Additionally, literature before the year 2000 was generally excluded, with a preference for papers published post-2010. Each paper was evaluated through the lens of each of the six key metrics outlined earlier, resulting in approximately 115 papers used for detailed analysis.

2.2 Carbon Capture Technologies

Carbon capture techniques can be broadly grouped into three categories: post-combustion carbon capture, pre-combustion carbon capture, and oxyfuel combustion capture. Multiple sub-categories exist within each main classification, and there are varying processes and methods of gas separation for each sub-category. A high-level decomposition of some of the more common carbon capture technologies can be seen in Figure 2.3. This thesis primarily focuses on post-combustion carbon capture, mainly absorption, adsorption, and membranes.

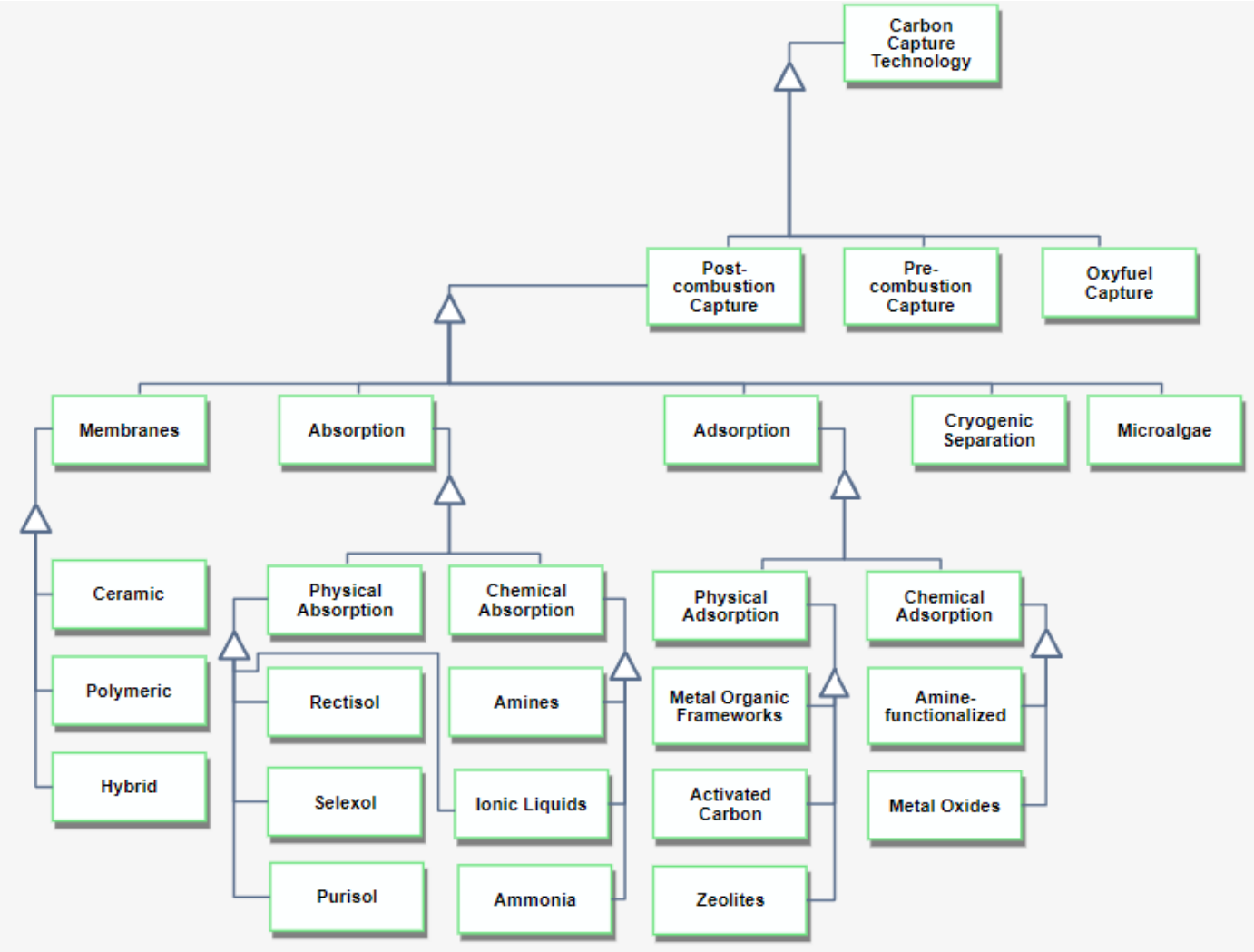

Figure 2.3: Decomposition of Common Carbon Capture Technologies. Note ionic liquids can absorb CO_2 by both physical and chemical processes

2.2.1 Post-Combustion Carbon Capture

Post-combustion carbon capture refers to the point source separation and capture of CO_2 from exhaust flue gas generated during combustion. There are various methods used to separate the CO_2 from the exhaust gas, such as absorption, adsorption, membranes, cryogenic, and microalgae capture. These techniques will be further reviewed in Section 2.3. It is generally viewed as a more mature technology than pre-combustion or oxyfuel combustion capture, as some of the capture processes, such as amine scrubbing, have been used since the 1930s in natural gas sweetening to separate CO_2 from natural gas [35]. This technical maturity results in post-combustion capture often being cheaper than pre-combustion and oxyfuel-combustion capture [36]. Furthermore, post-combustion carbon is generally viewed as the most suitable method for retrofitting existing power plants with CCS equipment as it does not require extensive additional equipment or significantly change the plant's configuration [37]. Post-combustion capture also creates operational flexibility, allowing plants to implement partial CCS or bypass the capture equipment completely during periods of peak demand where rapid power output takes priority. Some methods of post-combustion capture also allow for the integration of renewable energy, such as solar PV, to provide the energy for solvent regeneration. Post-combustion capture is widely applicable to other heavy industries such as steel, cement, and petrochemicals.

One key challenge of post-combustion carbon capture is the difficulty in separating the CO_2 from the flue gas stream. CO_2 concentrations can range from 3%-4% for natural gas-fired plants to 12%-15% for coal-fired plants [38]. Separating CO_2 from flue gas at these low concentrations requires significant energy due to the low CO_2 partial pressure and is a primary barrier to widespread implementation. An additional challenge to post-combustion carbon capture is the presence of impurities in the flue gas, such as particulate matter, sulfur dioxide, and nitrogen oxide. These impurities are found in higher concentrations in coal-fired flue gas than gas-fired flue gas, and they can reduce the effectiveness of the carbon capture process [39]. The energy required to separate the CO_2 from the flue gas often results in significant penalties to the plant's thermal efficiency.

The CCE of post-combustion carbon capture varies considerably based upon the specific technology being used, the CO_2 concentration of the flue gas, and the type of power plant. Amine-based chemical absorption has demonstrated capture efficiencies of 85%-95% in pilot studies across both coal flue gas and natural gas flue gas[40],[41],[42]. Multiple pilot programs for post-combustion capture have been executed, such as the Boundary Dam Power Station in Estevan, Saskatchewan, the Petra Nova project in Thompsons, Texas, and the Bellingham, Massachusetts NGCC plant. A full list of post-combustion carbon capture-related U.S. as tracked by the National Energy Technology Laboratory is shown in Figure 2.4. In total, there are 37 active projects out of 68 total projects being tracked, with the remainder either inactive or retired.

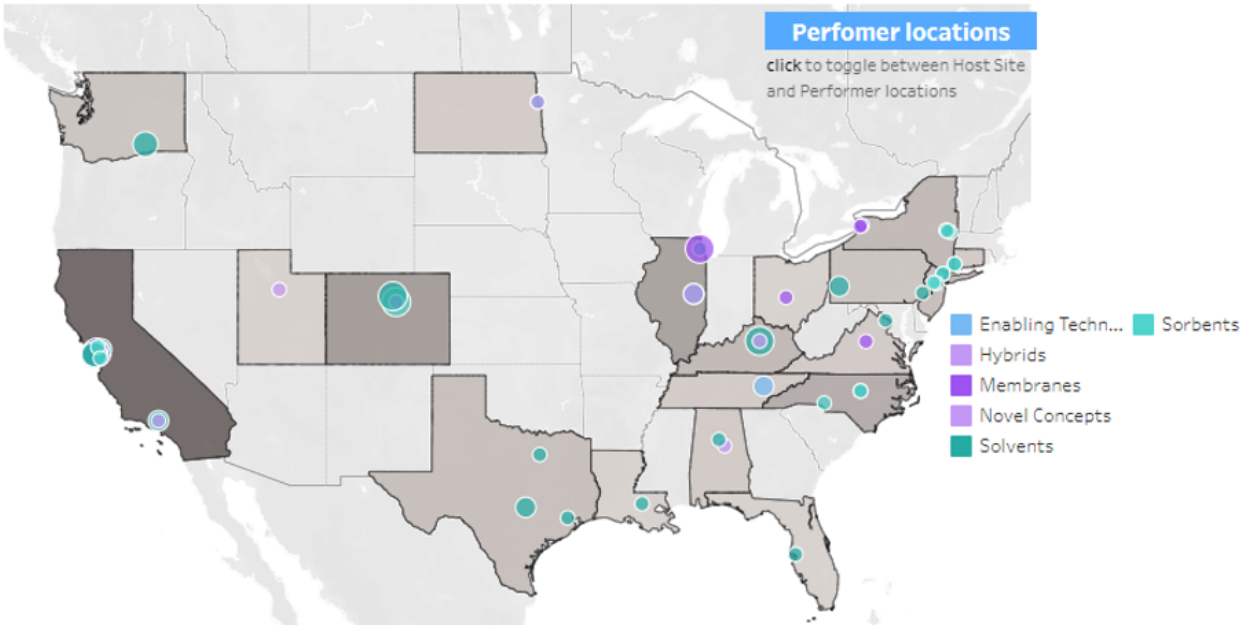

Figure 2.4: Map of Current Post-Combustion Carbon Capture Projects [43]

2.2.2 Pre-Combustion Carbon Capture

In contrast to post-combustion carbon capture, pre-combustion carbon capture removes the CO_2 prior to completing the combustion process. For natural gas systems, this process functions by converting methane into syngas, composed of hydrogen and carbon monoxide, via steam methane reforming or partial oxidation. Steam methane reforming is the primary method of producing hydrogen gas and requires reacting methane with steam and a high-temperature catalyst [44]. The steam methane reforming process can be represented by the following chemical reaction:

$$CH_4 + H_2O \longrightarrow CO + 3\,H_2$$

Next, the syngas undergoes a water-gas shift reaction in a reactor, where the carbon monoxide is reacted with steam and a low-temperature catalyst to produce carbon dioxide and hydrogen. The water-gas shift reaction can be represented by the following chemical reaction:

$$CO + H_2O \longrightarrow CO_2 + H_2$$

The resulting hydrogen is burned in the gas turbine to generate electricity, similar to standard combined cycle gas turbine plants [45]. The overall process flow for pre-combustion carbon capture can be seen in Figure 2.5. The gas separation technique itself is largely the same as what is available for point-source post-combustion carbon capture, including technologies such as absorption, adsorption, and membranes. Physical or chemical adsorption are the methods of gas separation most commonly used to separate the CO_2 from the syngas stream. Pre-combustion capture methods may benefit from physical solvents, which mix less strongly with CO_2, as the circumstances for CO_2 separation are very different from those

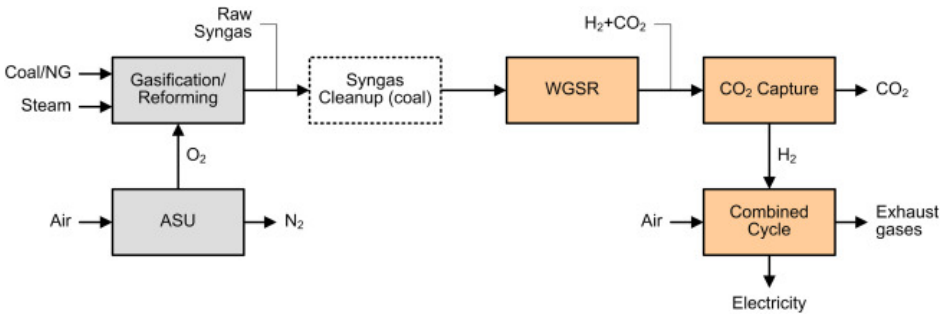

Figure 2.5: Pre-Combustion Carbon Capture Process flow [46]

in post-combustion capture procedures. Physical solvents exhibit a higher CO_2 capacity at pre-combustion conditions, allowing for CO_2 separation at lower stripper pressures, hence reducing energy usage during regeneration [45].

Pre-combustion carbon capture is generally an efficient method of carbon capture, able to capture 90%-95% of CO_2. The resulting gas mixture after the water-gas shift reaction contains up to 55% CO_2, and this higher CO_2 concentration facilitates a more efficient capture process [47]. The higher concentration in the gas stream reduces the energy required to separate the CO_2 from the H_2, resulting in a smaller energy penalty to the plant's thermal efficiency. IGCC plants average an energy penalty, defined as a percent decrease in the plant's thermal conversion efficiency due to the carbon capture process, between 6%-10% [48]. Comparatively, leading post-combustion carbon capture technologies incur an energy penalty from 6%-14%, depending on the specific technology used [49]. Pre-combustion carbon capture has the smallest impact on the plant's overall thermal efficiency compared to post-combustion carbon capture and oxyfuel carbon capture [50]. This is true for both natural gas-fired and coal-fired power plants.

This technology has been most thoroughly evaluated for coal-fired power plants, specifically integrated gasification combined cycle (IGCC) coal plants. Coal requires extensive processing prior to combustion due to its higher CO_2 content, sulfur content, and particulates. Furthermore, IGCC plants already require the gasification of coal, so incorporating pre-combustion carbon capture can leverage the existing equipment and processes. Conversely, NGCC power plants require minimal pre-processing and provide relatively high thermal efficiencies without the need for a gasifier or reformer, so pre-combustion carbon capture has not been extensively studied for these plants. Including a reforming unit and a shift reactor would require a substantial redesign of existing NGCC power plants, adding major expenses and making pre-combustion carbon capture an unattractive option for retrofitting existing plants. All current projects on pre-combustion carbon capture are focused on coal-fired plants or hydrogen generation for industrial usage. A list of pre-combustion projects involving the power sector in the U.S. is presented in Table 2.2.

Table 2.2: Summary of Pre-Combustion Carbon Capture Related Projects [43]

Performer	Key Technology	Project Status	Ending Scale	Performer State	Performer City
Arizona State University	Membranes	Inactive	Laboratory	AZ	Tempe
Media and Process Technology, Inc.	Membranes	Active	Bench	PA	Pittsburgh
Membrane Technology and Research, Inc.	Membranes	Inactive	Bench	CA	Newark
Ohio State University	Membranes	Inactive	Laboratory	OH	Columbus
Pacific Northwest National Laboratory	Solvents	Inactive	Laboratory	WA	Richland
SRI International	Membranes	Inactive	Bench	CA	Menlo Park
State University of New York	Membranes	Inactive	Laboratory	NY	Amherst
TDA Research, Inc.	Sorbents	Active	Small Pilot	CO	Wheat Ridge
TDA Research, Inc.	Sorbents	Inactive	Small Pilot	CO	Wheat Ridge
University of Southern California	Hybrid	Inactive	Bench	CA	Los Angeles

2.2.3 Oxyfuel Combustion Capture

Oxyfuel combustion capture is the third main category of carbon capture methods. In oxyfuel combustion, the source fuel is burned in the presence of nearly pure oxygen instead of air. Air is composed of approximately 78% nitrogen, 21% oxygen, and 1% other gases[51]. Combusting natural gas with air results in a flue gas composition that also contains large amounts of N_2, with smaller amounts of CO_2, O_2, and H_2O [52]. Typical flue gas from an NGCC power plant contains less than 5% CO_2 and approximately 75% N_2. As discussed in Section 2.2.1, these low concentrations make separating the CO_2 from the N_2 a difficult, energy-intensive process. Oxyfuel combustion seeks to remedy this issue by replacing air with pure oxygen and recycled flue gas. The process begins by using an air separation unit to separate the oxygen from the air, usually via a cryogenic distillation air separation process. Cryogenic gas separation is further discussed in Section 2.3.4. The resulting gas is nearly pure oxygen, which is then fed into the combustion chamber. This reduces the nitrogen content in the chamber prior to combustion. The source fuel is then ignited in the presence of pure oxygen and recycled flue gas, consisting of mostly CO_2 and water vapor. The resulting flue gas is approximately 70%-80% CO_2, by volume [53]. Some of the resulting

flue gas is recycled back into the combustion chamber in order to control the temperature and ensure appropriate heat transfer during the combustion process. The flue gas is then cooled to allow the water vapor to condense and be separated from the CO_2 before being processed to remove any impurities. The CO_2 rich gas is compressed and captured without requiring any physical or chemical sorbents [54]. An overview of this process is demonstrated in Figure 2.6.

Figure 2.6: Oxyfuel Block Diagram Process Flow [55]

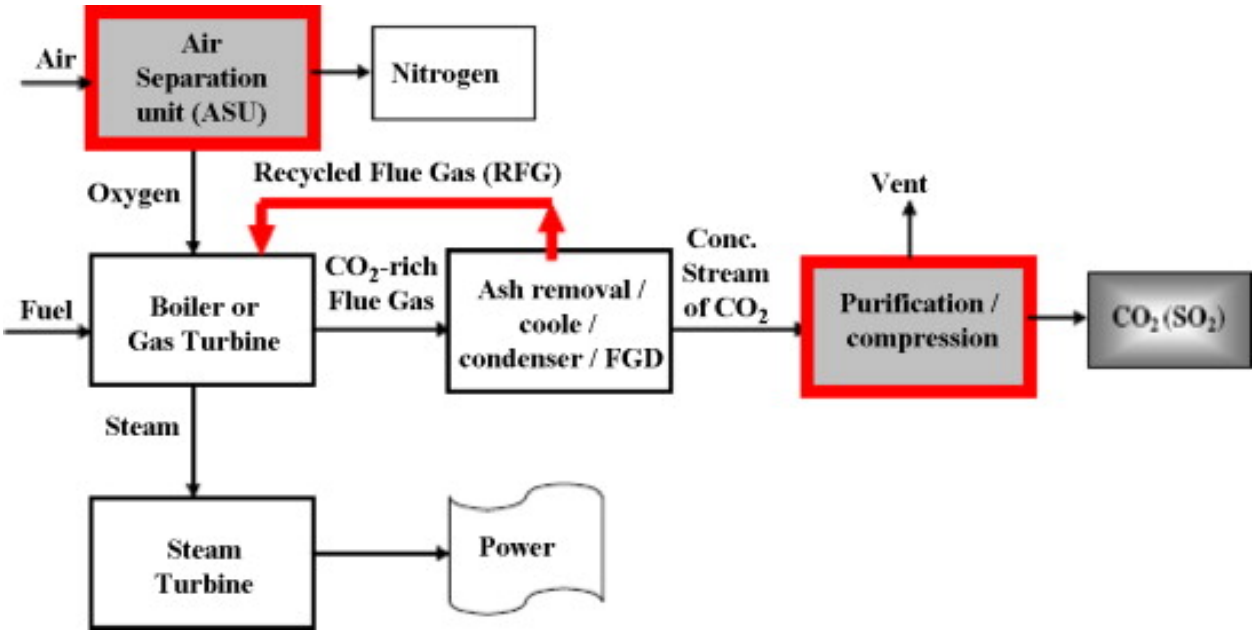

Oxyfuel combustion carbon capture can be a highly efficient method of separating and capturing CO_2 from power plant flue gas, capturing over 90% of CO_2 and theoretically capable of capturing up to 100% of CO_2 [56]. This high carbon capture efficiency is driven by the high CO_2 concentration in the flue gas as a result of removing the nitrogen prior to the combustion process. An additional benefit to oxyfuel combustion carbon capture is that nitrogen oxide (NO_x) production is significantly reduced due to the removal of nitrogen [53]. The overall volume of flue gas from oxyfuel combustion is also approximately reduced by 75%-80%, resulting in requiring smaller emissions control equipment [37].

The primary challenge in oxyfuel combustion is the requirement of large volumes of high-purity oxygen to be used in the combustion process. Separating oxygen from the air is an energy-intensive process, and adding cryogenic carbon capture to power plants can reduce the plant's thermal efficiency by 18%-20% [57],[50]. The air separation unit is responsible for the majority of the reduction in thermal efficiency. Oxyfuel combustion carbon capture is most often considered for coal-fired power generation. Application of oxyfuel combustion capture to NGCC plants is somewhat limited. A key strength of these plants is their ability to operate at a relatively high thermal efficiency and produce less CO_2 per unit of electricity than coal power plants. Further, retrofitting them with an air separation unit and other required equipment for oxyfuel combustion capture is a difficult, expensive process that is

difficult to justify economically. Thus, most research on oxyfuel combustion carbon capture focuses on coal-fired power plant applications.

2.3 Post-Combustion Carbon Capture Separation Methods

This section reviews the specific methods and techniques for post-combustion carbon capture. As discussed in Section 2.2.1, post-combustion carbon capture is generally regarded as the most suitable method of retrofitting existing power plants, so this paper will focus primarily on post-combustion capture analysis.

2.3.1 Absorption

Absorption is the most established method for post-combustion carbon capture. The two main techniques of absorption for carbon capture are chemical absorption and physical absorption. Both methods involve absorbing gaseous CO_2 into a solvent. Chemical absorption requires a chemical reaction where chemical bonds are formed between the absorbate, the substance being absorbed, and the absorbent, the material that absorbs the substance. In the context of carbon capture, this refers to CO_2 being absorbed into a solvent, oftentimes an amine-based solvent, by a chemical reaction. It typically creates stronger bonds, such as covalent or ionic bonds, as opposed to physical absorption. It also may function at elevated temperatures in contrast to physical absorption, and it is often irreversible. Chemical absorption is typically preferred to physical absorption due to its higher absorption capacity in the presence of low CO_2 partial pressure associated with flue gas composition [58]. Physical absorption is the process in which the absorbate is dissolved into the absorbent without forming any major chemical bonds. The process is facilitated by the presence of weak Van der Waals forces between the molecules of the absorbate and the absorbent. Physical absorption generally occurs at lower temperatures and has the potential to be reversed. The degree of absorption follows Henry's Law and is contingent upon partial pressures and temperature. Common physical solvents include Rectisol, Selexol, Fluor, Purisol, and Sulfinol [59].

Chemical absorption is the most mature carbon capture process and is regarded as the leading candidate for retrofitting power plants with CCS equipment [60]. In absorption carbon capture, the exhaust gas is cooled before being sent to an absorption column. The absorption column contains an aqueous solution with a solvent, such as monoethanolamine (MEA), that reacts with and captures the CO_2 in the exhaust gas mixture. As the solvent captures increasing amounts of CO_2, it begins to saturate and requires regeneration. It is pumped through a heat exchanger into a desorption column, where it is heated until the CO_2 is released. The captured CO_2 is then sent to be compressed and stored, and the regenerated solvent is recirculated back through the heat exchanger to the absorption column. This entire process is displayed in Figure 2.7.

The most common type of chemical absorption uses amine-based solvents, with 30 wt% MEA being the most well-known and often used as the industry standard for benchmarking [62]. An amine is an organic molecule that is derived from ammonia (NH_3) by substi-

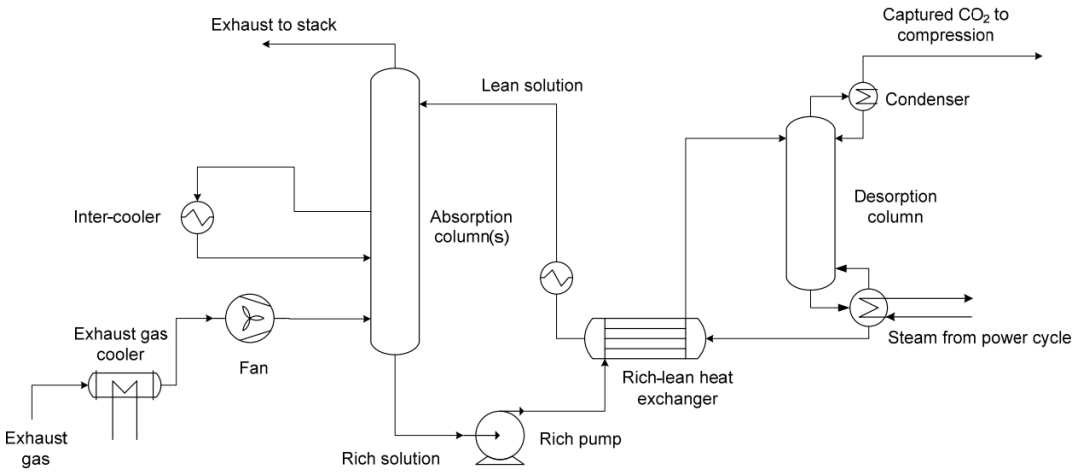

Figure 2.7: Flow Diagram of Absorption-Desorption CO_2 Capture Process [61]

tuting one or more hydrogen atoms with alkyl or aryl groups [63]. Other common solvents include diethanolamine (DEA), diglycolamine (DGA), di-isopropanolamine (DIPA), 2-amino-2-methyl-l-propanol (AMP), and methyl diethanolamine (MDEA) [64]. Picking the appropriate solvent is a critical decision for chemical absorption carbon capture, and extensive research is being conducted on different types of solvents, including blended amines and ionic liquids. Public solvent formulations, such as MEA, are often used in studies to facilitate easier comparison of results, though private formulations have exhibited improved performance. The technology readiness levels of these solvents range from a 9 for very mature solvents such as traditional amines and physical solvents to a 2 for ionic liquids [58].

Chemical absorption offers a variety of advantages relative to other capture methods. First, it provides a high carbon capture efficiency under steady-state conditions, ranging from 85%-95% in pilot studies [40]. Solvents used for chemical absorption have a high CO_2 selectivity, supporting the high capture efficiencies and enabling the system to handle large volumes of gas [34]. It is also the most suitable technology for retrofitting existing power plants as it does not impact the upstream combustion process. Absorption is a mature, well-established technology that is implementation-ready for power plants today. Finally, absorption provides increased removal of gaseous impurities such as NO_x and SO_x from the emissions stream [65]. However, absorption-based carbon capture also comes with a variety of challenges that make it difficult to adopt at scale. As mentioned in 2.2.1, the low CO_2 concentration in flue gas makes it difficult to separate. This results in requiring large-scale equipment capable of handling large volumes of gas, leading to high capital costs [66]. Solvent degradation is another barrier to absorption-based carbon capture. As the aqueous amine solvent interacts with impurities, typically NO_x for NGCC plants, it undergoes irreversible chemical reactions. These reactions result in the loss of solvent and reduced capture efficiency [67]. Strzisar et al. continue to contend that equipment corrosion due to solvent degradation products is another key issue, resulting in the requirement to keep solvent concentrations low. The primary challenge with absorption-based carbon capture, however, is that it requires a very high amount of energy to regenerate the solvent. The heat duty for conventional 30 wt% MEA ranges between 3.6-4.0 GJ/tonne of CO_2 but has been demonstrated as low as 2.0

GJ/tonne of CO_2 for other solvents [32]. This reduces the plant's net operating efficiency by 6%-14% [49]. Between 60%-80% of the total energy used for absorption-based carbon capture is associated with solvent regeneration, with the remainder going towards compression and other associated processes [68].

While multiple pilot studies have been conducted for coal-fired power plants (Boundary Dam[69], Petra Nova[70]), limited tests have been conducted for gas-fired power plants. The Bellingham, Massachusetts NGCC plant utilized Fluor's Econamine FG PlusSM™ solvent to capture 85%-95% of the emissions from a 40 MW slipstream from 1991-2005, and it is one of the extremely few cases where carbon capture technology was applied to a gas-fired power plant beyond lab testing [71]. Pilot studies have been conducted more recently at Technology Centre Mongstad using new solvents such as CESAR-1, but overall studies beyond modeling work are limited to carbon capture applied to NGCC plants [72].

2.3.2 Adsorption

Another method of post-combustion carbon capture is adsorption. Where absorption separates CO_2 by utilizing liquid solvents, adsorption uses solid materials, called adsorbents, to separate the CO_2 from the flue gas. The key difference between adsorption and absorption is the way in which the molecules are bound. Absorption involves the molecules being dissolved or reacted in a liquid solvent, but in adsorption, the molecules adhere to the surface of a porous solid sorbent instead [59]. The process begins with flue gas passing through a chamber containing adsorbent materials. The CO_2 is captured on the surface of the absorbent, allowing the N_2 to flow uninhibited to the exhaust column. As increasing amounts of CO_2 are captured by the absorbent, equilibrium is reached, and the adsorbent requires regeneration. The desorption process then begins, similar to amine-based solvent carbon capture. Adsorption capacity is dependent upon both pressure and temperature, so the solid absorbent can be regenerated by either pressure swing adsorption (PSA) or temperature swing adsorption (TSA). PSA involves reducing the pressure to release the CO_2 and regenerate the adsorbent, and TSA requires increasing the temperature to separate the CO_2 and regenerate the absorbent material [73]. PSA has been historically preferred to TSA for adsorption-based carbon capture for two primary reasons, although recent research has trended toward exploring TSA. PSA generally requires less energy, as TSA must heat the adsorbent to high temperatures for regeneration. Further, PSA has shorter cycle times than TSA and is able to achieve more rapid desorption due to pressure changes occurring quicker than temperature changes. The adsorption and desorption cycles in TSA take significantly longer than PSA because of the effects of thermal inertia [74]. A variation of PSA, called vacuum swing adsorption, also exists, and it regenerates the adsorbent by lowering pressure to a vacuum level.

Similar to absorption, there are two main categories of adsorption: chemical adsorption, or chemisorption, and physical absorption, or physiosorption. The characteristics of chemisorption and physiosorption are the same as those of liquid absorption, with the former involving a chemical reaction and the latter involving Van der Waals forces. Physiosorption is the most common type of adsorption for carbon capture, and its adsorption capacity increases with pressure [59]. Physiosorption creates weaker bonds between CO_2 and the adsorbent, resulting in a faster rate of adsorption and desorption. Due to these weaker bonds,

it also requires less energy for the desorption process [75]. Physical adsorbents include metal-organic frameworks, activated carbon, silica gels, alumina, and zeolites [76]. Chemisorption creates strong bonds, via ionic or covalent bonding, between the adsorbate and adsorbent. These strong bonds make the desorption process difficult, requiring significant amounts of energy. Chemisorption is able to capture CO_2 at lower concentrations than physiosorption and has higher selectivity due to the chemical reactions [77]. Chemical adsorbents typically consist of metal oxides, such as calcium oxide (CaO) and magnesium oxide (MgO) [78]. Amine-functionalized materials, where traditional porous solid adsorbents are chemically modified to add amines to their surface, are also being researched due to their higher adsorption capacity and regeneration requirements [79].

Adsorption-based carbon capture is a viable yet not thoroughly explored technology for reducing emissions from NGCC power plants. It is well understood that selecting the appropriate adsorbent is critical for adsorption-based carbon capture. Ideally, the adsorbent should have the following characteristics: [80]

- High adsorption capacity
- High CO_2 selectivity
- Tolerant of moisture and other impurities without adversely impacting capture rate
- Exhibit a rapid adsorption and desorption cycle time
- High mechanical and thermal stability

Zeolites, metal-organic frameworks, and activated carbon are viewed as the most promising adsorbents for carbon capture, but this paper will not focus on the various types of solid sorbents as it has been extensively covered in literature elsewhere [59],[76],[78],[80],[81]. In addition to the absorbent selection, the performance of adsorbents also depends on the configuration of the gas-solid reactor. Multiple gas-solid reactor configurations are currently being studied, including fixed bed reactors, moving bed reactors, and fluidized bed reactors [80]. This combination of absorbent material, gas-solid reactor configuration, and adsorbent regeneration method results in a large number of potential outcomes when evaluating adsorption-based carbon capture for NGCC power plants. Historical literature indicates that adsorption can capture 85% - 90% of CO_2 emissions from gas-fired power plants [30],[82] and recent modeling studies have demonstrated the potential to increase CCE up to 96% via moving bed temperature swing adsorption using Zeolite 13X [83]. However, no commercial-scale projects utilizing adsorption-based carbon capture have been implemented in gas-fired power plants, so literature and field data on capture efficiencies remain limited. A 60% carbon capture efficiency was recorded in the lone coal-fired power plant pilot program conducted as part of the CO2CRC/H3 Capture Project on a lignite-fired power plant in the Latrobe Valley, Victoria, Australia [84]. In their analysis of the project, Qadar et al. suggest the capture efficiency would be much higher in an optimized scenario without process interruptions.

One advantage of adsorption-based carbon capture is that it can have a lower energy penalty relative to most absorption-based methods, depending on the specific adsorbent, configuration, and regeneration method used [83]. However, this is highly contingent upon the specific combination being used. Recent studies have shown various adsorption-based

carbon capture methods would actually have a higher energy penalty than a traditional amine solvent absorption process [32]. Estimates of energy penalty for adsorption range from 5% - 10% [32],[83]. Similar to absorption, adsorption is also a reasonable option for retrofitting existing NGCC power plants. Only limited additional equipment would be required, such as vacuum pumps (for vacuum swing adsorption (VSA)) and an adsorption vessel. No upstream modifications would be required to the power plant, significantly reducing retrofitting complexity and cost.

Multiple challenges exist with utilizing adsorption-based carbon capture for gas-fired power plants. First, for the majority of adsorbents being investigated, the adsorption capacity is greatly reduced in the presence of water [80]. This is especially true for physical adsorbents, and it is a primary challenge in using steam for temperature swing adsorption to regenerate the adsorbent. Combined with the relatively large volume of water vapor typically found in flue gas, this necessitates that the adsorbents undergo a drying process prior to recycling, increasing the energy penalty. The energy requirements for pressure swing adsorption require the capture of CO_2 at high pressures and thereby require compressing large volumes of flue gas. This leads to a high energy penalty and reduces the adsorbent CO_2 selectivity due to the increased pressure [85]. Vacuum swing adsorption does not require compression of the exhaust gas, as it captures the CO_2 at atmospheric conditions and then reduces the pressure to vacuum levels for the desorption process. However, studies have shown this results in lower CO_2 recoveries, typically less than 85% for single-stage vacuum pumping [86]. Multi-stage VSA is likely required to achieve capture efficiencies above 90%, though that introduces additional energy consumption associated with vacuum pumping [27].

2.3.3 Membranes

Membranes are a third primary method of carbon capture and storage currently being investigated for use in the power sector. Membranes are composed of layers of permeable or semi-permeable materials that utilize selective permeance to separate CO_2 from the flue gas. They are designed to selectively allow CO_2 to permeate through the medium via partial pressure differences while retaining other gases, such as N_2. This requires a pressure differential across both sides of the membrane. There are two methods for creating the pressure differential. The feed-side gas can be compressed before it enters the membrane system, or the permeate-side can be placed under vacuum pumping [87]. Merkel continues to assert that vacuum pumping generally exhibits lower energy consumption but requires a larger membrane area, necessitating highly permeable membranes. Under either scenario, the process begins with flue gas being fed into the membrane system. As the flue gas enters the membrane system, different individual gases diffuse through the membrane at different rates. The membranes are designed so that CO_2 permeates through it faster than N_2, effectively separating the gases [66]. The gas strain that passes through the membrane is referred to as the permeate strain, and the gas that is retained is the retentate strain [88]. The permeate strain, ideally mostly CO_2, is sent to be compressed and stored, while the retentate gas, composed mostly of N_2, is safely vented. A diagram demonstrating the membrane separation process is shown in Figure 2.8

There are two key metrics that must be considered when evaluating membranes for gas

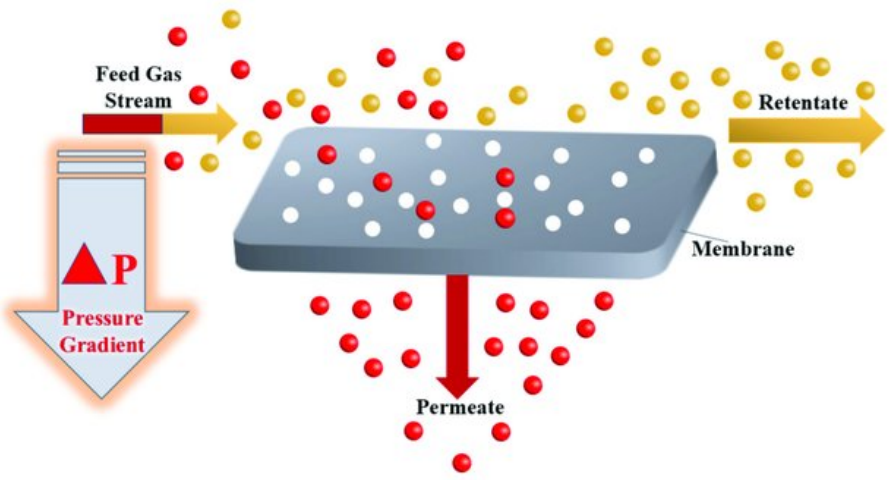

Figure 2.8: Membrane Separation Process [89]

separation: selectivity and permeability [90]. Park et al. define permeability as the intrinsic ability of a material to allow a gas to pass through it and selectivity as the degree to which CO_2 is separated from the other gases. In the context of membranes, permeance is often used, which is defined as the permeability, P, divided by the membrane thickness.

$$Permeance = \frac{P}{t_{\text{membrane}}}$$

Selectivity, α, is determined by the ratio of gas permeabilities and can be calculated as

$$\alpha = \frac{P_1}{P_2} = \frac{D_1}{D_2} * \frac{S_1}{S_2}$$

where D_x represents the diffusion coefficient of the gas within the membrane, and S_x is the sorption coefficient, which connects the gas concentration within the membrane to the adjacent gas pressure [87]. These criteria are often in tension, as membranes with a higher selectivity typically exhibit lower permeability, and those with high permeability exhibit low selectivity [65]. High permeability is desirable as it enables the membrane to quickly handle large volumes of gas. Given the relatively low CO_2 concentration in NGCC power plant flue gas, the membranes must be able to process large volumes of gas quickly to avoid limiting power plant output. High selectivity is also necessary to ensure the captured CO_2 in the permeate strain meets the established 90% capture rate and 95% purity outlined by the Department of Energy. Highly selective membranes often have an associated low permeability, and highly permeable membranes often have poorer selectivity [91].

There are three main classifications of membranes considered for carbon capture: polymeric membranes, inorganic/ceramic membranes, and hybrid membranes. Polymeric membranes are composed of organic polymers, such as polysulfone, and have been utilized for various separation processes across multiple industries [92]. They typically exhibit relatively good permeability and selectivity [93]. However, they are susceptible to degradation and fouling when subjected to harsh conditions, high temperatures and pressures, and corrosive environments [31]. This can lead to reduced stability over time. Inorganic membranes are

composed of inorganic materials, such as ceramic, zeolite, or silica. They have been rising in prominence in the literature recently due to their capability to handle these adverse conditions often found in natural gas-fired power plant flue gas processing [94]. Fard et al. highlight that they are chemically and thermally stable and able to withstand high temperatures and other chemical impurities. However, they are generally more expensive and more brittle than polymeric membranes, leading to higher costs. The third class of membranes are hybrid membranes. These membranes combine organic and inorganic components to capture the advantages offered by each type of membrane. This is usually accomplished in a mixed matrix membrane, consisting of inorganic material such as zeolites, silica, or graphene embedded in a polymer matrix [95]. The exact performance of the hybrid membrane is dependent upon the inorganic filler selected, the polymer compatibility, and the configuration. They have the potential to offer greater selectivity, permeability, and stability over polymeric membranes [96]. However, these membranes are less technically mature compared to traditional polymeric and inorganic membranes. It is also challenging to fabricate defect-free mixed matrix membranes without adversely impacting their mechanical stability [97].

Overall, membranes possess certain desirable characteristics for carbon capture in the power sector. They are suitable candidates for retrofitting existing power plants as they do not require modifications to the steam cycle or combustion process, resulting in less capital expenditures and less complexity [93]. Further, unlike absorption and adsorption, they generally do not require any energy for regeneration [98]. However, their main limitation is currently related to their carbon capture efficiency. Membranes have shown promise for CO_2 concentrations greater than 20%, but their application at lower concentrations has been limited. Historically, membranes have not been able to effectively meet the 90% capture requirements without incurring dramatic energy penalties [33]. Single-stage membrane separation typically cannot meet capture efficiency and purity requirements, so multi-stage membrane separation is required. The additional stages, each requiring additional energy for compression, lead to extensive reductions in thermal efficiency. Subramanian et al. determined that a 90% CCE would result in a reduction of NGCC plant thermal efficiency to 34.9%, an energy penalty of nearly 24%. This can be somewhat mitigated by utilizing exhaust gas recirculation by increasing the CO_2 concentration, but the energy penalty is still 12%, worse than most other technologies. Recent studies have indicated that it is extremely unlikely to achieve both 90% CCE and 95% CO_2 purity using a single-stage membrane, as the membrane performance is limited by the pressure differential [87]. Therefore, multi-stage membrane processes and designs are being tested for improved performance. A pilot study of a multi-stage membrane was sanctioned by the Department of Energy at Technology Centre Mongstad that demonstrated capture rates above 90% with purity above 95%. However, the inlet CO_2 concentration was varied from 14%-26%, and the capture rate was found to rapidly decrease as a function of flue gas flow rate [87]. Other model-based studies have been conducted, showing capture rates of 90% with energy penalties between 7%-8%, but these have yet to be validated on a pilot-scale demonstration [99].

2.3.4 Cryogenic Separation

Cryogenic-based carbon capture (CCC) is another method for separating CO_2 from other gases. Conventionally, it relies on cryogenic distillation, leveraging the different boiling

points of gases to selectively liquefy CO_2. CO_2 has a boiling temperature of -109.3 °F (-78.5 °C) [100], much higher than that of N_2 at -320.1 °F (-195.8 °C) [101] and O_2 at -297.3 °F (-183 °C) [102]. The process begins by cooling the flue gas to a very low temperature, often at high pressures, utilizing heat exchangers and refrigeration cycles. As the temperature drops, water vapor condenses and is removed. When the temperature drops low enough, the CO_2 condenses while the other gases remain in a gaseous phase. The liquid CO_2 is then separated and sent for transportation and storage [103]. The primary advantage of CCC is that it results in a high purity CO_2 stream without requiring chemical solvents or sorbents [104]. It is capable of achieving carbon capture efficiencies greater than 90% and up to 99% depending on the temperature and pressure configuration utilized [105]. It is also appropriate for retrofitting existing power plants as it does not require steam or alter the upstream combustion processes.

However, the primary challenge with CCC is associated with the CO_2 concentration in flue gas. Literature indicates that cryogenic distillation is historically not economical for post-combustion carbon capture due to the vast energy required to cool the gas to the appropriate temperatures at such low concentrations of CO_2 [106],[103]. Newer methods of CCC that utilize techniques other than distillation, such as anti-sublimation, Stirling coolers, and CryoCell®, have shown more promise with reduced energy penalties but are yet to be commercially proven [107]. Cryogenic methods for carbon capture are currently better suited for higher CO_2 concentration applications, including pre-combustion, oxyfuel combustion, and heavy industry applications. Further research is also exploring the potential of hybrid technologies combining cryogenic carbon capture with membranes, energy storage, and adsorption processes [32],[108]. Lab and modeling results thus far have been favorable, so cryogenic-based carbon capture should be monitored for future suitability in retrofitting NGCC power plants.

2.3.5 Calcium Looping

Calcium looping (CaL) is the final method of carbon capture that will be addressed in this thesis. It is a subset of a larger category of processes, chemical looping, and it has a higher technology readiness level (TRL) than most other solid looping techniques [58]. It is still considerably less mature than conventional amine-based carbon capture methods, however. CaL operates by leveraging the reversible chemical reactions between CaO and CO_2. It utilizes some of the principles of adsorption, as discussed in Section 2.3.2. Flue gas enters a carbonator, where it encounters a solid sorbent, CaO, and reacts to form $CaCO_3$ via carbonation, as shown below:

$$CO_2 + CaO \longrightarrow CaCO_3$$

This reaction in the carbonator typically occurs at high temperatures between 600 - 700 °C. The flue gas, with most of the CO_2 removed, is subsequently vented. The $CaCO_3$ is then transported into the calciner, where it is subjected to high temperatures of 850 - 900 °C, causing the $CaCO_3$ to decompose back into CaO and CO_2, reversing the initial reaction [109]. The CaO is recycled back into the carbonator, and the process repeats. The CO_2 released in the calciner is generally quite pure, so it is relatively simple to capture and store. The process flow is shown in Figure 2.9.

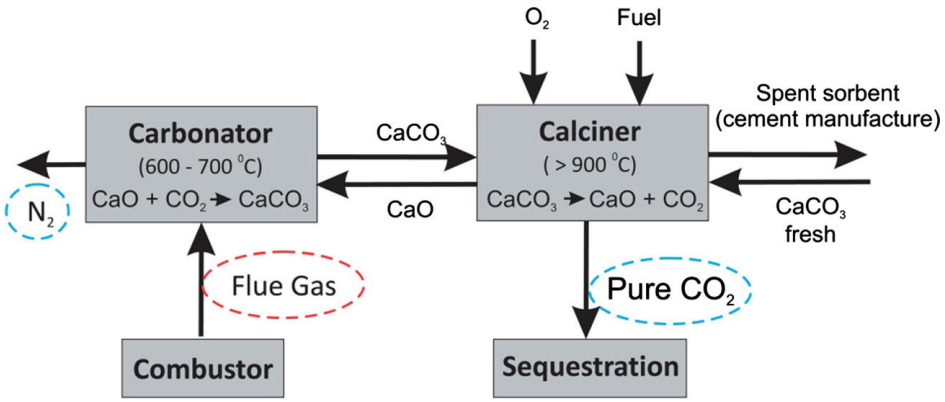

Figure 2.9: Calcium Looping Process Diagram [110]

Calcium looping has shown promise as a carbon capture technique. CaL can often achieve good carbon capture efficiencies, with literature indicating CCE upwards of 90% is possible [111]. A small pilot project was conducted on a 1.7 MW_{th} power plant that supported capture rates of 90% while operating under steady-state conditions [28]. However, those studies were conducted on coal-fired fuel gas compositions with higher CO_2 concentrations. The overall carbonation reaction depends on the partial pressure of CO_2 in the flue gas, so lower concentrations require that the carbonation process is operated at lower temperatures [112]. It is preferable for the carbonation and calcination temperatures to be as close as possible to minimize the fuel requirements of heating the $CaCO_3$ during the calcination process. This results in an increased energy penalty for NGCC CaL application to achieve 90% CCE. The energy penalty of CaL for NGCC power plants ranges from 7.4% - 15.5%, although this can be improved with exhaust gas recirculation [113],[112]. This indicates CaL may require more energy than traditional 30 wt% MEA carbon capture by amine absorption, as discussed in Section 2.3.1. The reduction in plant thermal efficiency is generally driven by the large energy requirements to operate the carbonator and calciner. Additionally, most calciners used are oxy-calciners, which require an air separation unit to provide concentrated oxygen [114]. This further reduces the plant's thermal efficiency. Future developments are underway to improve the thermal efficiency of this process, including methods such as utilizing supercritical steam cycles, integration with chemical looping combustion, and improvements to sorbent capacity [115],[116]. Overall, CaL is making notable improvements, but it is currently less technically mature and less suitable for carbon capture at NGCC power plants than conventional amine absorption.

2.3.6 Summary Comparison

The post-combustion carbon capture technologies previously reviewed are summarized in Table 2.3. The comparative table covers key metrics for each technology, giving ranges in areas of uncertainty.

Table 2.3: Comparison of Carbon Capture Technologies for NGCC Power Plants

Technology	**Steady-state Capture Efficiency (%)**	**Energy Penalty (%)**	**Retrofitting Complexity**	**Cost ($/ton CO2)**[1]	**Technical Maturity Level**	**Operational Challenges**	**References**
Absorption	85-95	6-14	Low	48-70	2-9[2]	Corrosion, solvent loss, regeneration cost	[49], [71], [117], [118]
Adsorption	81-90	5-15	Low	51-100	5-9[3]	Adsorbent degradation, water sensitivity, regeneration cost	[117], [32], [83], [85],[119]
Membranes	70-90	7-24	Low	90-122	2-7[4]	Membrane fouling, permeance/selectivity issues, scalability, requires higher CO_2 concentrations	[33], [87], [117],[120]
Cryogenics	85-99	25-30	Moderate	50-96	3-6	High energy requirement, technical immaturity, requires higher CO_2 concentrations, water sensitivity	[121], [105], [106], [117]
Calcium Looping	up to 90	7.4 - 15.1	Moderate	>90	5-7	High temperature, sorbent degradation and capacity	[111], [109], [122], [28][123]

2.3.7 Non-Steady State Carbon Capture

To facilitate the modeling process, this thesis elects to focus on absorption-based CCS. As illustrated in Table 2.3, absorption-based CCS remains the leading candidate for retrofitting NGCC power plants. It is a significantly more mature technology than most other post-combustion methods, with continuous improvements underway in solvent performance. It offers a high capture efficiency under steady-state conditions, and it is capable of handling the very large quantities of gas required for natural gas power plants. Absorption-based CCS also provides a relatively low level of complexity associated with retrofitting equipment and is highly competitive on costs and energy penalties with other techniques. Furthermore, given

[1] Excludes transportation and storage costs

[2] Amine-based and physical solvent-based absorption are TRL 9; ionic liquids and other emerging solvent are TRL 2-7

[3] PSA/VSA adsorption is TRL9. TSA adsorption is TRL 7. Other separation techniques not considered.

[4] Gas separation membranes are TRL 9 for natural gas sweetening but lower for power plant carbon capture

the technical immaturity of most other technologies, there is extremely limited literature on the use of adsorption, membranes, cryogenics, and calcium looping systems at a pilot scale or larger for NGCC plants. The studies on these technologies that were discovered in the literature search are mostly limited to modeling studies, lab tests, or small studies using flue gas that more closely represents a coal-fired power plant with a higher CO_2 concentration.

The literature search process found few studies that focused on understanding the relationship between carbon capture efficiency and startup and shutdown plant operations. The most comprehensive report on this subject was published in the 2022 International Energy Agency Greenhouse Gas (IEAGHG) technical report, Start-up and Shutdown Protocol for Natural Gas-fired Power Stations with CO_2 Capture [72]. This thorough report will serve as the basis for the start-up penalty assumptions used in the modeling work to follow. The study was conducted at Technology Centre Mongstad in Norway using flue gas from a natural gas-fired power plant. It utilized the CESAR-1 solvent, consisting of AMP and Piperazine (PZ). The factors investigated in that study that are relevant to this thesis are the differentiation between carbon capture unit performance during hot start-ups and cold start-ups and the capture performance during steady-state and shutdown operations. The results suggest that CCE is not materially impacted by changes in load once steady-state conditions are reached. NGCC plants are generally flexible enough to operate at high capture efficiencies during load-following conditions as long as the CO_2 capture unit is coordinated with changes in load. Similarly, CCE is relatively unchanged by shutdown operations, although this is highly contingent upon the energy source used to generate steam for solvent regeneration. Regenerating the solvent during shutdown operations can result in increased heat rates or energy penalties. However, a tangible reduction in CCE and an increase in heat rate was observed during cold start-up operations. In cold start-ups, the capture rate is initially quite high, assuming the solvent is lean to begin with. The capture rate rapidly decreases as the solvent undergoes rich loading and is unable to be regenerated quickly enough due to insufficient heat. Upon reaching target reboiler temperatures, the capture rates recover and trend upwards again. This behavior is illustrated in Figure 2.10.

To simplify the capture rate behavior observed in the literature, a linear approximation is used. A linear approximation ensures that the modeling work performed in Chapter 3 and Chapter 4 avoids encountering quadratic formulations, reducing the resources required to solve the optimization problem. Figure 2.11 shows the linear approximation of the instantaneous carbon capture rate compared against the observed data. Note that the observed data is also an approximation of the real data shown in Figure 2.10 as the raw data was unavailable. The linear approximation performs adequately, underestimating the early capture rates while overestimating the capture rates after one hour, eventually converging on the observed data. Literature indicates most cold start-ups last approximately three hours until the plants reach steady-state conditions. The cumulative capture rate over time is calculated over the three-hour window to ensure the linear approximation sufficiently represents the observed behavior. Figure 2.12 indicates that both the observed data and the linear approximation capture approximately 77% of the CO_2 emissions during the cold start-up operation. This validates the linear approximation as a suitable representation of cold start-up behavior over the three-hour window. A summary of the findings of the literature search highlighting the transient duration, capture rate impacts, and heat rate impacts for various operating modes is shown in Table 2.4. The associated capture rate impact and additional reboiler

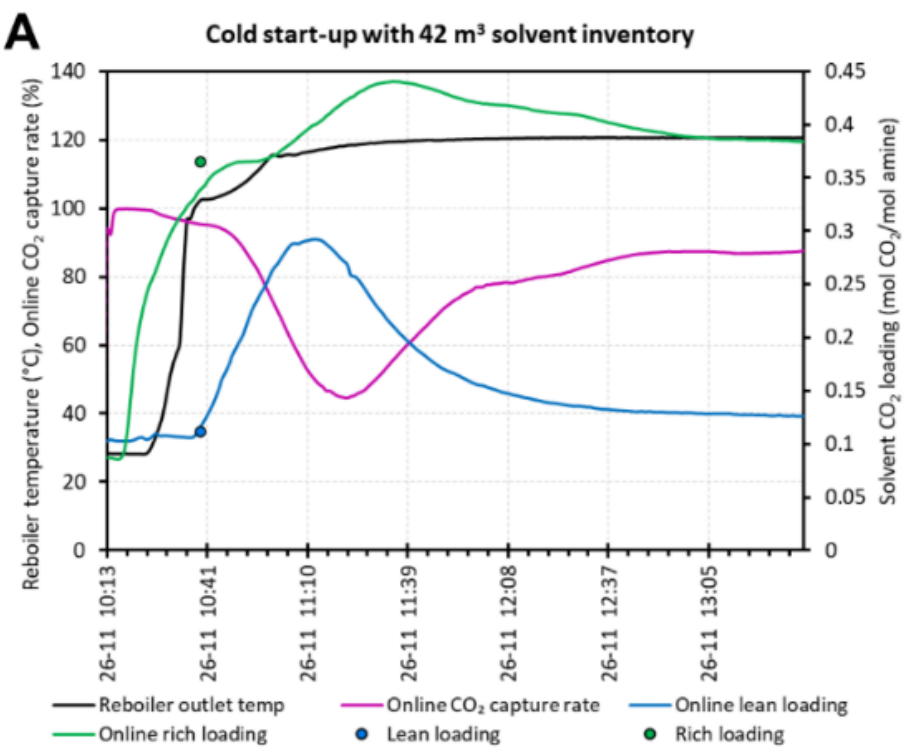

Figure 2.10: Pilot Plant Data for Cold Start-up Operations [72]

energy consumption are only in effect during the transient period. Note that auxiliary boiler emissions are excluded.

Table 2.4: Impact of Operating Modes on Capture Rate and Heat Rate

Operating Mode	**Transient Duration**	**Relative Capture Rate Reduction**	**Reboiler Duty MJ/kgCO_2**
Cold Start (>8 hours)	3 hours	18%-22%	4.9
Hot Start (<8 hours)	< 1 hour	0%	3.7
Shutdown	< 1 hour	0%	5.63
Load-following	0 hours	0%	0

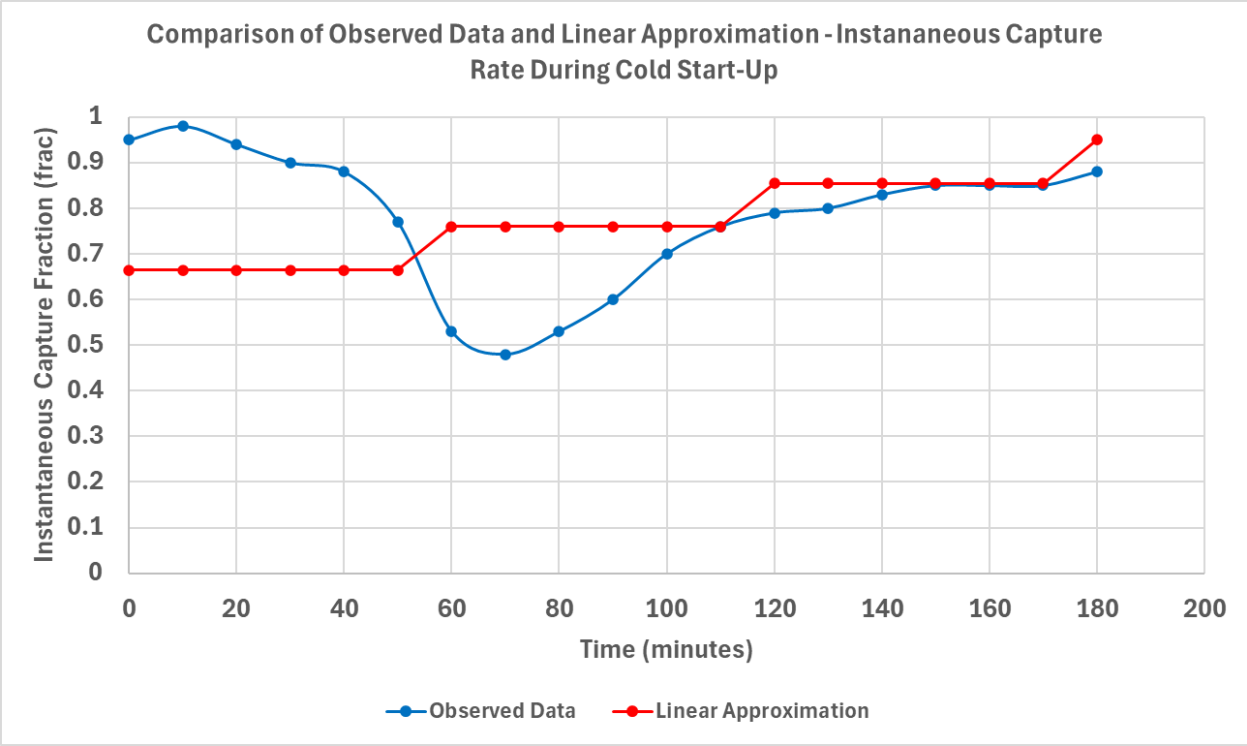

Figure 2.11: Comparison of Observed Data with Linear Approximation Used in Model - Instantaneous Capture Rate

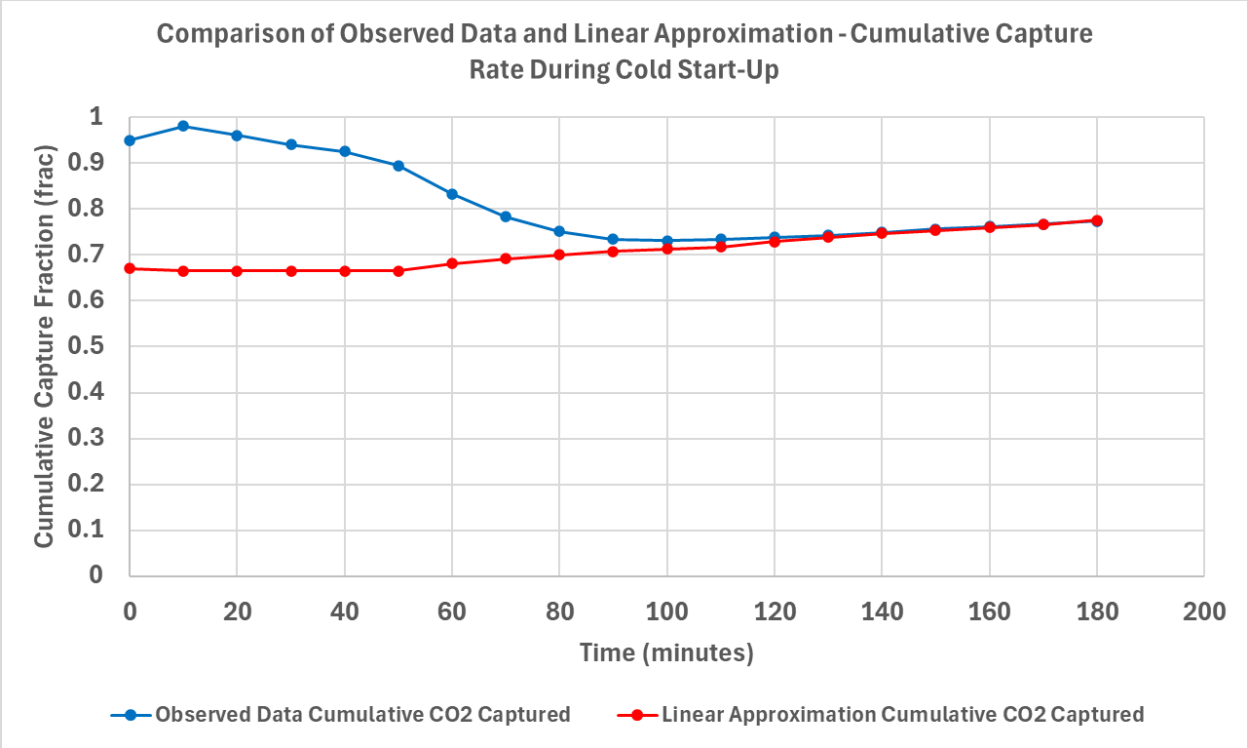

Figure 2.12: Comparison of Observed Data with Linear Approximation Used in Model - Cumulative Capture Rate

Chapter 3

GenX Model Overview and Validation

This chapter of this thesis describes the tools and techniques used to evaluate the impact of the findings from the literature search process using optimization modeling. Section 3.1 describes the GenX model, highlighting key uses, parameters, inputs, and outputs. Next, a basic GenX model is generated to test the impact of capture rate penalties, start-up conditions, and heat rate impacts on two simple systems. Last, a set of equations is defined that creates a modified model that seeks to replicate the advanced penalties model results.

3.1 GenX Overview

GenX, a "configurable electricity capacity expansion model" developed by the Massachusetts Institute of Technology and Princeton University, was used to evaluate different scenarios [20]. GenX is an adaptable, open-source model developed in Julia that is designed to optimize the operation and investment decisions in power systems. It aims to determine the least-cost pathways for system development given various constraints. The model is particularly useful for examining situations with significant levels of renewable energy sources, energy storage, fluctuating demand, and other emerging technologies, such as post-combustion carbon capture. GenX utilizes a constrained mixed integer or linear programming framework to solve optimization problems. It is capable of simulating both short-term operational decisions and long-term investment choices within the electricity grid. Various inputs, such as demand profiles, emissions information, technology costs, resource availability, and others, are evaluated. The model also incorporates environmental, reliability, policy, and other constraints. GenX then identifies the optimal mix of generation, storage, and transmission resources to minimize the system cost and meet demand. Figure 3.1 displays the range of potential configurations for GenX along three key axes. GenX typically requires five key inputs and up to eight secondary, optional inputs. The first required input is fuel data, describing the fuel type, associated emissions intensity, and fuel price over time. For this analysis, it mainly refers to natural gas, via NGCC power plants, with and without CCS. The second input describes the network data system. The network data provides the number of model zones, the transmission flows, and existing capacities. Third, demand data is required. This includes hourly electricity demand data and penalties for non-served energy. Next, data on each type of generator, such as solar, wind, or natural gas, is incorporated into the model.

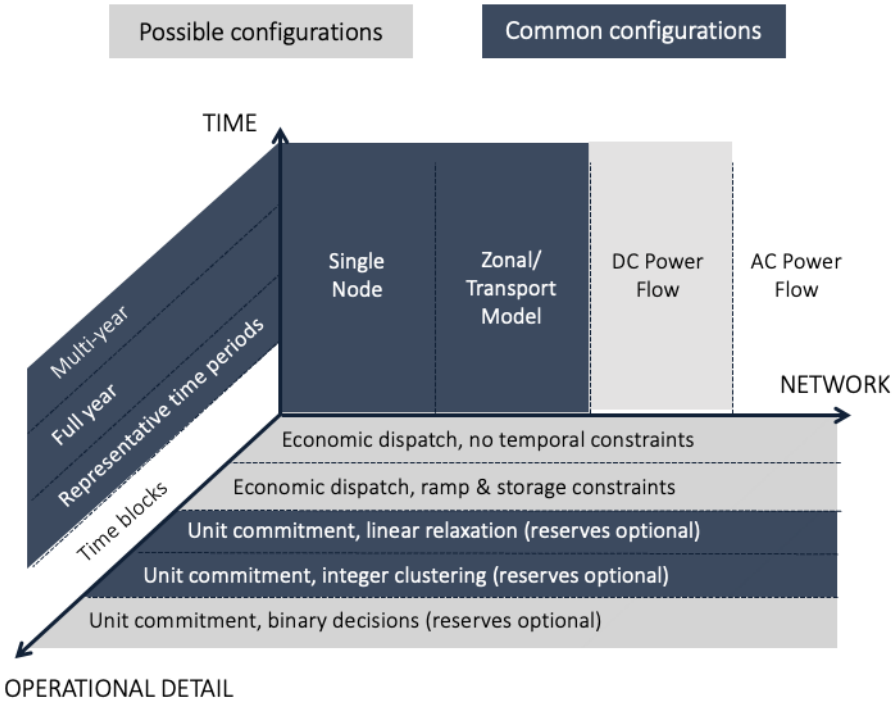

Figure 3.1: Potential GenX Configuration Options [20]

Each generator is assigned associated cost, capacity, and performance values. The model also includes information on generator variability, specifying the time-series availability and capacity factor of each resource type. Finally, the model can be given additional optional inputs, including CO_2 emissions limits, energy share requirements, operational reserve requirements, capacity reserve margin requirements, minimum regional technology capacity requirements, variable renewable energy (VRE) availability for co-located resources, and hydrogen demand. The general process flow with selected parameters is shown in Figure 3.2.

Additionally, GenX provides flexibility when determining clustering methods for thermal plant unit commitment and start-up and shutdown decisions. Users can elect to use integer clustering, linearized clustering, or no clustering. Integer clustering for thermal power plant unit commitment groups thermal plants into clusters where the commitment status and the output levels are represented by integer variables. This creates an exact representation, as all units within the integer cluster will be treated as online or offline. However, it can be much more computationally expensive than linearized clustering. In linearized clustering, the commitment and dispatch decisions are approximated using continuous variables rather than discrete integers. This simplifies the optimization and greatly speeds up model runtime. Beyond unit commitment, GenX also incorporates time domain reduction as a second clustering method for time-series data like demand and VRE availability. This setting breaks down the comprehensive time-series dataset into a smaller subset of representative periods and uses those in the optimization algorithm to decrease the required computational resources. For a yearly model, each representative period contains 8,760 time-steps due to the hourly format of the data. Representative periods are determined using k-means clustering,

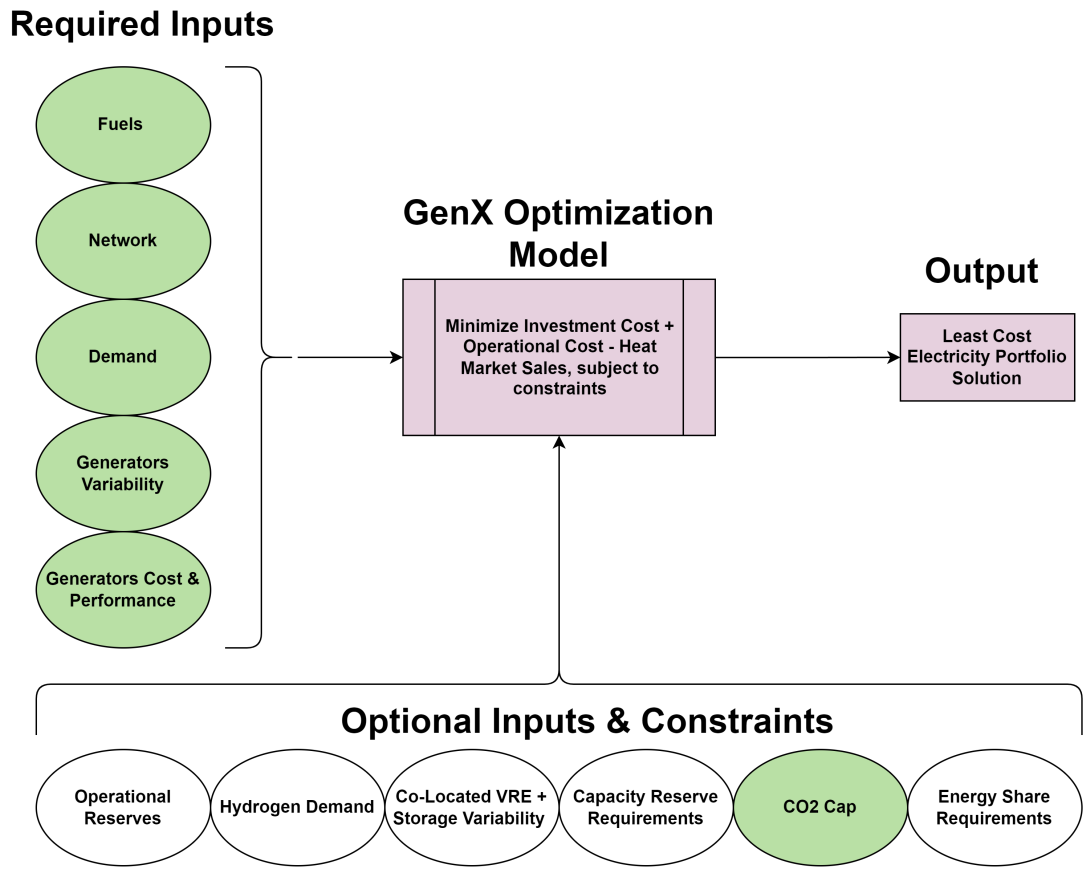

Figure 3.2: Graphical View of GenX Inputs, Constraints, and Outputs. Inputs used in this analysis are highlighted in green.

an optimization method that creates centroids and clusters data based on the distance of each individual point from the center of the cluster, as seen in Equation 3.1.

$$\arg\min_{S} \sum_{i=1}^{k} \sum_{x \in S_i} \|x - \mu_i\|^2 \tag{3.1}$$

GenX can be forced to include extreme periods, requiring k-means clustering to include the highest and lowest points and ensuring outliers are used. This is critical when dealing with energy demand and supply due to the nature of VRE and peaking demand. Periods with maximum load, minimum solar, and minimum wind are automatically included as extreme periods. Additional information on GenX temporal resolution and time domain reduction is addressed in Mallapraganda et al. [124]. The model can apply time-domain reduction via k-means clustering to demand data, wind data, solar data, and fuel prices.

3.2 Default GenX Start-up Calculations

To test the theoretical impacts of NGCC start-up and shutdown behavior, modifications were made to the base GenX code to incorporate additional carbon capture rate and heat rate penalties during cold start-ups. Recall that with unit commitment activated ($y \in UC$), GenX tracks the number of thermal plants that are committed (online), off (tracked implicitly as not online), starting up, and shutting down for each hour. The number of start-ups is governed by a fairly standard set of unit commitment constraints, illustrated in Equation 3.2, Equation 3.3, and Equation 3.4. These constraints ensure that the total number of committed, starting up, and shutting down units is less than or equal to the total number of units in the fleet. Ramp rates, minimum stable power outputs, and other operating costs are also taken into consideration. The commitment state constraints are shown in Equation 3.5 and Equation 3.6 [20]. These ensure the proper accounting of start-ups and shutdowns over time.

Variable Definitions:

- $\nu_{y,z,t}$: Commitment state of generator cluster y in zone z at time t.
- $\chi_{y,z,t}$: Number of units started in generator cluster y in zone z at time t.
- $\zeta_{y,z,t}$: Number of units shut down in generator cluster y in zone z at time t.

Parameter Definitions:

- $\Delta_{y,z}^{\text{total}}$: Total installed capacity of generator cluster y in zone z.
- $\Omega_{y,z}^{\text{size}}$: Unit size of generator cluster y in zone z.

Capacity Constraints:

$$\nu_{y,z,t} \leq \frac{\Delta_{y,z}^{\text{total}}}{\Omega_{y,z}^{\text{size}}}, \quad \forall y \in UC, \forall z \in Z, \forall t \in T \tag{3.2}$$

$$\chi_{y,z,t} \leq \frac{\Delta_{y,z}^{\text{total}}}{\Omega_{y,z}^{\text{size}}}, \quad \forall y \in UC, \forall z \in Z, \forall t \in T \tag{3.3}$$

$$\zeta_{y,z,t} \leq \frac{\Delta_{y,z}^{\text{total}}}{\Omega_{y,z}^{\text{size}}}, \quad \forall y \in UC, \forall z \in Z, \forall t \in T \tag{3.4}$$

Commitment State Constraints:

$$\nu_{y,z,t} = \nu_{y,z,t-1} + \chi_{y,z,t} - \zeta_{y,z,t}, \quad \forall y \in UC, \forall z \in Z, \forall t \in T^{\text{interior}} \tag{3.5}$$

$$\nu_{y,z,t} = \nu_{y,z,t+\tau_{\text{period}}-1} + \chi_{y,z,t} - \zeta_{y,z,t}, \quad \forall y \in UC, \forall z \in Z, \forall t \in T^{\text{start}} \tag{3.6}$$

Start-ups appear in the GenX objective function as additional start-up costs and as additional start-up emissions. In the default GenX configuration, start-up penalties are only applied in the first hour following start-up, modeled as increased fuel consumption. The penalties are applied after all start-ups, regardless of the duration the unit was offline. No distinction is made between hot and cold start-ups. Therefore, there is no incentive for GenX to prioritize hot start-ups. The default GenX model accounts for start-up costs as shown in Equation 3.7, where the t subscript indicates the costs are calculated separately for each time-step.

$$C_t^{\text{startup}} = N_t^{\text{starts}} \times S \times \left(F_t \times F^{\text{startup}} + C^{\text{fee}}\right) \tag{3.7}$$

where:

- C_t^{startup} is the startup cost at time t ($)
- N_t^{starts} is the number of starts at time t
- S is the unit size (MW)
- F_t is the fuel cost at time t ($/MMBTU)
- F^{startup} is the startup fuel required per start (MMBTU/MW/start)
- C^{fee} is the startup fee, applied to each thermal plant or clustered fleet of plants in the same zone. This includes additional maintenance, staff, and other costs required for start-ups ($/MW/start)

Under this equation, the start-up costs are scaled to the unit size, not the actual unit output during the first hour of operation. This results in a unit that comes online at 50% power in the first hour incurring the same start-up costs as one coming online at 100% power. This is a simplifying assumption made in order to reduce the computational burden. The

more precise formulation would require multiplying the power output of the generators and the number of generators starting in that hour, making the resulting problem quadratic and much more difficult to solve. Further, the unit is required to pay variable O&M costs and fuel costs separately, based on its output power. Thus, the error associated with the linearized approximation is not too large.

The second area where start-ups impact the objective function is in the emissions calculations. In the default version of GenX, emissions are calculated via Equation 3.8. Similar to the start-up costs, the start-up emissions are scaled to the total unit size, not the actual output in the first hour.

$$E_t^{\text{startup}} = N_t^{\text{starts}} \times S \times E^{\text{fuel}} \times F^{\text{startup}} \times (1 - CCR^{\text{steady}}) \tag{3.8}$$

where:

- E_t^{startup} is the startup emissions at time t
- N_t^{starts} is the number of starts at time t
- S is the unit size
- E^{fuel} is the fuel emissions per unit of fuel, based upon pre-CCS emissions intensity (tonne CO_2/MMBTU)
- F^{startup} is the startup fuel required per start
- CCR^{steady} is the steady state capture rate

3.3 Advanced Start-up Capture & Heat Rate Penalties

In attempting to improve this model, the same challenge faced by the original designers is encountered: avoiding a quadratic formulation. Two options are available to avoid this scenario. First, the penalties can be scaled to the maximum output, as is currently implemented in GenX. Alternatively, the penalties can be scaled to the median possible output of the plant. For a plant with an output range between 50%-100%, it might be more accurate to assume production at 75% power during the start-up transient period. However, there is no guarantee that any given plant or clustered fleet will produce power across its entire possible range. A peaker unit, for example, is likely to produce either 0% or 100% of its output, resulting in an average of 100% when operating. Therefore, penalties are scaled to unit size to facilitate easier comparison with the existing GenX method.

The model introduces cold starts and hot starts. The number of hot starts is a variable, while the number of cold starts is a derived expression. The number of hot starts must be less than the number of hot units in shutdown, and each unit remains hot for τ hours after shutdown. The model assumes that hot shutdown units are always preferred over cold shutdown units whenever available. The hot start-ups are governed by the simple constraints shown in Equation 3.9, with the number of units available for hot start-ups calculated in Equation 3.10.

$$0 \leq N_t^{\text{hot}} \leq N_t^{\text{total}} \tag{3.9}$$

$$N_t^{\text{hot}} \leq \sum_{t'=1}^{\tau} \left(N_{t-t'}^{\text{shutdown}} - N_{t-t'}^{\text{hot}} \right) \tag{3.10}$$

where:

- N_t^{hot} is the number of hot starts at time t
- N_t^{total} is the total number of starts at time t
- $N_{t-t'}^{\text{shutdown}}$ is the number of shutdowns at time $t - t'$
- τ is the duration of time a unit remains hot after shutting down

As previously mentioned, the number of cold start-ups is derived from the total number of start-ups and the number of calculated hot start-ups, as shown in Equation 3.11.

$$N_t^{\text{hot}} + N_t^{\text{cold}} = N_t^{\text{total}} \tag{3.11}$$

Next, the existing formulation for start-up costs and start-up emissions is modified so that the system is encouraged to maximize the number of hot start-ups whenever possible. The aforementioned literature addressed in Chapter 2 provides the foundation for detailing the impact of start-up operations on carbon capture rates and heat rates. A modified set of equations is created, utilizing advanced carbon capture rate and thermal heat rate penalties during cold start-up operations. Penalty parameters are introduced for heat rate, χ, and carbon capture rate, ϵ. These parameters make the heat rate and carbon capture rate χ and ϵ percent worse, respectively, immediately following cold start-up before linearly returning to steady state value over the following τ hours. After t' hours, the heat rate of the unit is calculated by Equation 3.12. Note that t' ranges from 0 to $T - 1$. Thus, as t' increases, the transient heat rate gets closer to the steady state heat rate. At T hours, the transient heat rate and steady-state heat rate are equivalent.

$$H_{t'}^{\text{transient}} = H^{\text{steady}} \times \left(1 + \chi \left(1 - \frac{t'}{T} \right) \right) \tag{3.12}$$

where:

- $H_{t'}^{\text{transient}}$ is the transient heat rate at time t'
- H^{steady} is the steady state heat rate
- χ is a penalty scaling factor to worsen heat rate
- t' is the specific time period within the transient phase
- T is the total duration of the transient phase

In order to calculate only the additional fuel used due to start-up, the steady-state rate must be subtracted, resulting in the net heat rate penalty due to start-ups shown in Equation 3.13.

$$P_t^{\text{heat rate startup}} = \chi \left(1 - \frac{t'}{T}\right) \times H^{\text{steady}} \tag{3.13}$$

With the above equations defined, the start-up costs can be determined using Equation 3.14.

$$C_t^{\text{startup}} = N_t^{\text{cold}} \times S \times C^{\text{fee}} + S \times \sum_{t'=0}^{T-1} N_{t-t'}^{\text{cold}} \times P_{t-t'}^{\text{heat rate startup}} \times F_{t-t'} \tag{3.14}$$

where:

- C_t^{startup} is the startup cost at time t
- N_t^{cold} is the number of cold starts at time t
- S is the unit size
- C^{fee} is the startup fee
- T is the duration of the transient phase
- $P_{t-t'}^{\text{heat rate startup}}$ is the startup heat rate penalty at time $t - t'$
- $F_{t-t'}$ is the fuel cost at time $t - t'$

A similar approach is utilized to calculate the transient emissions rate during cold start-up operations, shown in Equation 3.15.

$$CCR_{t'}^{\text{transient}} = CCR^{\text{steady}} \times \left(1 + \epsilon \left(\frac{t'}{T} - 1\right)\right) \tag{3.15}$$

where:

- $CCR_{t'}^{\text{transient}}$ is the transient capture rate at time t'.
- CCR^{steady} is the steady state capture rate.
- ϵ is a penalty scaling factor to worsen capture rate
- t' is the specific time period within the transient phase.
- T is the total duration of the transient phase.

The transient emission rate and emissions rate penalty above the steady-state rate can be calculated using Equation 3.16, Equation 3.17, Equation 3.18, and Equation 3.19. The transient emission rate at time t' is given by:

$$E_{t'}^{\text{transient}} = H_{t'}^{\text{transient}} \times E^{\text{fuel}} \times \left(1 - CCR_{t'}^{\text{transient}}\right) \tag{3.16}$$

where:

- $E_{t'}^{\text{transient}}$ is the transient emission rate at time t'.
- $H_{t'}^{\text{transient}}$ is the transient heat rate at time t'.
- E^{fuel} is the fuel emissions per unit of fuel.
- $CCR_{t'}^{\text{transient}}$ is the transient capture rate at time t'.

The steady-state emission rate is calculated as:

$$E^{\text{steady}} = H^{\text{steady}} \times E^{\text{fuel}} \times \left(1 - CCR^{\text{steady}}\right) \tag{3.17}$$

where:

- E^{steady} is the steady state emission rate.
- H^{steady} is the steady state heat rate.
- CCR^{steady} is the steady state capture rate.

The transient emission rate penalty, which is the difference between the transient and steady-state emission rates, is:

$$P_{t'}^{\text{emissions transient}} = E_{t'}^{\text{transient}} - E^{\text{steady}} \tag{3.18}$$

where:

- $P_{t'}^{\text{emissions transient}}$ is the transient emission rate penalty at time t'.

Thus, the total additional emissions due to startup are calculated as:

$$E_t^{\text{startup}} = S \times \sum_{t'=0}^{T-1} N_{t-t'}^{\text{cold}} \times P_{t-t'}^{\text{emissions transient}} \tag{3.19}$$

where:

- E_t^{startup} is the startup emissions at time t.
- S is the unit size.
- $N_{t-t'}^{\text{cold}}$ is the number of cold starts at time $t - t'$.

Therefore, by minimizing the number of cold start-ups by either reducing the total number of start-ups or preferentially utilizing hot start-ups, GenX will reduce the emissions and cost penalties at start-up conditions.

3.4 Carbon Capture Penalty Simplified Case

Prior to evaluating the impact of the start-up penalties on a real-world grid, the penalties were tested on simple models to determine the impact on system behavior. Two simplified models were created. Both models utilize the modified start-up penalties outlined in the previous section in addition to testing a case with no start-up penalties at all. Multiple parameters were varied to strengthen or weaken the impact of the start-up penalties, shown in Table 3.1. Emission intensity limits do not directly impact the start-up penalty calculations but do alter the system decisions and behaviors; thus, they were included as a variable to understand the system under different policy scenarios. The models were run using hourly time-steps for a period of one year.

Table 3.1: Operational Parameters and Changes

Parameter	**Values/Description**
Transient duration T	3 hours, constant
Time to cooldown τ	[1, 3, 6, 9, 12, 24, 36] hours
Heat rate change χ	[0, 5, 10, 15, 25, 30] % relative change
Capture rate change ϵ	[0, 5.26, 10.53, 15.79, 26.32, 31.58] % relative change
Emission intensity limit	[25, 30, 35, 40] gCO_2/kWh

3.4.1 Simple Solar and Natural Gas Model

The first model is a single zone, constant demand model that only includes solar PV and NGCC with CCS for generators and utilizes linearized clustering. The penalty for non-served energy is set at a very expensive value of $5,000,000/MWh, strongly encouraging the model to build capacity whenever feasible. In this model, the hourly availability of solar energy varies diurnally and seasonally but has a relatively consistent 12-hour cadence. Note that energy storage is not included in this simplified scenario. From running the models, it becomes immediately apparent that operating at an emissions intensity limit of 40 g/kWh results in a grid design that is exclusively natural gas. This is due to the NGCC with CCS energy intensity of baseload generation being approximately 37.76 g/kWh, therefore allowing the model to exclusively build nothing but gas plants instead of solar facilities. Despite solar facilities being cheaper to build, they are unable to meet overnight demand, so gas is always required. The solar plants built are driven by the emissions constraint more than the minimal cost objective. This trend is consistent: as emissions limits become more relaxed, there is a preference to utilize more gas for baseload generation. As emission limits become more strict, additional solar generation and less natural gas capacity are installed, as illustrated in Figure 3.3.

The second finding from the simplified solar model is that the cooldown period, τ, during which a unit can restart without incurring start-up penalties, does not materially differentiate

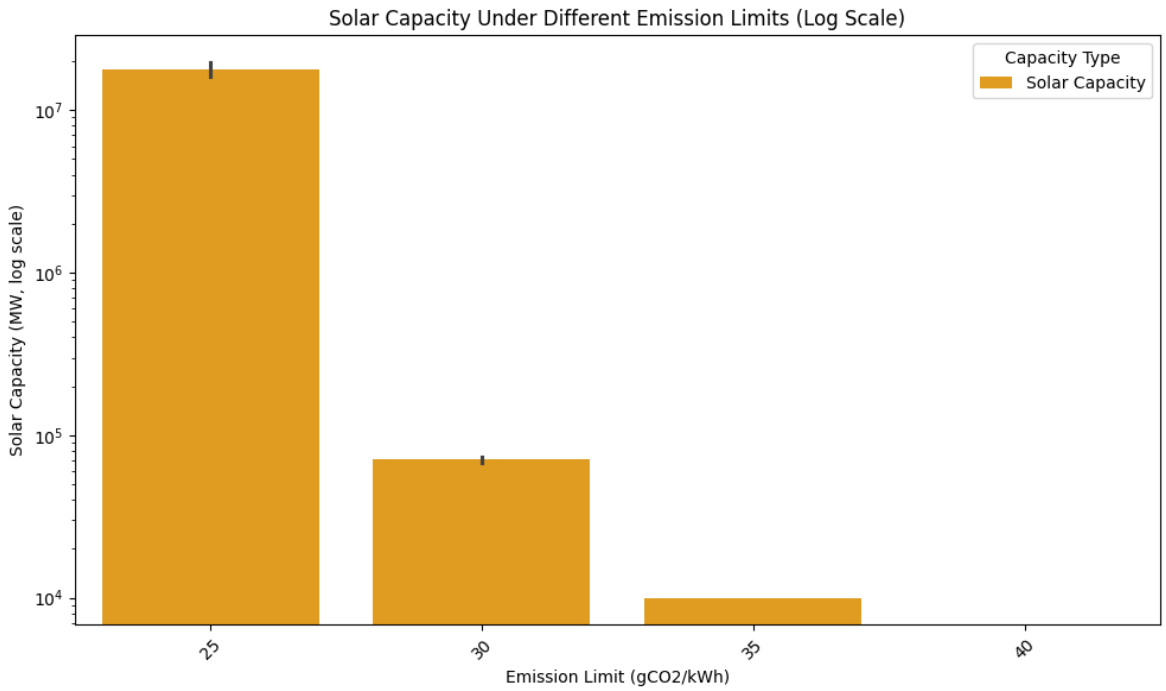

Figure 3.3: Installed Solar Capacity per Emissions Limit Constraint

scenarios when it is set to less than or equal to nine hours (τ<9). This is likely due to the fact that the diurnal solar availability dominates the start-up behavior penalties. In effect, the system has no available solar energy for 8-12 hours of the day, so a cooldown period of nine hours or less will rarely be able to achieve a hot start-up. The system essentially determines a very similar optimal solution and grid design for cooldown periods of one hour through nine hours, even under the harshest emissions limit and most severe heat rate and capture rate penalties. As the cooldown period for hot start-ups increases, a fairly broad distribution of hot start-up frequencies is observed. At 12 hours and beyond, the system does prioritize hot start-ups, as it now has available units under hot shutdown status that it can turn on without incurring penalties. The relationship between hot start-up frequency, cooldown period, and capture rate penalty is also investigated. The distribution of hot start-ups at capture rate penalties less than 15% ranges from 0% to approximately 80%, varying with the cooldown period. As capture rate penalties become more harsh and exceed 15%, the distribution of hot start-ups shifts markedly upwards, spanning from 60% to nearly 100%. It appears that a 15% capture rate penalty acts as the critical intersection where hot start-ups become significantly more important. This is most clearly illustrated in Figure 3.4. The data points that fall along the x-axis (zero hot start-ups) represent the cases where the advanced penalties logic is used but the cold start capture rate and heat rate penalties are set to zero.

The varying impacts of heat rate penalty and capture rate penalty are also studied under each emissions scenario. It appears that the capture rate penalty results in a moderately larger impact on total system cost than the heat rate penalty, especially under the more stringent emissions limits. At higher emissions limits, both penalties become less important

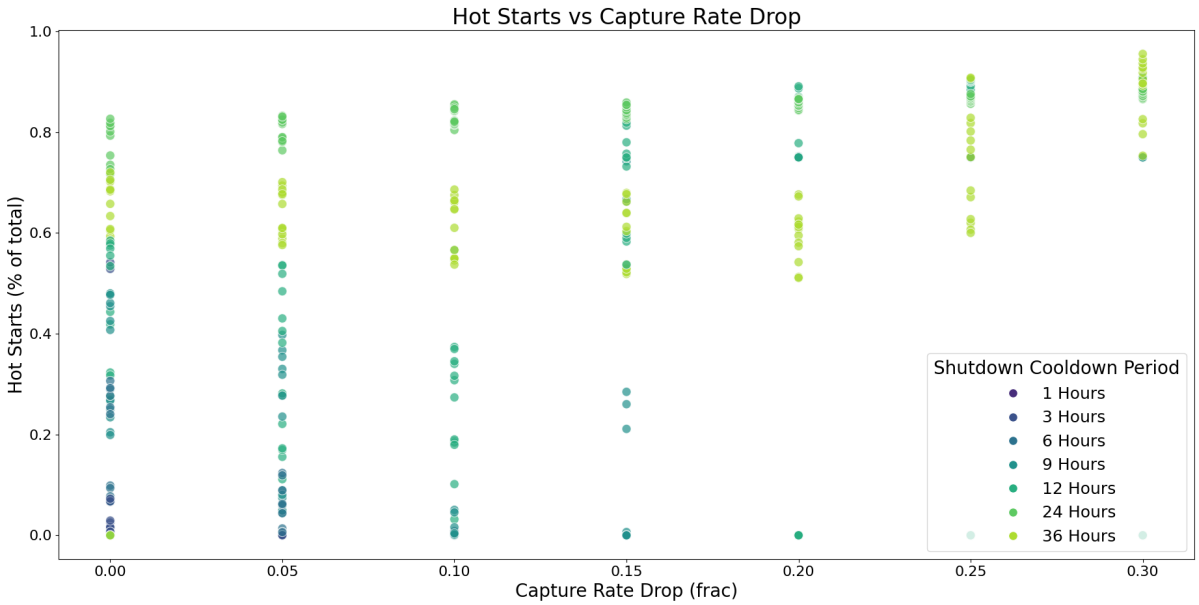

Figure 3.4: Hot Start-Ups vs Cold Start-Up Capture Rate Drop (25, 30 g/kWh emissions limit)

as the system is able to use gas more freely. As previously mentioned, under the 40 g/kWh emissions constraint, the system exclusively uses natural gas, so there is essentially zero variation in system behavior or cost. This analysis is displayed in Figure 3.5, comparing the trade-offs in heat rate and capture rate penalties while aggregating the mean system cost over all six cooldown periods. One can clearly observe an increasing trend in system cost associated with an increasing capture rate penalty. The heat rate penalty, however, displays a much more modest trend, only mildly increasing system cost with increased heat rate penalties.

Under the 25 g/kWh emissions intensity constraint, the impact of the start-up penalties is most noticeable. As the cold start-up capture rate penalty reaches 15% or greater, the system is unable to provide the required power while adhering to the emissions limit. This results in incurring the non-served energy penalty of $5,000,000/MWh, rapidly ballooning the total system cost. During periods where the cold start-up penalty is 15% or higher and the cooldown period for hot start-ups is 12 hours or less, the non-served energy penalty generally makes up over 90% of the total system cost. This is expected behavior given the extremely limited options presented in this simplified model, yet it indicates that the constraints and logic within the model are working appropriately. To better understand the impact of the advanced penalties, the results were compared to the model with default, one-hour penalties and the model with no start-up penalties at all, shown in Figure 3.6. The advanced penalty runs where the model was forced to pay the non-served energy cost due to strict emissions limits and harsh start-up penalties tend to dominate the data and skew the plot. As expected, the one-hour penalty and no penalties cases only show variance under different emissions constraints, as the other variables are not used in those models.

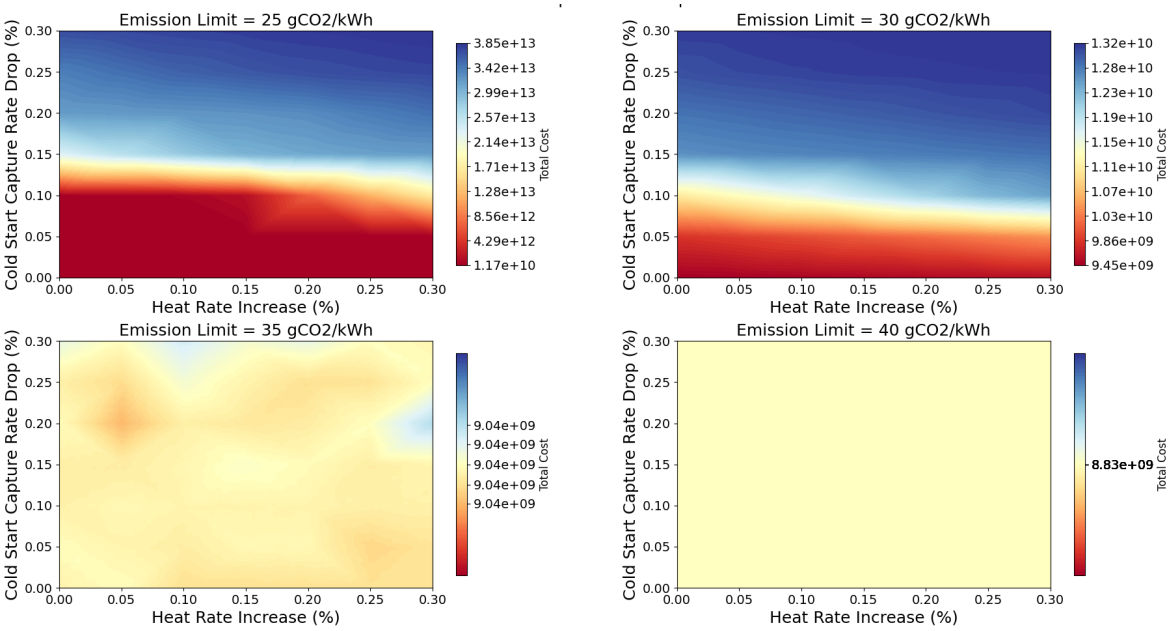

Figure 3.5: Heat Map of Heat Rate Penalty, Capture Rate Penalty, and Mean Total System Cost Under Each Emissions Intensity Limit.

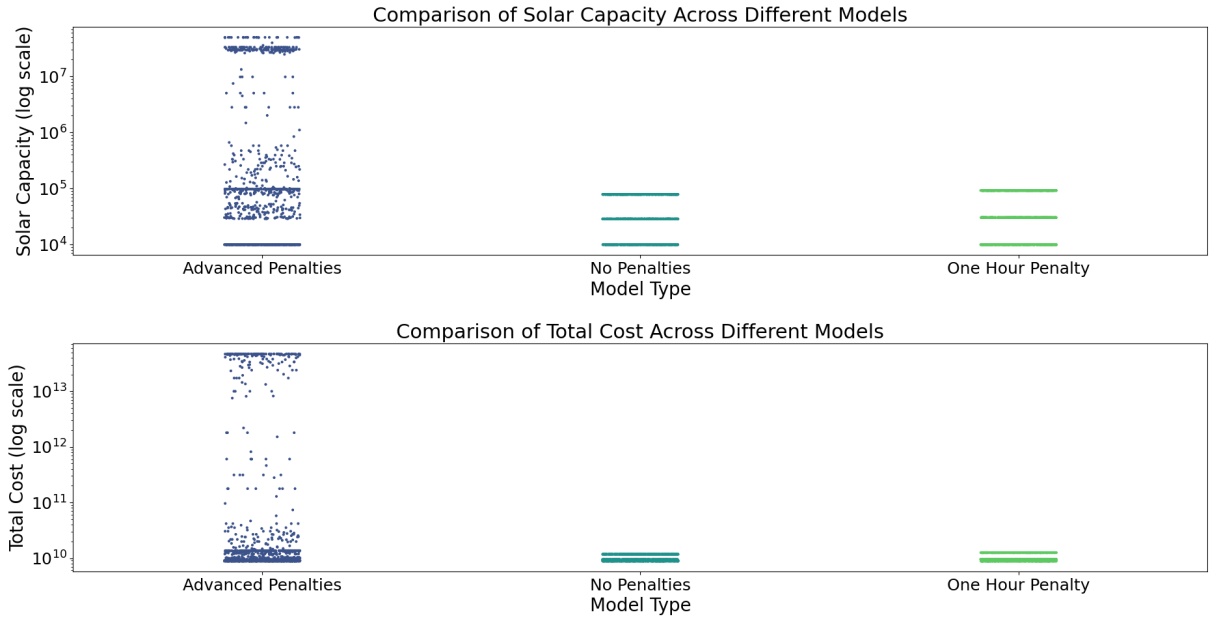

Figure 3.6: Comparison of Advanced Penalties, No Penalties, and One-Hour Penalties - Solar

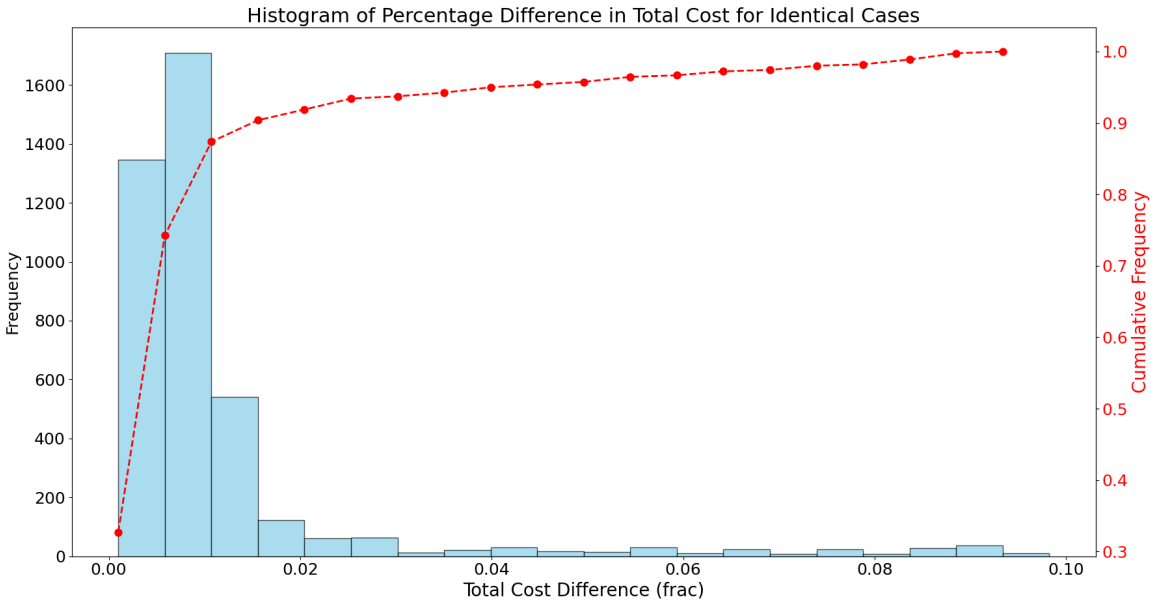

Figure 3.7: Percent Difference in Total Cost for Integer vs Linearized Clustering

3.4.2 Simple Onshore Wind and Natural Gas Model

Due to the diurnal nature of solar availability dominating the results of the cooldown variable and the large impact of the non-served energy component, a second simple model was created. Similar to the simple solar model above, the second model utilizes a single zone with constant demand. However, this model incorporates onshore wind instead of solar to better represent erratic resource availability. This ensures that brief and extended disruptions to wind power supply are incorporated to further evaluate the start-up penalties with natural gas plants, especially surrounding the impact of the cooldown period. This model was run twice, once using linearized clustering and once using integer clustering, to ensure comparable results. Overall, the linearized and integer clustering methods yielded similar results, with nearly 90% of cases having less than 2% difference in total cost. The vast majority of cases that did not fall within the 2% total difference were those that utilized the one-hour penalty logic. The one-hour penalty cases with the largest delta are generally those utilizing a combination of the strictest emissions limit coupled with the harshest capture rate and heat rate penalties. The advanced penalties models yield extremely similar total costs between linearized and integer clustering across all combinations of variables. The full breakdown is shown in Figure 3.7. As the linearized clustering method results in significantly faster run-time and is less computationally demanding, it will be used for the remaining analyses.

The first distinction from the solar model is that the onshore wind model builds some level of wind generation under all emissions scenarios. Whereas the solar model only used gas in the 40 g/kWh emissions limitation scenario due to the lack of solar availability overnight, the onshore wind availability is far more erratic, indicating some level of wind is optimal under all scenarios. Under each emissions scenario, similar levels of onshore wind and natural gas capacity are installed, shown in Figure 3.8.

As wind resource availability does not follow a cadence, it is expected that the cooldown

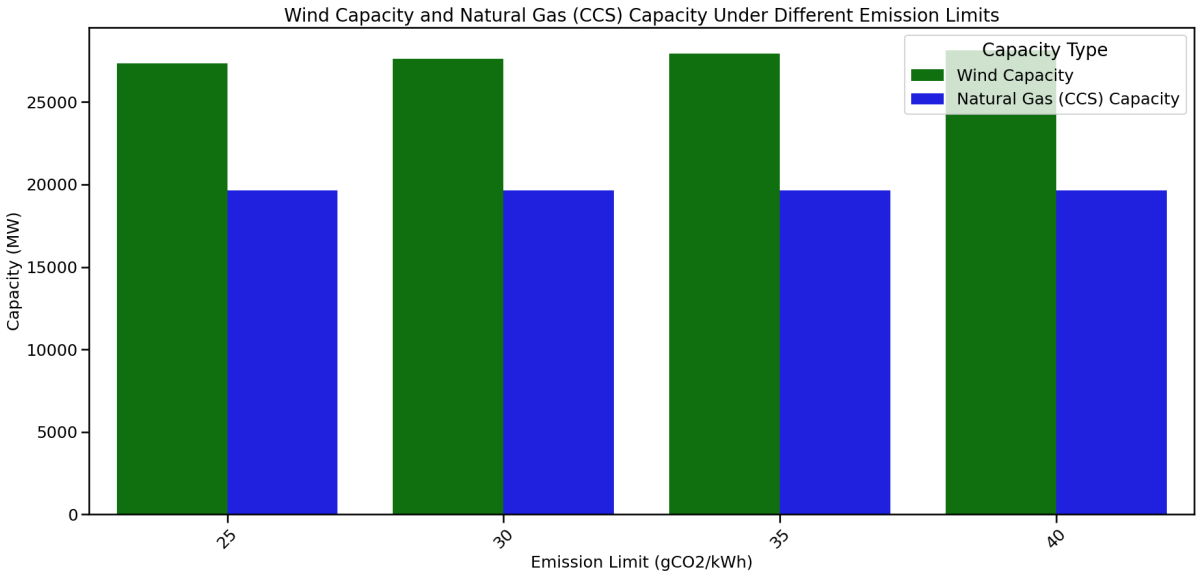

Figure 3.8: Onshore Wind and Natural Gas Capacity Under Each Emissions Intensity Limit

period allowing a plant to have a hot start-up without penalty will play a more significant role in determining the optimal solution. A tornado plot was generated to determine the relative impact of each variable on the total system cost. Figure 3.9 illustrates the relative impact of the variance for each variable on the total system cost. For the simple wind model, the cooldown period is the most significant variable driving total cost. The solar model did not show a significant impact for the cooldown period due to the diurnal nature of solar availability and the massive non-served energy penalties incurred during strict emissions scenarios. The wind model, however, has more irregular availability, leading to the cooldown period being more prominent and impacting total system cost. Further, the heat rate penalty actually has a larger impact on cost than the capture rate penalty, which is opposite to the solar model. The emissions limit has the least impact on total cost, as the system is able to generate enough capacity in all scenarios to avoid paying the non-served energy penalty. The relationship between increasing heat rate and decreasing cold start-up capture efficiency on total system cost is illustrated in Figure 3.10. The heat map suggests that the system is more sensitive to changes in heat rate than capture rate, especially heat rate penalties exceeding 15%. Capture rate penalties are more impactful during strict emission control scenarios, decreasing in importance as emissions limits increase. The two variables with the largest impact on system cost, cooldown period and heat rate, are also compared, with the results shown in Figure 3.11. In this comparison, it becomes clear how reducing the cooldown period in which a unit can have a hot start-up significantly increases system cost once that window falls below nine hours. Cooldown periods longer than 12 hours are able to largely offset the heat rate penalties, mainly due to the system utilizing more frequent hot starts under the more relaxed operational parameters.

Similar to the solar model, the wind model prioritizes hot start-ups as the emissions limits and capture rate and heat rate penalties become more severe. Large heat rate penalties

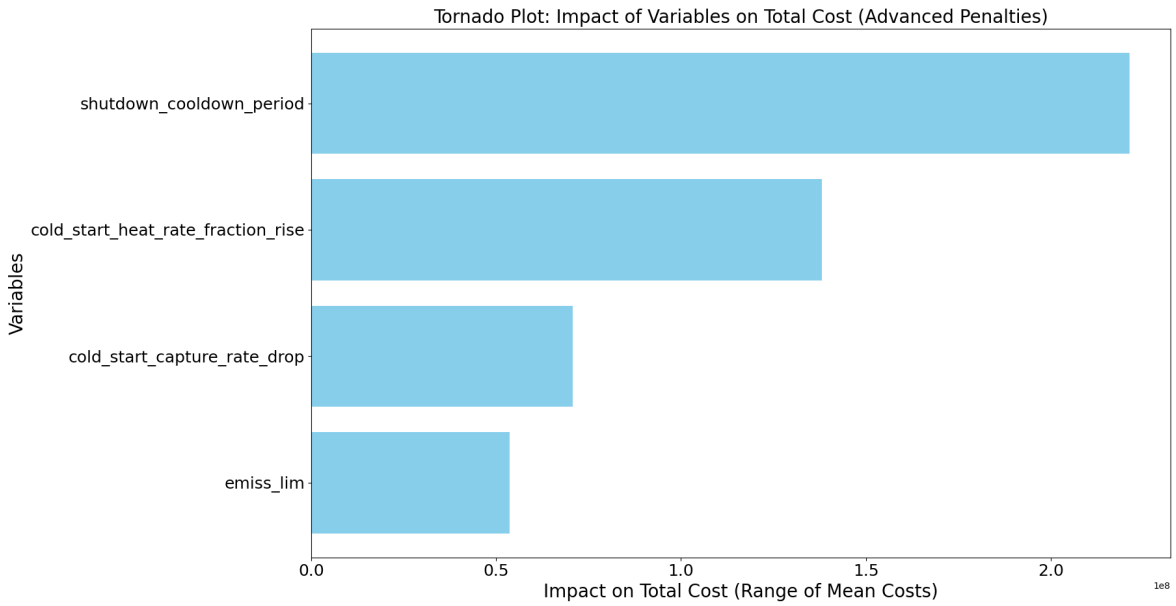

Figure 3.9: Tornado Plot for Simple Wind Model

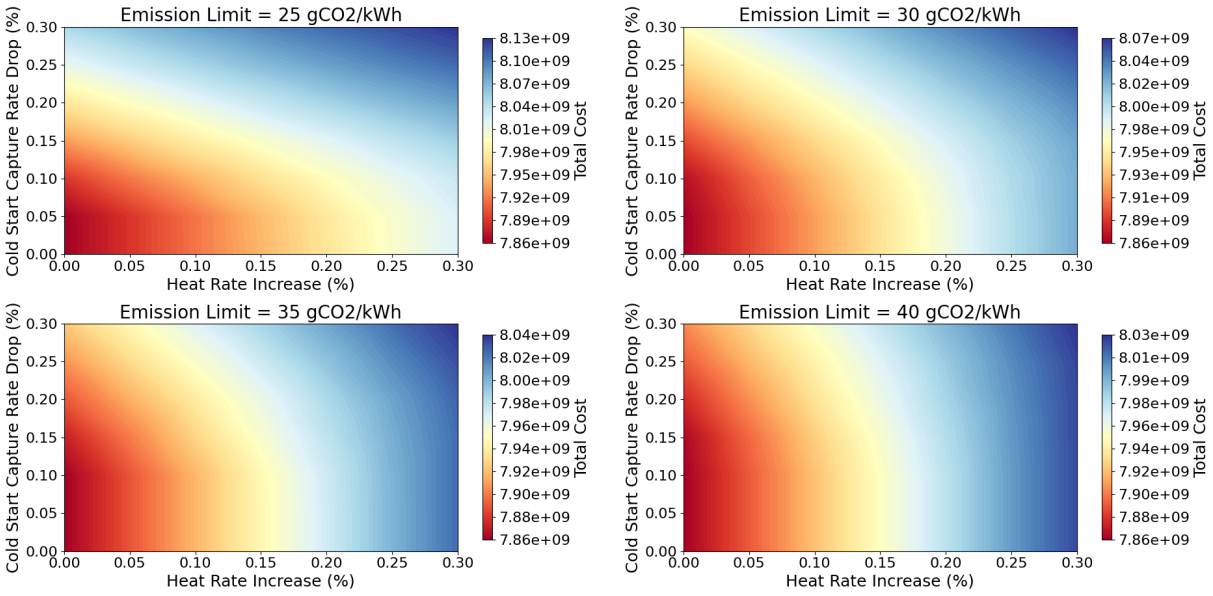

Figure 3.10: Heat Map of Heat Rate Penalty, Capture Rate Penalty, and Mean Total System Cost Under Each Emissions Intensity Limit - Wind

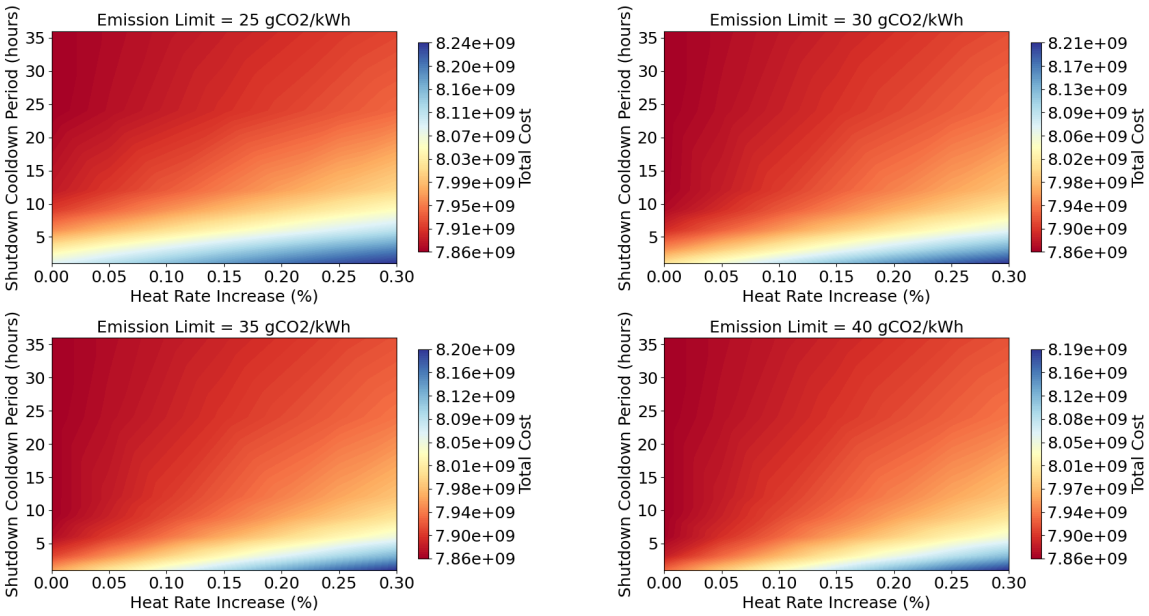

Figure 3.11: Heat Map of Heat Rate Penalty, Cooldown Period, and Mean Total System Cost Under Each Emissions Intensity Limit - Wind

result in the highest percentage of hot start-ups due to the significant impact on total cost. Large capture rate penalties also prioritize hot start-ups, though slightly less than heat rate penalties during long cooldown periods exceeding nine hours. Stricter emissions limits further encourage hot start-ups, although less so than either heat rate or capture rate penalties. This is demonstrated in Figure 3.12. Comparing the advanced penalties, one-hour penalty, and no penalties model shows that the system found a strong optimal solution for the one-hour and no penalties models. The same solution best satisfies the objective function under all four emissions intensity limits, as the optimal solution only results in an emissions intensity of 14.1 g/kWh and 17.2 g/kWh for the no penalties and one-hour penalty cases, respectively. Therefore, varying the emissions limits from 25 to 40 does not have an impact on the solution. As expected, the no-penalties model has the cheapest solution, followed by the one-hour penalty and, finally, the advanced penalties case. Interestingly, the one-hour penalty scenario builds less wind and more gas than the no-penalties case. This is possibly driven by the need for building additional gas plants and operating at higher capacity factors (41% vs 38%) in order to enable plants to run more continuously and avoid shutting down and the subsequent start-up penalties. The no penalties case also incorporates a 50% minimum power output constraint on thermal generators. The full results are displayed in Figure 3.13.

3.4.3 Modified One-Hour Penalty

After validating the advanced start-up penalties in the simple models and comparing the results against models using default one-hour fuel consumption penalties and no-penalties, a new model was created that seeks to replicate the advanced penalties behavior using a one-hour penalty as a proxy. To accomplish this, one must determine the value of the one-

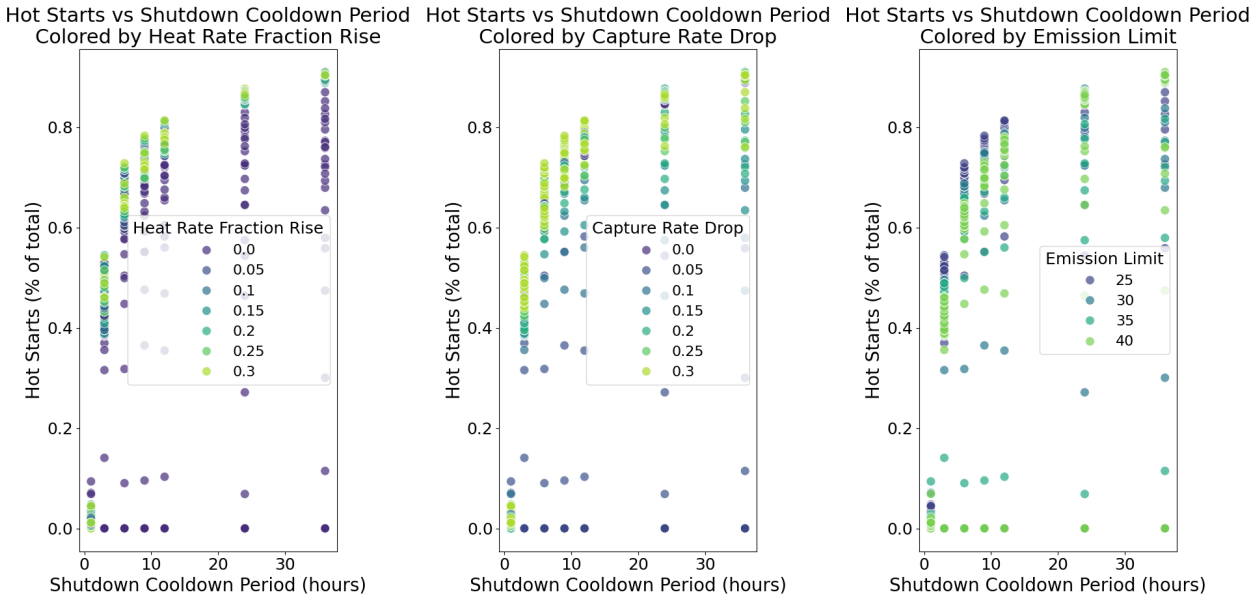

Figure 3.12: Comparison of Hot Start Percentage Under Varying Parameters

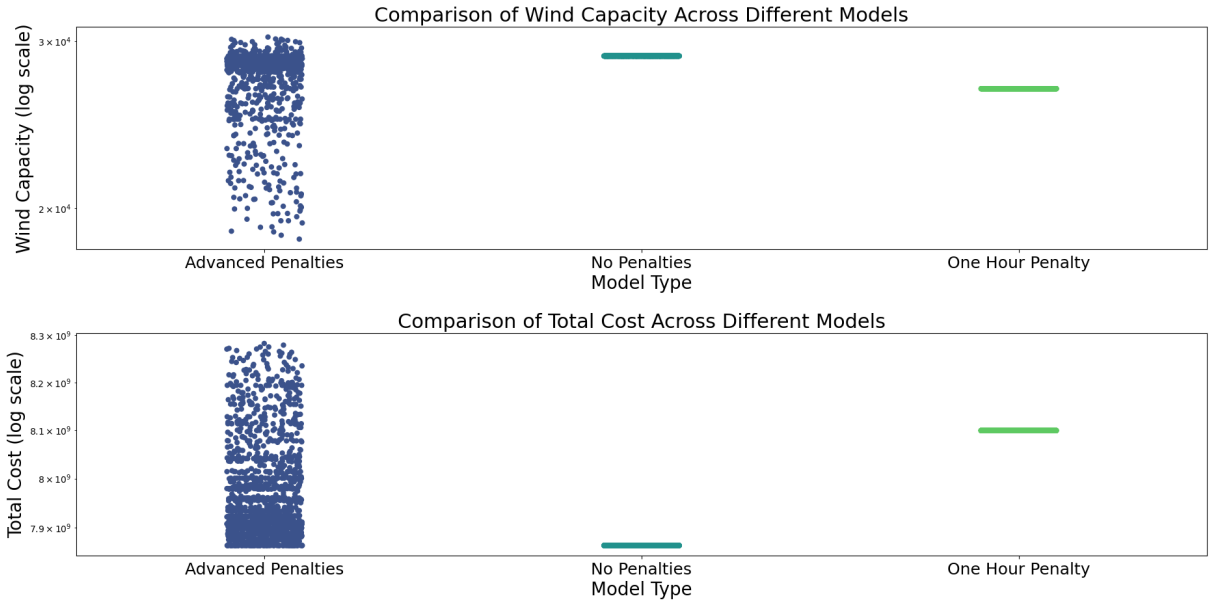

Figure 3.13: Comparison of Advanced Penalties, No Penalties, and One-Hour Penalties - Wind

hour fuel penalty that produces the same start-up emissions as calculated in the advanced penalties case. First, the carbon capture efficiency per hour is calculated during the transient period, increasing linearly from the initial value until it reaches the steady state value at the end of the transient stage. Next, the same process is followed for calculating the transient heat rate per hour. The total hate rate over the transient stage is calculated by summing the hourly heat rates. Finally, the transient emissions rate per hour is calculated and summed to yield the total emissions rate over the transient period. With the total emission rate during the transient period known, the equivalent start fuel required to match the start-up fuel penalty to the advanced penalty emissions is given in Equation 3.20.

$$F_{\text{required}} = \frac{E_{\text{transient}} - (T_{\text{transient}} \times R_{\text{steady, CCS, tonne/MMBtu}})}{R_{\text{steady, CCS, tonne/MWh}}} \tag{3.20}$$

where

- F_{required}: The equivalent start fuel required to match the start-up fuel penalty to the advanced penalty emissions
- $E_{\text{transient}}$: The total emissions rate over the transient period
- $T_{\text{transient}}$: The total transient heat rate over the transient period
- $R_{\text{steady, CCS, tonne/MMBtu}}$: The steady-state emissions rate with carbon capture and storage (CCS) in tonnes per MMBtu
- $R_{\text{steady, CCS, tonne/MWh}}$: The steady-state emissions rate with carbon capture and storage (CCS) in tonnes per MWh

Matching the emissions only solves half of the problem, however. With the increased fuel consumption required to match the emissions comes additional start-up costs. To avoid over-penalizing the start-up costs while matching emissions, a negative start-up cost variable must be added. First, the additional transient fuel required is calculated by subtracting the steady-state heat rate from the total transient period heat rate. Next, the difference between the fuel required for emissions and the calculated additional transient fuel is determined. That difference is then multiplied by the average fuel cost, yielding a start-up cost adjustment. Finally, the original start-up cost per MW is added, resulting in a start-up cost per MW per start. With this value known, the correct start-up cost with fuel can be calculated, displayed in the equations below.

$$F_{\text{additional, transient}} = H_{\text{total, transient}} - H_{\text{steady}} \times T_{\text{transient}} \tag{3.21}$$

$$\Delta F = F_{\text{required}} - F_{\text{additional, transient}} \tag{3.22}$$

$$C_{\text{adjustment}} = \Delta F \times C_{\text{fuel, avg}} \tag{3.23}$$

$$C_{\text{start, per MW}} = C_{\text{adjustment}} + C_{\text{start, original}} \tag{3.24}$$

$$C_{\text{start, total}} = C_{\text{start, per MW}} + C_{\text{fuel, avg}} \times F_{\text{required}} \tag{3.25}$$

With the proxy equations defined, an additional run was performed on both the simple solar and simple wind models. The proxy model, defined as Modified One-Hour Penalty, was compared to the advanced penalties model to determine how closely it can replicate system behavior. The modified one-hour penalty does not adequately represent the solar model, although this is likely due to the unique structure of that model. With harsh start-up penalties and strict emissions constraints, the model is unable to produce power during periods when solar is unavailable, resulting in many instances where the model pays the maximum non-served energy penalty in addition to building gas and solar facilities. For the wind model, the one-hour penalty modified proxy appears to do a reasonable job of calculating a total system cost similar to that of the advanced penalties model. This suggests that the negative start-up cost is adequately offsetting the additional fuel consumption required to match overall emissions during start-up. When comparing all runs across both models, the modified one-hour penalty tends to overestimate the total system cost relative to the advanced penalties model, shown in Figure 3.14. However, recall that the modified one-hour penalty is applied to all start-ups and does not differentiate between a hot start and a cold start. It is more appropriate to only compare instances of the advanced penalties model where nearly 100% of all start-ups occurred as cold start-ups. Filtering these cases, the modified one-hour penalty model appears to serve as a reasonable proxy for the advanced penalties model, achieving an average error of 0.45%. Figure 3.15 illustrates the performance of the two models filtered to cold start-up conditions for the advanced penalties model.

Therefore, the simple models underscore the significant role that start-up penalties play in shaping both system cost and operational behavior. Capture rate penalties, heat rate penalties, and reduced cooldown duration all lead to increased system costs, although the relative impact of each variable varies depending on the specific system. A modified model utilizing fuel consumption as a proxy for more advanced start-up penalties yields similar, though not identical, total system costs.

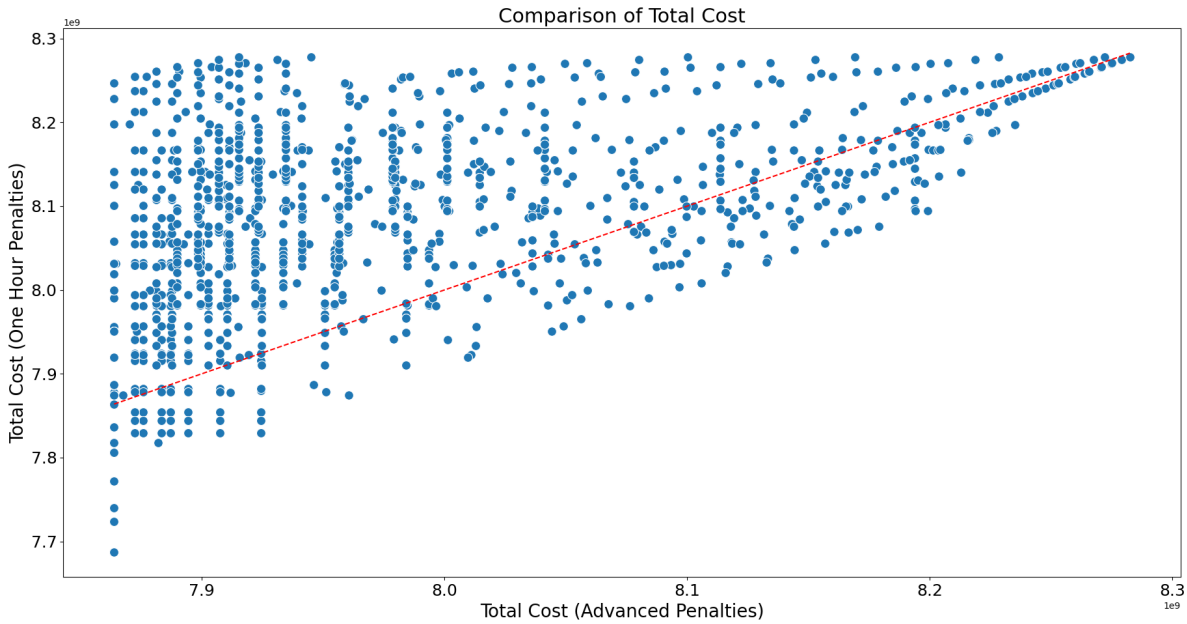

Figure 3.14: Advanced Penalties (All Starts) vs Modified One-Hour Penalties - Total Cost

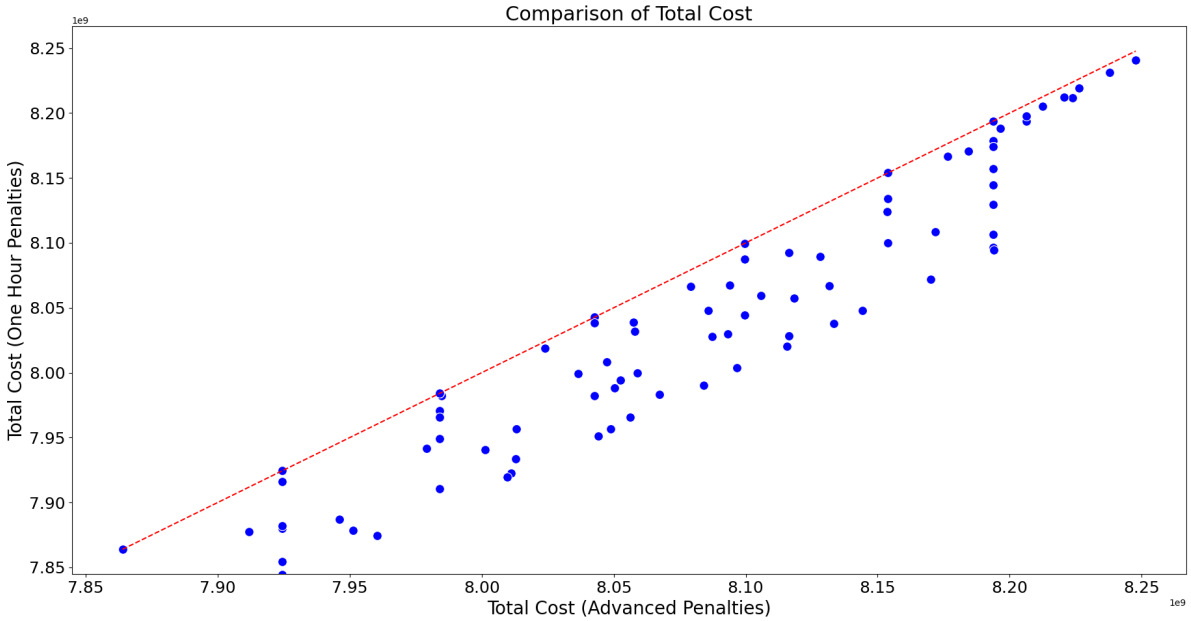

Figure 3.15: Advanced Penalties (Cold Starts Only) vs Modified One-Hour Penalties - Total Cost

Chapter 4

GenX Optimization Modeling on the ISO New England Grid System

After testing the impact of varying start-up CCE and heat rate penalties under different emissions constraints and cold start-up thresholds on the simple models, a real-world model was tested. This chapter builds on the foundation established in Chapter 3 using a complex model of the New England grid system. First, the ISO-New England model is introduced, defining key inputs, assumptions, and parameters. After describing the system, the impacts of the advanced start-up penalties are investigated. System operational behavior, grid design, and resource capacities are calculated under sets of given assumptions and constraints. Finally, the model explores how including start-up penalties for natural gas power plants can influence the relative value of other energy technologies.

4.1 ISO New England Model Overview

This section examines the GenX model of the ISO New England (ISO-NE) grid system. An existing GenX model of the ISO-NE grid was used as the baseline model. This model is configured to determine the least cost electricity generation, storage, and transmission portfolio to meet demand in the year 2050, subject to CO_2 emissions constraints. The model assumes a high electrification scenario in 2050, leveraging the electrification potential of transportation, industry, heating, buildings, and other technologies [125]. The model is divided into two discrete zones. Zone one represents Quebec, which is connected to New England via a shared transmission line. The Hydro-Quebec existing hydropower plant is the only generator modeled in zone one, as it supplies approximately 10% of New England's power needs [126]. Zone two includes Maine, New Hampshire, Vermont, Massachusetts, Rhode Island, and Connecticut, representing the ISO New England network. The model includes the existing 345kVAC and 450kVDC transmission lines but does not permit transmission expansion due to the complexity associated with international transmission. Fixed resistive losses per MWhe transmitted are included. Twenty weather-years of correlated demand and VRE availability are incorporated, with two representative two-week periods of VRE availability shown in Figure 4.1 and Figure 4.2, highlighting summer and winter conditions.

New England demand data is comprised of twenty 1-year time-series representing the

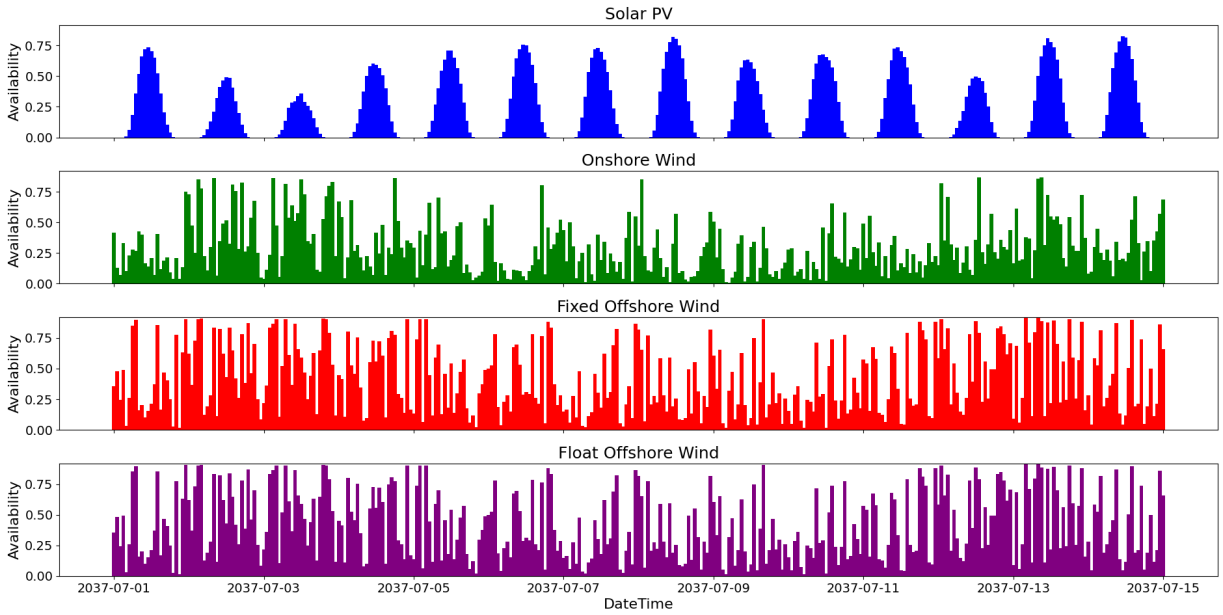

Figure 4.1: Two Week View of VRE Availability, Summer

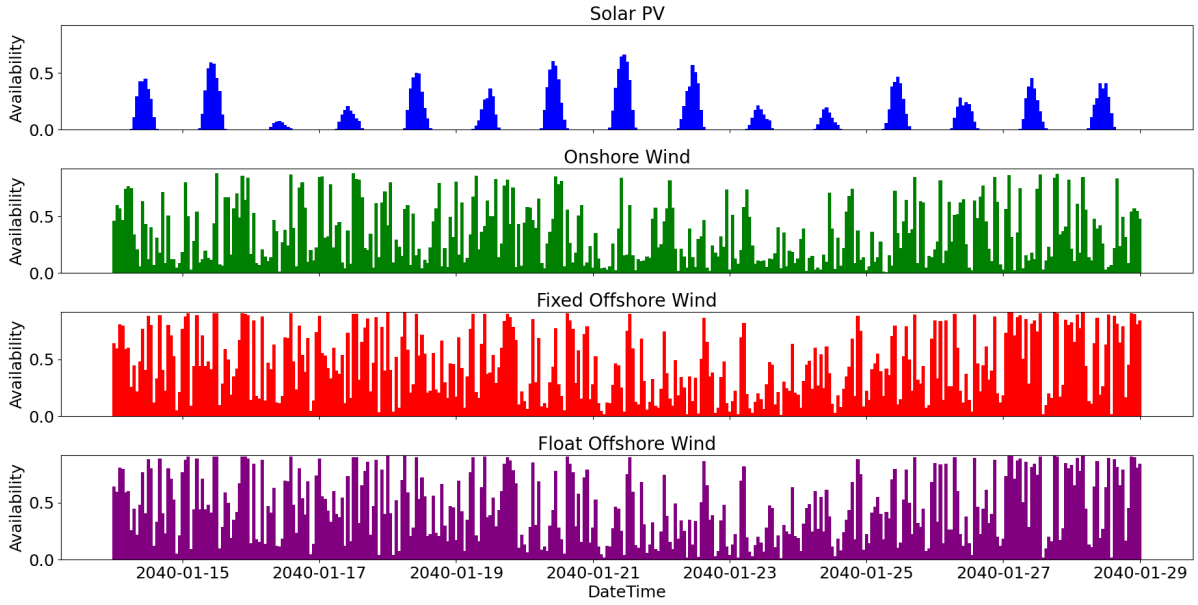

Figure 4.2: Two Week View of VRE Availability, Winter

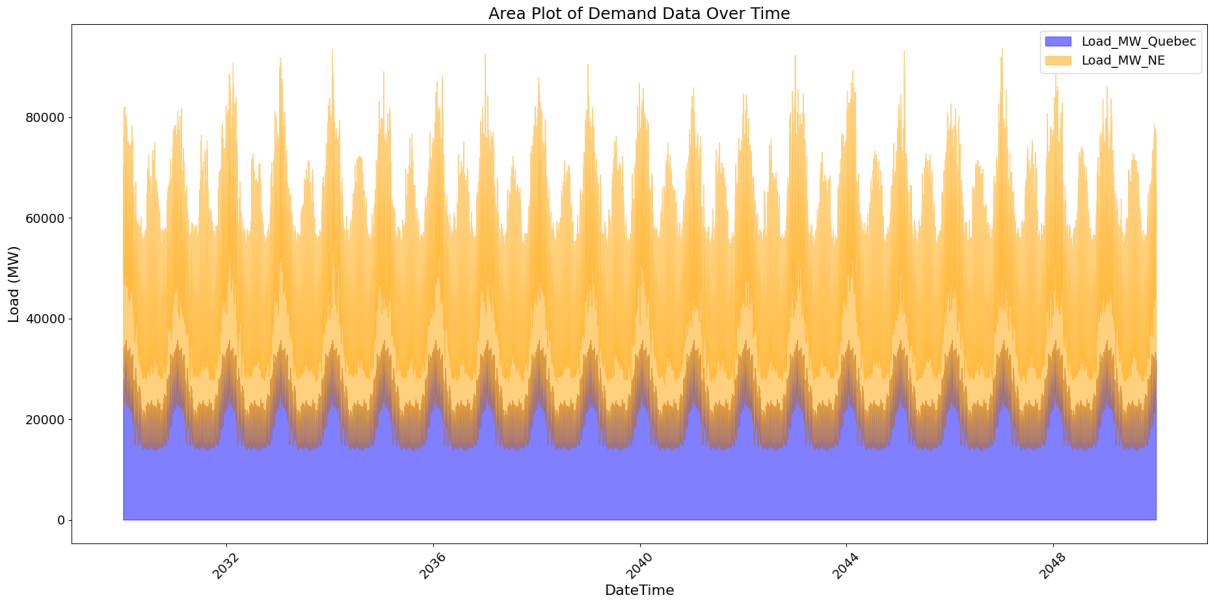

Figure 4.3: Demand Data

hourly load in New England. Each projection represents the projected 2050 electricity demand, determined by analyzing the weather pattern data acquired between 2001 and 2020 [127]. Due to the high electrification scenario, these modifications result in New England's electricity demand being highest during the winter season for most cases. Quebec demand leverages the work done by Dimanchev et al. It incorporates a single weather scenario and utilizes the 2012 load pattern, modified to account for load growth from 2012 to 2050 while ensuring Quebec maintains net exporter status [128]. Further information on the demand and VRE availability forecasting and methodology can be found in the research published by Khorramafar et al.[129]. The demand profile is displayed in Figure 4.3.

The model also includes a variety of energy generation and storage technologies, including reservoir hydropower (Quebec only), NGCC without CCS, NGCC with CCS, residential solar PV, commercial solar PV, utility solar PV, onshore wind, offshore wind (floating platform), offshore wind (fixed platform), battery (4-hour lithium-ion), nuclear fission, run-of-the-river (ROR) hydropower, and pumped hydro storage (PHS). Each of the resources is assigned an associated cost, capacity, and availability. The model does not allow for capacity expansion or new builds of Quebec hydropower, pumped hydroelectric storage, and run-of-the-river hydroelectric. Other VRE sources, such as solar photovoltaic and wind, are permitted to expand with a cap on maximum capacity. Solar photovoltaic is divided into three categories: utility-scale solar PV, commercial solar PV, and residential solar PV. Wind is divided into onshore wind, fixed platform offshore wind, and floating platform offshore wind. Maximum capacity expansion for utility-scale solar PV and wind generation is based upon the 2020 Net-Zero New England report, and it factors in land-use constraints and political considerations [130]. For commercial and residential rooftop solar PV, the constraint is calculated based upon the historical rate of rooftop installations, leveraging previously conducted studies from Massachusetts and extrapolated to other states [131],

Table 4.1: Resource Allocation for ISO-NE and Quebec with Expansion Capacities

Resource	ISO-NE Existing Capacity (MWe)	QC Existing Capacity (MWe)	ISO-NE Expansion Allowed	Max Expansion Capacity (MWe)
Reservoir Hydro	0	41,108	No	N/A
NGCC without CCS	0	0	Yes	Uncapped
NGCC including CCS	0	0	Yes	Uncapped
Residential Solar PV	0	0	Yes	6,000
Commercial Solar PV	0	0	Yes	12,000
Utility Solar PV	0	0	Yes	22,000
Onshore Wind	0	0	Yes	9,000
Offshore Wind (fixed platform)	0	0	Yes	37,000
Offshore Wind (floating platform)	0	0	Yes	275,000
Battery Storage	0	0	Yes	Uncapped
Fission	0	0	Yes	Uncapped
ROR Hydropower	1,961	0	No	N/A
PHS	1,830	0	No	N/A

[132]. The existing capacity, if any, and expansion capability for these resources by zone are displayed in Table 4.1.

Each of the above resources is assigned an associated cost, capacity, and availability. The model assumes that coal will be eliminated by 2050 and all-natural gas-fired power plants will be combined cycle plants. Natural gas fuel prices were forecast based on the historical ratio of ISO-NE hub spot fire compared to the Henry Hub spot price from 2016-2019. Next, the median trend was calculated by normalizing each monthly futures price by the corresponding annual average price from 2026-2031. The ISO-NE price is then calculated in Equation 4.1 [127].

$$\text{ISO-NE Price} = \left(\frac{H_{\text{futures}}}{H_{\text{annual}}}\right) \times H_{2050} \times R_{\text{ISO-NE/HH}} \tag{4.1}$$

$$\begin{aligned} H_{\text{futures}} &: \text{Henry Hub Futures Price (Month)} \\ H_{\text{annual}} &: \text{Annual Average Henry Hub Futures Price} \\ H_{2050} &: \text{EIA 2050 Henry Hub Price} \\ R_{\text{ISO-NE/HH}} &: \text{Historical ISO-NE/Henry Hub Price Ratio} \end{aligned}$$

All other cost, lifetime, and performance data were obtained from the 2024 National Energy Research Laboratory (NREL) Annual Technology Baseline database [133]. For the VRE resources, availability estimates were obtained from Khorramafar et al.'s correlated demand and availability model and are shown in Table 4.2. A list of key input resource parameters is shown in Table 4.3.

Table 4.2: VRE Annual Availability

Resource	**NREL ATB Resource Class**	**Annual Availability (%)**
Onshore Wind	Class 7	36.0
Fixed Offshore Wind	Class 1	51.1
Floating Offshore Wind	Class 11	51.1
Utility Solar PV	Class 9	16.8
Commercial Solar PV	Class 9	9.6
Residential Solar PV	Class 9	8.9

The ISO New England GenX model was subsequently run, with GenX seeking to determine the optimal solution. As mentioned previously in Section 3.1, GenX utilizes an objective function to minimize the total cost of the system while honoring all constraints. The initial GenX settings relevant to the ISO-NE model are displayed in Table 4.4.

Table 4.3: Generator Data for Baseline Model

Resource	Capital Cost $/MW	Fixed O&M Cost $/MW	Fixed O&M Cost $/MWh	Variable Cost $/MWh
Reservoir Hydro	$ 6,399,260	$ 620,000	$ -	$ -
NGCC without CCS	$ 1,660,173	$ 480,000	$ -	$ 1.61
NGCC with CCS	$ 2,434,378	$ 780,000	$ -	$ 3.32
Residential Solar PV	$ 955,014	$ 260,000	$ -	$ -
Commercial Solar PV	$ 1,301,055	$ 200,000	$ -	$ -
Utility Solar PV	$ 1,690,918	$ 280,000	$ -	$ -
Onshore Wind	$ 1,382,828	$ 460,000	$ -	$ -
Offshore Wind (fixed platform)	$ 3,933,764	$ 1,420,000	$ -	$ -
Offshore Wind (floating platform)	$ 6,363,042	$ 1,220,000	$ -	$ -
Battery Storage	$ 530,258	$ 140,000	$ 70,000	$ -
Fission	$ 9,241,956	$ 3,040,000	$ -	$ 2.00
ROR Hydropower	$ 5,909,262	$ 374,000	$ -	$ -
PHS	$ 9,090,391	$ 940,000	$ -	$ -

Table 4.4: Initial GenX Settings

Parameter	Setting
Network Expansion	Not Active
CO_2 Cap	Load + rate-based emission limit constraint
Solver	Gurobi 11.02
Unit Commitment	Linearized Clustering
Capacity Reserve Requirement	Not Active
Energy Share Requirement	Not Active
Minimum Capacity Requirement	Not Active

4.2 ISO New England Model Results

The GenX model of ISO-NE seeks to provide information around three key narratives. The first question surrounds understanding how these advanced start-up penalties and cooldown periods influence the overall system behavior. Next, the total generation, capacities, and capacity factors of natural gas plants are investigated to better understand their role in providing energy under various constrained scenarios. The last narrative explores how varying the flexibility of natural gas using start-up penalties can alter the value of other energy resources. Four versions of the ISO-NE model were generated to understand the impact. First, a no-penalty model was created that allows NGCC plants to cycle on and off with no capture rate penalty or additional fuel consumption. Second, the baseline ISO-NE model was generated, incorporating a one-hour fuel consumption penalty for NGCC start-ups. Third, an advanced penalties model that incorporates a reduction in CCE and increased heat rate after a cold start-up was generated. Finally, the modified one-hour model was created, which attempts to mimic the advanced penalties start-up parameters using one-hour fuel consumption as a proxy. The four models here follow the same framework as the simple models outlined in Section 3.4, executed under four distinct emissions intensity limits representing emission control policies ranging from very strict to relaxed: 2.5 g/kWh, 4.0 g/kWh, 12.0 g/kWh, and 35.0 g/kWh. The selected parameters for the advanced penalties model are shown in Table 4.5.

4.2.1 Impact of Start-Up Penalties on System Operational and Behavioral Decisions

To explore the impact of these start-up penalties on the system behavior, system power output by resource type was calculated and graphed. This provides visibility into how the system elects to optimize the operation of natural gas plants by showing power output over time. The total time-series of 175,200 time-steps was divided into 18 segments sampled every

Table 4.5: Advanced Start-Up Penalties Parameters

Resource	**Shutdown Cooldown Period**	**Cold Heat Rate Duration**	**Cold Start Heat Rate Increase**	**Steady Capture Rate**	**Cold Start Capture Rate**	**Start Cost per MW**
NGCC	6 hours	1 hour	10%	0%	0%	$50
NGCC with CCS	6 hours	3 hours	20%	95%	70%	$80

10,000 hours apart in order to ease the computational burden. Each segment shows two weeks of power generation data. Two representative segments, during a period of high and low solar availability, are shown in Figure 4.4 and Figure 4.5, respectively. While the total output from the thermal generators varies considerably over time, these results suggest that natural gas will nevertheless play a role in continuing to meet energy demand. It also highlights the difference in system behavior. Under the no-penalties operating condition, the system cycles multiple NGCC plants off and on each hour. Under the one-hour model, the modified one-hour model, and the advanced penalties model, the system adopts a steady-state approach, often operating the plants at continuous, lower outputs rather than cycling on and off to avoid paying start-up penalties. The difference in behavior between the one-hour models and advanced penalties model appears modest, suggesting that while incorporating any start-up penalties materially changes system behavior, the difference between the advanced penalties, one-hour penalty, and one-hour modified penalty results in similar system decisions. The advanced penalties model does show more variation in Figure 4.4 and Figure 4.5 likely due to having hot start-ups as an option to restart plants and avoid associated penalties.

The total system cost under each model is also evaluated as shown in Figure 4.6. The total system cost is the objective function of the optimization model, seeking to meet demand while honoring constraints at minimum cost. As expected, the no-penalty model yields the lowest total system cost as it is able to freely use natural gas in a dispatchable manner without incurring any start-up penalties to capture rate or heat rate. The original one-hour model, which includes a static increase in fuel consumption for all scenarios, has the second lowest cost. The advanced penalties model yields the second highest cost for the total solution, and the modified one-hour model is the most expensive. This is intuitive, as it is expected that adding start-up penalties will result in additional costs. The modified one-hour model applies the start-up penalty to all start-ups, compared to the advanced model, which only penalizes cold start-ups, so it is reasonable that it has the highest system cost. Despite this assumption, the modified one-hour model produces total system costs similar to the advanced penalties model, indicating an improvement over the default start-up configuration. Under very strict emissions intensity limitations, the differences between the models are smaller. This is likely due to the overall reduction of natural gas generation across all models in an ultra-low emissions environment, reducing the impact of start-up penalties. In less emissions-constrained scenarios, however, natural gas is utilized more prominently, and the differences

between the models are greater, especially compared to the no-penalties case.

4.2.2 Impact of Start-Up Penalties on Resource Capacity

The second narrative looks at the installed capacity, capacity factors, and overall generation by resource. This primarily evaluates the role of natural gas, although other resources are considered. As of 2023, the average capacity factor of all NGCC power plants in the United States was 57%. As gas transitions towards less of a baseload generator and becomes more sensitive to demand and VRE availability, it is reasonable to expect that capacity factor to decrease. First, the total installed generation capacity, capacity factors, and total power output were calculated for thermal generators with and without CCS across all four models for the four emissions constraints. From this analysis, a few key trends are observed. As expected, the no-penalties model installs the most natural gas with CCS capacity across all four emissions scenarios, largely due to the lack of start-up penalties and additional associated emissions. Despite the no-penalties model installing and utilizing the most natural gas, the capacity factors for all four models are similar when under strict to moderate emissions constraints. At the highest emission intensity limit of 35 g/kWh, the no penalties model has the highest capacity factor for natural gas with CCS. This can likely be attributed to the fact that an emissions intensity limitation that high nearly enables natural gas with CCS to operate uninhibited as baseload generation with only mild curtailment.

For the other emissions intensity constraints, the capacity factors across all four models are very similar despite having different installed capacities and total generation. This is somewhat counter-intuitive, as one may have expected that the introduction of start-up penalties would result in gas facilities operating at higher capacity factors, even during periods of renewable energy availability, to avoid paying start-up penalties. The similarity in capacity factors can possibly be attributed to the method of calculation, where the sum of the 20-year total power generation is used and divided by the total installed capacity multiplied by 20 years. This method of determining capacity factors is a reasonable summary of broad system behavior and is illustrated in Figure 4.7.

While a 20-year perspective on capacity factor effectively summarizes overall system behavior, it may overlook the finer details of daily or hourly operations. Extended periods of no natural gas usage can disproportionately influence capacity factor plots when viewed over such a long time scale. To gain a more detailed understanding, a new approach was developed that examines the behavior of natural gas plants on a finer scale. The 20 years of hourly data were aggregated into 14,600 twelve-hour periods. For each period, the average power output of natural gas plants with CCS was calculated and then divided by the total installed capacity, yielding a normalized power output, or periodic capacity factor. This metric represents the average gas capacity factor during each 12-hour interval. Periods with an average capacity factor of less than 1.0% were excluded from the analysis to enhance clarity and focus on times when natural gas was actively utilized. The resulting histogram is displayed in Figure 4.8.

This analysis provides an alternative perspective compared to the initial 20-year assessment of capacity factors. The finer-scale analysis reveals that, under stricter emissions control policies, gas plants tend to operate at lower capacity factors when they are active, consistent with the long-term trends observed in the 20-year view. However, when focusing

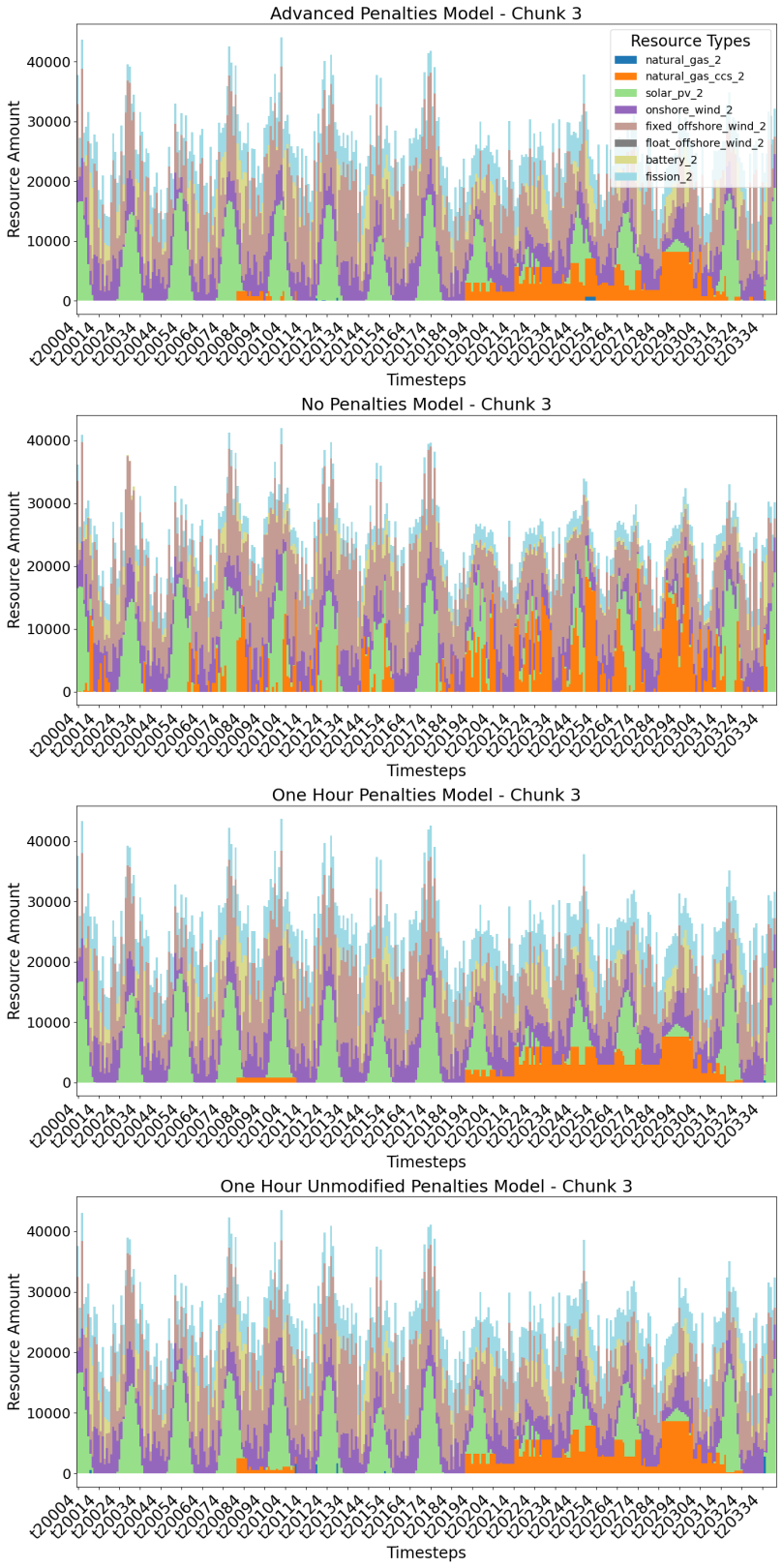

Figure 4.4: Power Output by Resource - High Solar Availability (12g/kWh emissions limit)

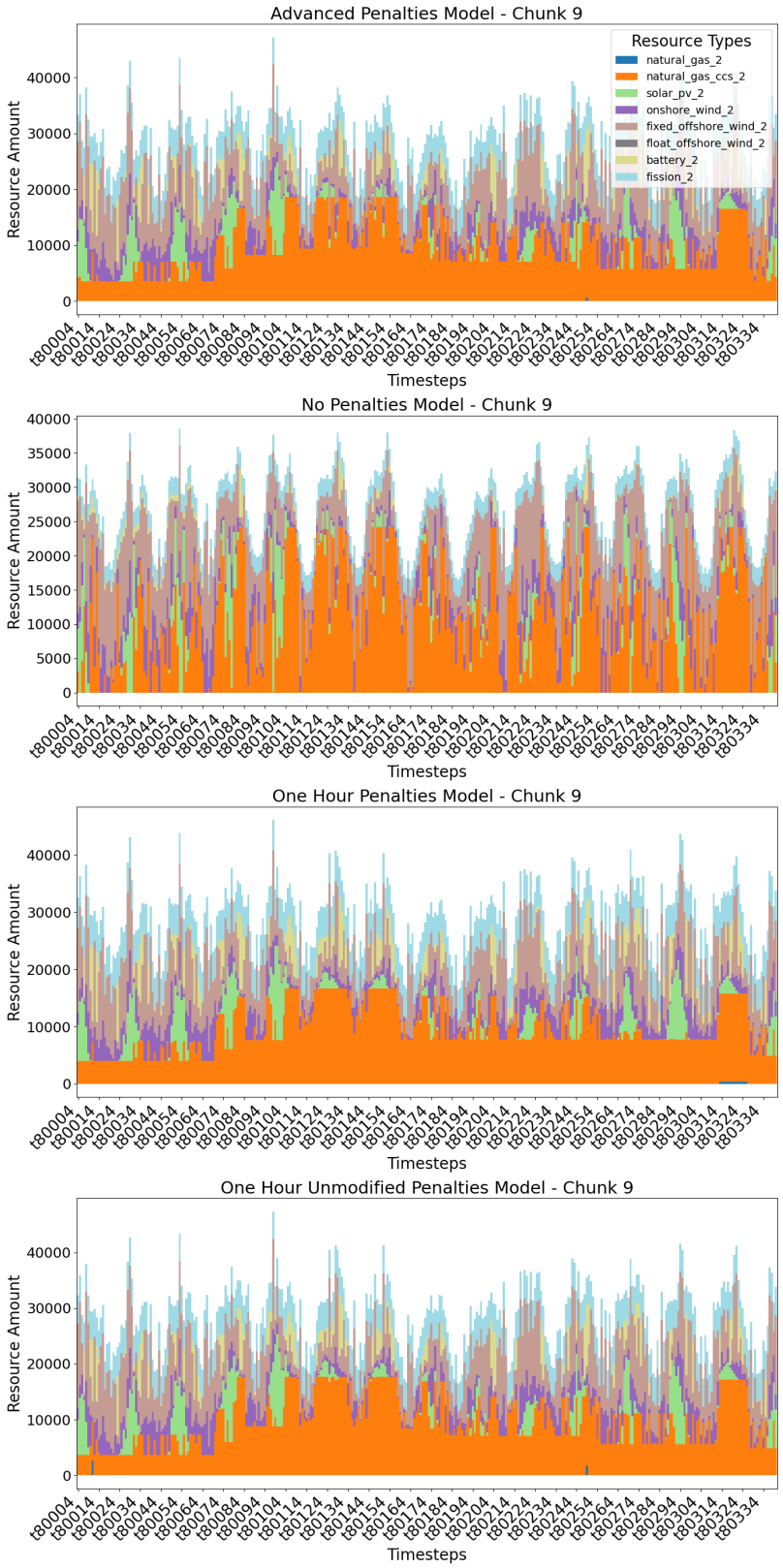

Figure 4.5: Power Output by Resource - Low Solar Availability (12g/kWh emissions limit)

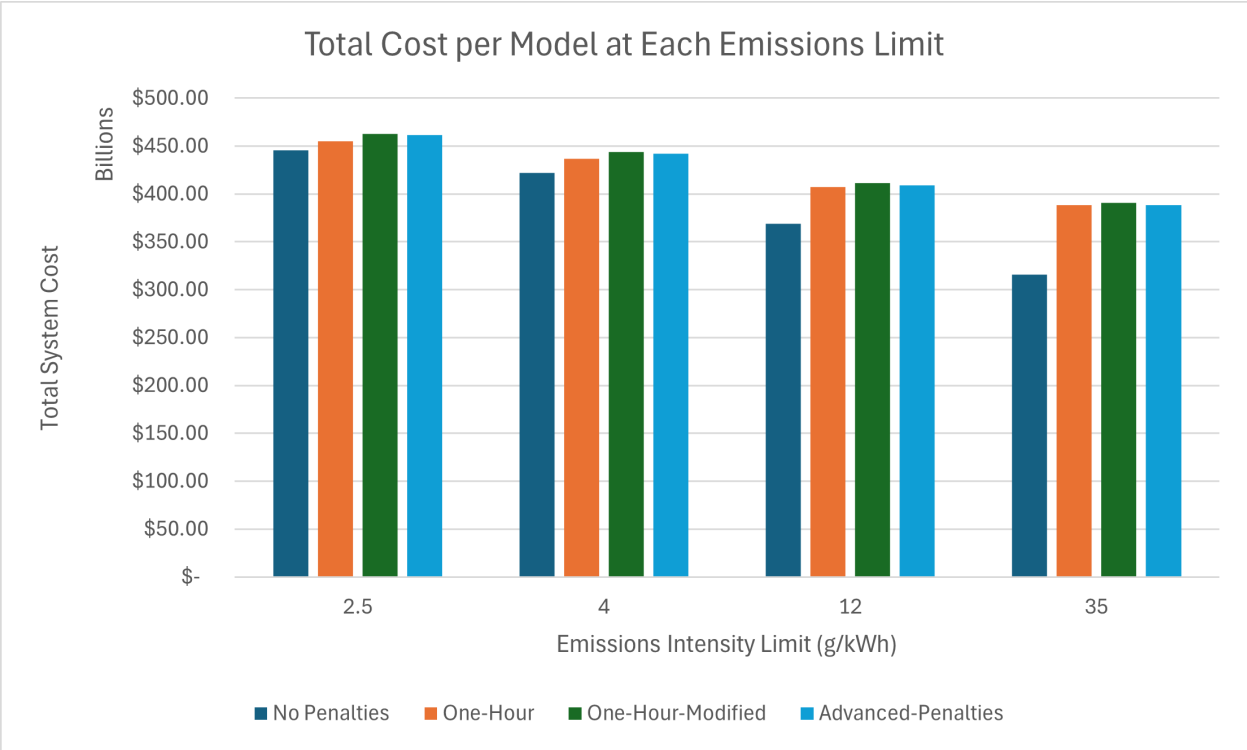

Figure 4.6: Total System Cost for Optimized Solution

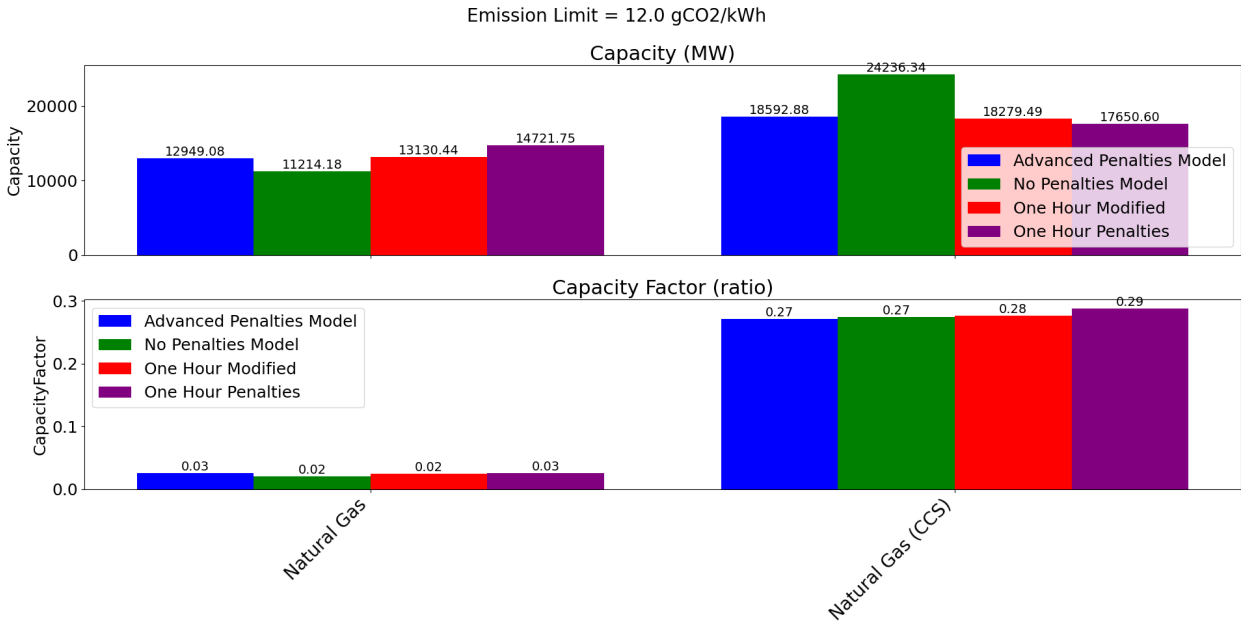

Figure 4.7: Capacity Factors for NGCC and NGCC with CCS

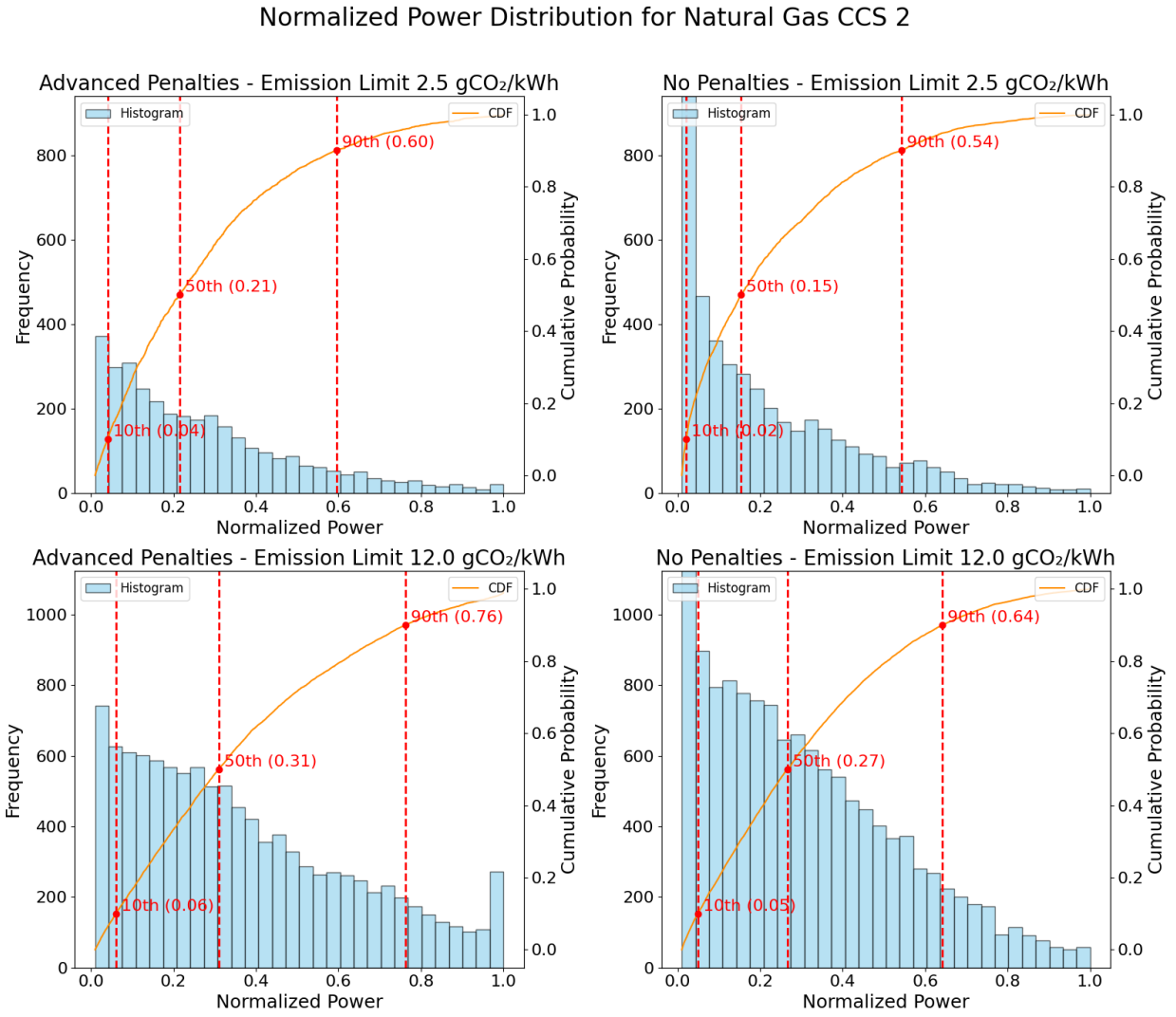

Figure 4.8: 12-Hour Capacity Factor Distributions for NGCC with CCS, Excluding Periods of Gas Utilization $< 1.0\%$. Bins and CDF truncated at 1.0%

specifically on periods of active natural gas usage, a clear distinction emerges between the operational strategies of the advanced penalty and no-penalty scenarios. In the advanced penalty scenario, gas plants operate at higher capacity factors under both the 2.5 g/kWh and 12.0 g/kWh constraints—an insight that was not evident in the broader 20-year analysis. The advanced penalty model consistently exhibits higher capacity factors across the distribution, as indicated by the 10^{th}, 50^{th}, and 90^{th} percentiles. This suggests that while the overall capacity factors between the advanced penalty and no penalty models may appear similar over the long term, the advanced penalties model leaves natural gas plants with CCS offline more frequently. Consequently, the stricter start-up penalties in the advanced penalties model likely result in fewer gas plant start-ups overall, but when these plants are brought online, they operate at higher capacity factors than they would under the no penalty scenario.

4.2.3 Impact of Start-Up Penalties on Value of Alternative Energy Generation

In this analysis, the economic implications of start-up penalties on natural gas plants with CCS on the value of a specific resource type are investigated. The primary objective is to determine how these penalties influence the maximum allowable capital expenditure per kilowatt that justifies investment in these alternative technologies. This is accomplished by allowing the model to build varying amounts of resource capacity up to a predetermined maximum. The model can build this resource at no capital cost, meaning the investment cost to install additional capacity is effectively set to $0. However, the resource still incurs operational and maintenance costs. The model's objective function is to minimize the total system cost, which includes both operational costs and penalties for emissions, under various constraints. To determine the economic value of building more capacity of a specific resource, the model calculates the "dual value," a derivative indicating the change in the objective function (total system cost) if the maximum capacity of that resource was increased by 1 MW. This value represents the marginal benefit of adding more capacity. From this, the maximum allowable capital expenditure per kW is calculated, which would justify installing additional capacity of this resource. Essentially, if the cost of installing more capacity is less than this calculated capital expenditure per kW, it would be economically beneficial to invest in more of the resource. The model spans a one-year period under two distinct emissions limits: 2.5 g/kWh and 12.0 g/kWh. The analysis includes the advanced penalties, no penalties, and modified one-hour penalty models, and the results are displayed in Figure 4.9 through Figure 4.12.

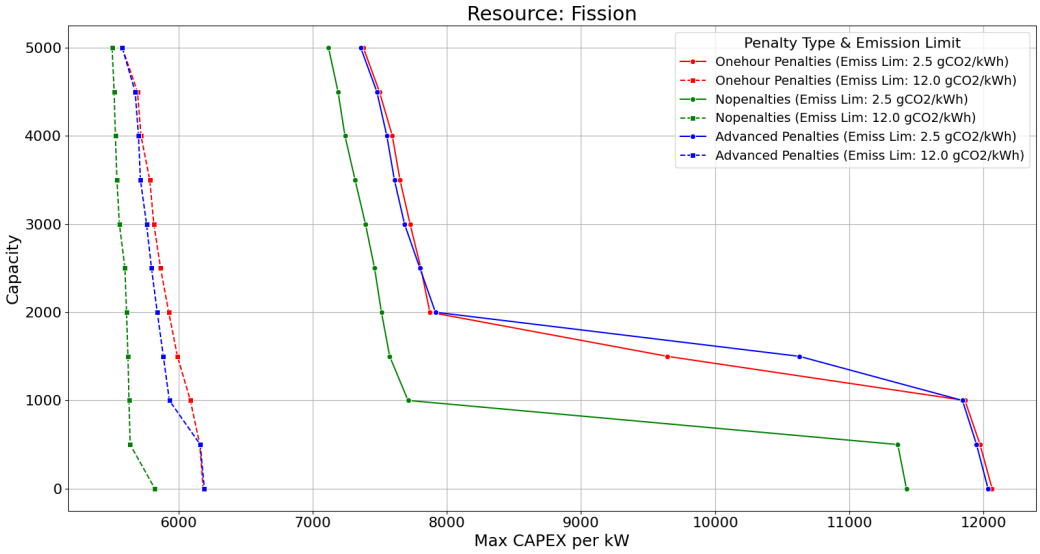

Figure 4.9: Maximum Capex per kW vs Maximum Installed Fission Capacity

The first observation that can be drawn from the analysis is that the initial capacity expansion is generally the most valuable in reducing total system cost, but subsequent ex-

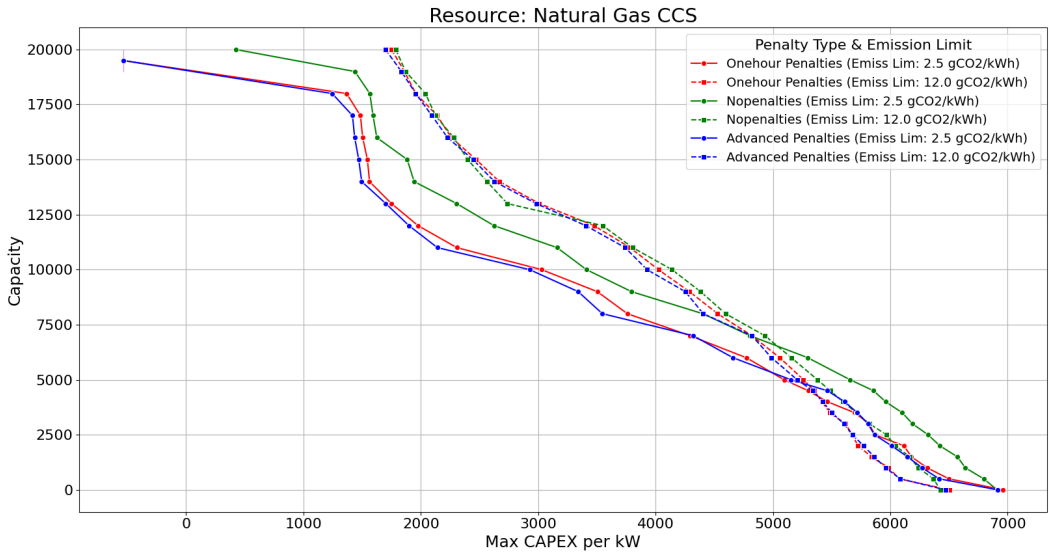

Figure 4.10: Maximum Capex per kW vs Maximum Installed NGCC Plant Capacity

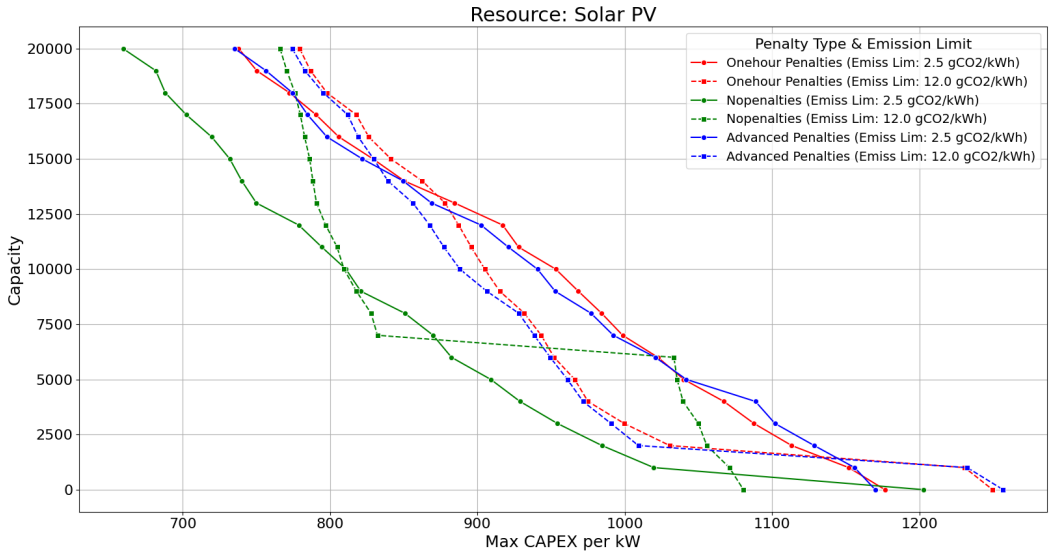

Figure 4.11: Maximum Capex per kW vs Maximum Installed Solar Capacity

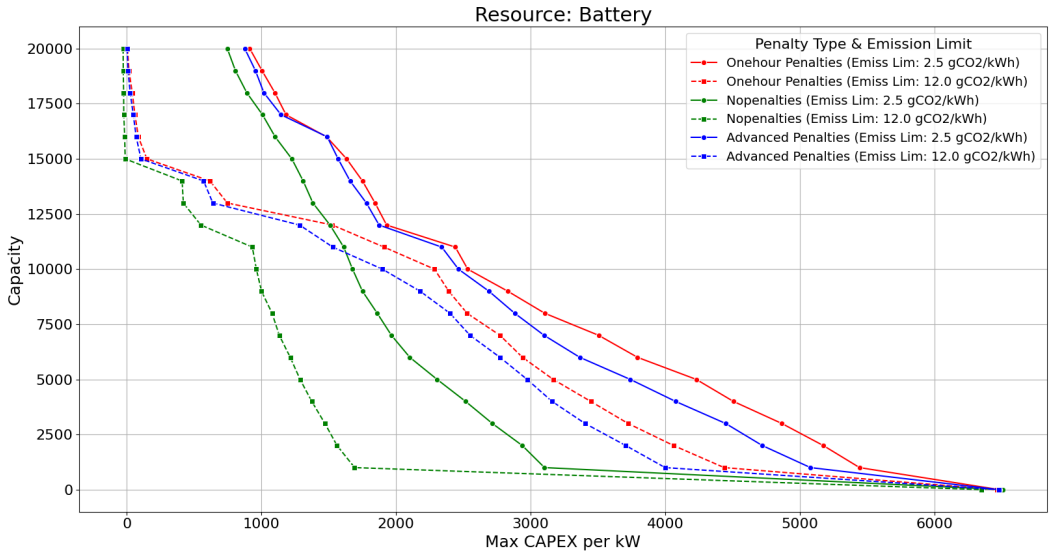

Figure 4.12: Maximum Capex per kW vs Maximum Installed Battery Capacity

pansion becomes more economically difficult to justify. This trend is consistent across fission, solar, and battery power generation. For example, in the advanced penalties model under a 2.5 g/kWh emissions limitation, adding the first 500 MW of nuclear fission will reduce the total system cost as long as the price of fission does not exceed $11,947 per kW. However, to add 2,000 MW of fission capacity, fission must cost no more than $7,915 per kW to remain economically viable. Installing greater than 2,000 MW of fission appears to result in a regime with a linear relationship between increasing capacity and decreasing maximum allowable cost per kW. This is an intuitive result, as each resource plays a distinct role in the grid such that a small amount is very valuable. Gradually, the value of that generator is saturated as additional capacity is installed. The rate of this decline is determined by the cost of competing or supporting technologies.

Comparing the no-penalties scenario versus the scenarios incorporating start-up penalties highlights how the inclusion of capture rate and heat rate penalties on NGCC plants increases the economic viability of fission under a strict emissions control policy. The no-penalties scenario would require fission to cost less than $7,710 per kW to add 1,000 MW of capacity, whereas the advanced penalties scenario is able to economically add 1,000 MW of fission up to a price of $11,842 per kW. All scenarios under the 2.5 g/kWh emissions constraint illustrate diminished returns after installing between 1,000 MW and 2,000 MW of fission capacity. Conversely, a different trend is observed for fission under the 12.0 g/kWh emissions constraint. Allowing more emissions significantly reduces the impact of the start-up penalties of natural gas, forcing fission to meet stricter cost per kW thresholds to truly reduce the overall system cost. This trend is nearly linear from the first 500 MW until 5,000 MW for all three penalty scenarios. Nevertheless, there is still marginal value to fission in start-up penalty scenarios compared to the case without any start-up penalties.

As expected, the impact of start-up penalties on natural gas capacity exhibits an inverse

relationship to the other resource types. While start-up penalties on natural gas generally lead to other resources becoming more economically attractive, they subsequently increase the economic hurdle required to justify additional gas capacity expansion. During the 2.5 g/kWh emissions constraint, the advanced penalties and modified one-hour penalty models require cheaper natural gas plant capital costs when compared to the no-penalties case at all points along the curve. However, it is noteworthy that the differences between the three models in maximum capital per kW under the 12.0 g/kWh emissions constraint are significantly reduced. Under this constraint, the differences in maximum allowable cost never exceed $300 per kW, and after installing 10,000 MW, the cost becomes essentially identical. This implies that allowing higher emissions intensities reduces the impact of start-up penalties on gas plants. This behavior is intuitive, but it is interesting that after adding approximately 10,000 MW, the penalties essentially cease having an impact on the economic threshold for capacity expansion. This may imply that with enough installed capacity, the system can operate in a manner that largely avoids having to perform cold start-ups and, therefore, avoids paying the penalty altogether.

Evaluating the impact of start-up penalties on the value of solar PV is not completely intuitive. During the strict 2.5 g/kWh emissions constraint, the impact on solar is similar to what was observed when viewing the impact on fission. The advanced and one-hour modified penalties result in solar being more valuable relative to natural gas, as compared to the case with no start-up penalties. The behavior during the more relaxed 12.0 g/kWh emissions limit is unique and inconsistent with other analyses noted so far. The results suggest that initially adding solar capacity does result in solar being more valuable in the scenarios incorporating start-up penalties than in the scenario without penalties. However, the scenarios with penalties reach an inflection point where solar becomes less valuable much earlier than in the no penalties scenario, approximately after installing 2,000 MW of capacity. During periods in which 2,000 MW to 6,000 MW of solar capacity are installed, the maximum allowable capital cost for solar is actually lower in the scenarios that include penalties than in the scenario without penalties. That inflection point is reached after 6,000 MW of solar capacity in the no-penalties model, at which point the value of solar is reduced, and the behavior reverts back to the standard trend. As solar capacity continues to increase, all three scenarios appear to be converging near 20,000 MW. This phenomenon indicates a possible operational constraint coming into effect much earlier for the scenarios with penalties than the scenario without penalties. This may suggest that there is a certain capacity up to which adding solar is easy, as it is always producing less than demand and is easily supported by flexible, dispatchable generation. Beyond this capacity, significant losses in the value of solar are observed as increased support is required per additional kW of solar capacity added. As NGCC with CCS becomes less flexible due to emissions penalties, this inflection point occurs at a lower installed solar capacity. However, the initial installed solar capacity remains more valuable as the alternative technology (natural gas with CCS) is more expensive. Further investigation into the solar model, including specific operational constraints and adding capacity expansion beyond 20,000 MW, is recommended and addressed in Chapter 5.

The interaction between battery storage and start-up penalties on natural gas mirrors the patterns observed in the fission analysis. Notably, the imposition of start-up penalties on NGCC plants increases the maximum allowable capital expenditure per kW for battery

storage at a given capacity compared to scenarios without such penalties. This suggests that start-up penalties make battery storage a more economically viable option, as the costs associated with bringing additional gas capacity online rise. This holds true under both emissions constraints, but unlike fission, the incremental value associated with adding battery capacity remains significant under the 12.0 g/kWh emissions constraint. This suggests that battery storage may benefit more than fission and be a more viable option for capacity expansion under moderate emissions control policies. Additionally, it can be observed that adding the initial battery capacity is extremely valuable, with the system justifying costs exceeding $6,000 per kW. The incremental value of battery expansion rapidly decreases with the first 1,000 MW added. This indicates that having zero energy storage capacity via batteries results in a large detrimental impact on the total system cost, but diminishing returns are rapidly encountered. This appears to exhibit logarithmic behavior, as each installed MW of new capacity is worth less than the previous MW. Note that in the 12.5 g/kWh emissions limit scenario, the maximum capital per kW for added battery capacity actually becomes negative at very large quantities of installed capacity. This is likely due to the battery system still incurring associated operations and maintenance costs while adding energy storage capacity beyond what is required to meet demand.

Chapter 5

Conclusion and Future Studies

This thesis examines the carbon capture rate efficiency and heat rate for natural gas combined cycle power plants operating at varying conditions. It initially describes the current energy landscape, illustrating the role of natural gas and reviewing the climate challenges associated with fossil fuel consumption. It also discusses the transitioning role of natural gas from a baseload energy generator to an intermittent generator likely to support variable renewable energy sources. The literature review introduces the process and methodology employed to acquire information on carbon capture associated with NGCC power plants, defines the system boundary, and compares various carbon capture technologies. Post-combustion carbon capture, specifically absorption-based carbon capture, appears to be a preferred technology for retrofitting existing NGCC plants. Non-steady-state carbon capture and heat rate behavior are examined, leveraging the existing study conducted by the IEAGHG as the foundation for the subsequent modeling work. With baseline assumptions drawn from literature, this thesis next describes the GenX model used for performing the analysis. The GenX model is then reviewed, detailing the default model behavior and modifications made to incorporate start-up penalties during non-steady-state operations. A proxy model incorporating new equations and constraints can adequately replicate the advanced start-up penalties and total system cost by using additional fuel consumption and modified start-up costs. The final modeling results and broader implications for overall grid design are discussed. Finally, this chapter addresses research limitations and recommendations for future studies.

Incorporating detailed penalties during start-up operations provides a deeper understanding of how natural gas may be utilized in 2050. Carbon capture efficiency reductions and heat rate increases associated with cold start-ups reduce the flexibility and viability of using natural gas as a load-following thermal generator in emissions-constrained environments. Utilizing GenX and the ISO-NE grid, the impact of these modifications is explored under various technical and policy constraints and scenarios. Accounting for start-up penalties changes system operational behavior, as less natural gas is used but often operates at higher capacity factors while online. It also leads to higher total system costs associated with the reduced thermal output, higher costs for CCS, and increased emissions during start-up transient periods. This results in other energy sources, such as nuclear fission, solar photovoltaic, and battery storage, incurring lower economic barriers to capacity expansion relative to natural gas units with CCS.

This thesis is a foundational piece supporting future exploration in this area of study.

This work focused exclusively on post-combustion carbon capture, specifically absorption-based capture. While that technology appears best suited for retrofitting NGCC plants, other technologies have shown promise and should continue to be explored. Extremely limited information exists in the literature on the overall performance of the capture unit and its associated impact on the plant's heat rate during variable operating conditions, such as during a cold start-up. Additional studies should be conducted to validate the existing literature on variable operating performance for different solvents in absorption-based carbon capture and how other capture technologies may perform under variable conditions. Moreover, this thesis focuses primarily on start-up operations, differentiating between hot and cold starts. The energy required to regenerate the solvent during shutdown operations is assumed to be obtained from a net zero emissions energy source. Factoring in an auxiliary fossil-fuel-powered boiler will likely alter these findings and should be investigated further. Concurrently, Chapter 3 demonstrates that the cooldown period significantly impacts the system's behavior and performance. This thesis only explored a linear relationship among parameters where a unit was assigned a binary status of hot or cold. Additional studies exploring the non-linear behavior and warm start-up regime may prove useful. This research can also be expanded to examine the impacts on other grid systems, such as the Electric Reliability Council of Texas grid and the California ISO grid. Finally, one may incorporate the findings of this thesis into multi-sector models, such as Dolphyn, to explore sectors such as hydrogen production from steam methane reforming or autothermal reforming with CCS. Dolphyn could further investigate the capture, transportation, and storage of CO_2 and the associated impacts.

Thus, this thesis demonstrates three key takeaways. First, natural gas combined cycle power plants equipped with carbon capture units will likely play a role in meeting energy demand, even under highly constrained emissions scenarios. Next, the performance of these carbon capture units, as currently modeled, is not constant at all conditions but is degraded during a transient period after cold start-ups. Hot start-ups do not appear to impact unit performance significantly. This performance degradation during cold start-ups results in additional emissions, reduced power output, and increased cost for the overall system. As these start-up penalties become increasingly harsh, the value of natural gas as an intermittent power generator is reduced relative to other technologies. Finally, in some scenarios, it seems likely that natural gas will be operated continuously, even during periods of renewable energy availability, to minimize the cost and emissions associated with frequent cold start-ups.

References

[1] K. Calvin, D. Dasgupta, G. Krinner, *et al.*, *IPCC, 2023: Climate change 2023: Synthesis report, summary for policymakers. contribution of working groups i, II and III to the sixth assessment report of the intergovernmental panel on climate change [core writing team, h. lee and j. romero (eds.)]. IPCC, geneva, switzerland*, P. Arias, M. Bustamante, I. Elgizouli, *et al.*, Eds., Jul. 2023.

[2] EIA, *World energy outlook 2023*, 2023. URL: www.iea.org/terms.

[3] E. Larson, C. G. J. Jenkins, E. Mayfield, *et al.*, *Net-Zero America: Potential Pathways, Infrastructure, and Impacts, Final Report Summary*, 2021. URL: https://netzeroamerica.princeton.edu/img/Princeton%20NZA%20FINAL%20REPORT%20SUMMARY%20(29Oct2021).pdf.

[4] EPA, *Inventory of U.S. Greenhouse Gas Emissions and Sinks | US EPA — epa.gov*, [Accessed 23-05-2024]. URL: https://www.epa.gov/ghgemissions/inventory-us-greenhouse-gas-emissions-and-sinks.

[5] EIA, *Frequently Asked Questions (FAQs) - U.S. Energy Information Administration (EIA) — eia.gov*, 2023. URL: https://www.eia.gov/tools/faqs/faq.php?id=74andt=11.

[6] EIA, *Annual energy outlook 2023*, 2023. URL: https://www.eia.gov/outlooks/aeo/pdf/AEO2023_Narrative.pdf.

[7] EIA, *Use of natural gas-fired generation differs in the United States by technology and region - U.S. Energy Information Administration (EIA) — eia.gov*, 2024. URL: https://www.eia.gov/todayinenergy/detail.php?id=61444#:~:text=Nearly%20all%20natural%20gas%2Dfired,when%20needed%20by%20the%20grid.

[8] D. Feldman, V. Ramasamy, A. R. Ran Fu, J. Desai, and R. Margolis, "U.s. solar photovoltaic system cost benchmark: Q1 2020," National Renewable Energy Laboratory, Tech. Rep., 2020.

[9] IEA, *Renewables 2023*, 2023. URL: https://www.iea.org/reports/renewables-2023/electricity.

[10] EPA, *Simple cycle stationary combustion turbine egus technical support document*, 2023. URL: https://www.epa.gov/system/files/documents/2023-05/Simple%20Cycle%20Stationary%20Combustion%20Turbine%20EGUs%20TSD.pdf.

[11] IPIECA, *Combined-cycle gas turbines (2022) | Ipieca — ipieca.org*, 2022. URL: https://www.ipieca.org/resources/energy-efficiency-database/combined-cycle-gas-turbines-2022.

[12] EIA, *Most combined-cycle power plants employ two combustion turbines with one steam turbine - U.S. Energy Information Administration (EIA) — eia.gov*, 2022. URL: https://www.eia.gov/todayinenergy/detail.php?id=52158.

[13] S. Shiozaki, T. Fujii, K. Takenaga, M. Ozawa, and A. Yamada, "6 - gas turbine combined cycle," in *Advances in Power Boilers*, ser. JSME Series in Thermal and Nuclear Power Generation, M. Ozawa and H. Asano, Eds., vol. 2, Elsevier, 2021, pp. 305–344, ISBN: 978-0-12-820360-6. DOI: https://doi.org/10.1016/B978-0-12-820360-6.00006-0. URL: https://www.sciencedirect.com/science/article/pii/B9780128203606000060.

[14] M. Islam, M. Hasanuzzaman, A. Pandey, and N. Rahim, "Chapter 2 - modern energy conversion technologies," in *Energy for Sustainable Development*, M. Hasanuzzaman and N. A. Rahim, Eds., Academic Press, 2020, pp. 19–39, ISBN: 978-0-12-814645-3. DOI: https://doi.org/10.1016/B978-0-12-814645-3.00002-X. URL: https://www.sciencedirect.com/science/article/pii/B978012814645300002X.

[15] P. Decoussemaeker, A. Nagasayanam, W. P. Bauver, L. Rigoni, L. Cinquegrani, G. Epis, and M.-E. Donghi, *Startup time reduction for combined cycle power plants*, 2016. URL: https://etn.global/wp-content/uploads/2018/09/STARTUP-TIME-REDUCTION-FOR-COMBINED-CYCLE-POWER-PLANTS.pdf.

[16] M. Oakes and M. Turner, *COST AND PERFORMANCE BASELINE FOR FOSSIL ENERGY PLANTS, VOLUME 5: NATURAL GAS ELECTRICITY GENERATING UNITS FOR FLEXIBLE OPERATION*, 2023. URL: https://netl.doe.gov/projects/files/CostandPerformanceBaselineforFossilEnergyPlantsVol5NatGasElectricityGenUnitsFlexOperation_050523.pdf.

[17] POWER, *Are Simple Cycles or Combined Cycles Better for Renewable Power Integration? — powermag.com*, 2015. URL: https://www.powermag.com/are-simple-cycles-or-combined-cycles-better-for-renewable-power-integration/.

[18] S. Krishnamurthy, V. R. Rao, S. Guntuka, P. Sharratt, R. Haghpanah, A. Rajendran, M. Amanullah, I. A. Karimi, and S. Farooq, "Co2 capture from dry flue gas by vacuum swing adsorption: A pilot plant study," *AIChE Journal*, vol. 60, no. 5, pp. 1830–1842, 2014. DOI: https://doi.org/10.1002/aic.14435. URL: https://aiche.onlinelibrary.wiley.com/doi/abs/10.1002/aic.14435.

[19] *Inflation reduction act of 2022*, 2022. URL: https://www.congress.gov/bill/117th-congress/house-bill/5376.

[20] M. E. Initiative and P. U. Z. lab, *GenX: A configurable power system capacity expansion model for studying low-carbon energy futures*, https://github.com/GenXProject/GenX, Accessed: 2024-07-09.

[21] URL: https://www.researchrabbit.ai/.

[22] R. Sharma, S. Gulati, A. Kaur, A. Sinhababu, and R. Chakravarty, "Research discovery and visualization using researchrabbit: A use case of ai in libraries," *COLLNET Journal of Scientometrics and Information Management*, vol. 16, no. 2, pp. 215–237, 2022. DOI: 10.1080/09737766.2022.2106167. URL: https://doi.org/10.1080/09737766.2022.2106167.

[23] D. Sulisworo, "Exploring research idea growth with litmap: Visualizing literature review graphically," *Bincang Sains dan Teknologi*, vol. 2, no. 02, pp. 48–54, 2023. DOI: 10.56741/bst.v2i02.323. URL: https://journal.iistr.org/index.php/BST/article/view/323.

[24] P. K. Behera, S. J. Jain, and A. Kumar, "Visual exploration of literature using connected papers: A practical approach," *Issues in Science and Technology Librarianship*, no. 104, 2023. DOI: 10.29173/istl2760. URL: https://journals.library.ualberta.ca/istl/index.php/istl/article/view/2760.

[25] M. D. Wilkes and S. Brown, "Flexible co2 capture for open-cycle gas turbines via vacuum-pressure swing adsorption: A model-based assessment," *Energy*, vol. 250, p. 123 805, 2022, ISSN: 0360-5442. DOI: https://doi.org/10.1016/j.energy.2022.123805. URL: https://www.sciencedirect.com/science/article/pii/S0360544222007083.

[26] M. Bui, P. Tait, M. Lucquiaud, and N. Mac Dowell, "Dynamic operation and modelling of amine-based co2 capture at pilot scale," *International Journal of Greenhouse Gas Control*, vol. 79, pp. 134–153, 2018, ISSN: 1750-5836. DOI: https://doi.org/10.1016/j.ijggc.2018.08.016. URL: https://www.sciencedirect.com/science/article/pii/S1750583618304250.

[27] L. Wang, Y. Yang, W. Shen, X. Kong, P. Li, J. Yu, and A. E. Rodrigues, "Co2 capture from flue gas in an existing coal-fired power plant by two successive pilot-scale vpsa units," *Industrial Engineering Chemistry Research*, vol. 52, no. 23, pp. 7947–7955, 2013. DOI: 10.1021/ie4009716. URL: https://doi.org/10.1021/ie4009716.

[28] B. Arias, M. Diego, J. Abanades, M. Lorenzo, L. Diaz, D. Martínez, J. Alvarez, and A. Sánchez-Biezma, "Demonstration of steady state co2 capture in a 1.7mwth calcium looping pilot," *International Journal of Greenhouse Gas Control*, vol. 18, pp. 237–245, 2013, ISSN: 1750-5836. DOI: https://doi.org/10.1016/j.ijggc.2013.07.014. URL: https://www.sciencedirect.com/science/article/pii/S1750583613002922.

[29] P. Tait, B. Buschle, I. Ausner, P. Valluri, M. Wehrli, and M. Lucquiaud, "A pilot-scale study of dynamic response scenarios for the flexible operation of post-combustion co2 capture," *International Journal of Greenhouse Gas Control*, vol. 48, pp. 216–233, 2016, FLEXIBLE OPERATION OF CARBON CAPTURE PLANTS, ISSN: 1750-5836. DOI: https://doi.org/10.1016/j.ijggc.2015.12.009. URL: https://www.sciencedirect.com/science/article/pii/S1750583615301560.

[30] M. Habib, A. M. Esquino, R. Hughes, *et al.*, "Flexible carbon capture using mof fixed bed adsorbers at an ngcc plant," *Carbon Capture Science Technology*, vol. 10, p. 100 170, 2024, ISSN: 2772-6568. DOI: https://doi.org/10.1016/j.ccst.2023.100170. URL: https://www.sciencedirect.com/science/article/pii/S277265682300074X.

[31] X. He, "A review of material development in the field of carbon capture and the application of membrane-based processes in power plants and energy-intensive industries," *Energy, Sustainability and Society*, vol. 8, no. 1, 2018, ISSN: 2192-0567. DOI: 10.1186/s13705-018-0177-9. URL: http://dx.doi.org/10.1186/s13705-018-0177-9.

[32] M. Bui, C. S. Adjiman, A. Bardow, *et al.*, "Carbon capture and storage (ccs): The way forward," *Energy Environ. Sci.*, vol. 11, pp. 1062–1176, 5 2018. DOI: 10.1039/C7EE02342A. URL: http://dx.doi.org/10.1039/C7EE02342A.

[33] A. S. R. Subramanian, K. Jordal, R. Anantharaman, B. A. Hagen, and S. Roussanaly, "A comparison of post-combustion capture technologies for the ngcc," *Energy Procedia*, vol. 114, pp. 2631–2641, 2017, 13th International Conference on Greenhouse Gas Control Technologies, GHGT-13, 14-18 November 2016, Lausanne, Switzerland, ISSN: 1876-6102. DOI: https://doi.org/10.1016/j.egypro.2017.03.1436. URL: https://www.sciencedirect.com/science/article/pii/S1876610217316211.

[34] U. Khan, C. C. Ogbaga, O.-A. O. Abiodun, A. A. Adeleke, P. P. Ikubanni, P. U. Okoye, and J. A. Okolie, "Assessing absorption-based co2 capture: Research progress and techno-economic assessment overview," *Carbon Capture Science and Technology*, vol. 8, p. 100 125, 2023, ISSN: 2772-6568. DOI: https://doi.org/10.1016/j.ccst.2023.100125. URL: https://www.sciencedirect.com/science/article/pii/S2772656823000295.

[35] G. T. Rochelle, "Amine scrubbing for co₂ capture," *Science*, vol. 325, no. 5948, pp. 1652–1654, 2009. DOI: 10.1126/science.1176731. URL: https://www.science.org/doi/abs/10.1126/science.1176731.

[36] M. Kheirinik, S. Ahmed, and N. Rahmanian, "Comparative techno-economic analysis of carbon capture processes: Pre-combustion, post-combustion, and oxy-fuel combustion operations," *Sustainability in Environment*, vol. 13, Dec. 2021. DOI: 10.3390/su132413567.

[37] L. Zheng, "1 - overview of oxy-fuel combustion technology for carbon dioxide (co2) capture," in *Oxy-Fuel Combustion for Power Generation and Carbon Dioxide (CO2) Capture*, ser. Woodhead Publishing Series in Energy, L. Zheng, Ed., Woodhead Publishing, 2011, pp. 1–13, ISBN: 978-1-84569-671-9. DOI: https://doi.org/10.1533/9780857090980.1.

[38] NETL, *9.2. Carbon Dioxide Capture Approaches — netl.doe.gov*. URL: https://netl.doe.gov/research/carbon-management/energy-systems/gasification/gasifipedia/capture-approaches.

[39] *Comparison Against Other Fossil Fuels — swarthmore.edu*, [Accessed 22-05-2024]. URL: https://www.swarthmore.edu/environmental-studies-capstone/comparison-against-other-fossil-fuels.

[40] J. Fagerlund, R. Zevenhoven, J. Thomassen, *et al.*, "Performance of an amine-based co2 capture pilot plant at the fortum oslo varme waste to energy plant in oslo, norway," *International Journal of Greenhouse Gas Control*, vol. 106, p. 103 242, 2021, ISSN: 1750-5836. DOI: https://doi.org/10.1016/j.ijggc.2020.103242. URL: https://www.sciencedirect.com/science/article/pii/S1750583620306678.

[41] G. Kennedy, "W.a. parish post-combustion co2 capture and sequestration demonstration project (final technical report)," Mar. 2020. DOI: 10.2172/1608572. URL: https://www.osti.gov/biblio/1608572.

[42] J. Cichanowicz, "2021 status of carbon capture utilization and sequestration for application to natural gas-fired combined cycle and coal-fired power generation," 2021. URL: https://www.publicpower.org/system/files/documents/CCUS%20Status_Final_2022.pdf#page=9.10.

[43] NETL, *Point Source Carbon Capture Project Map — netl.doe.gov*. URL: https://netl.doe.gov/carbon-management/carbon-capture/psc-map.

[44] A. Basile, S. Liguori, and A. Iulianelli, "2 - membrane reactors for methane steam reforming (msr)," in *Membrane Reactors for Energy Applications and Basic Chemical Production*, ser. Woodhead Publishing Series in Energy, A. Basile, L. Di Paola, F. l. Hai, and V. Piemonte, Eds., Woodhead Publishing, 2015, pp. 31–59, ISBN: 978-1-78242-223-5. DOI: https://doi.org/10.1016/B978-1-78242-223-5.00002-9. URL: https://www.sciencedirect.com/science/article/pii/B9781782422235000029.

[45] NETL, *9.2. Carbon Dioxide Capture Approaches — netl.doe.gov*. URL: https://netl.doe.gov/research/carbon-management/energy-systems/gasification/gasifipedia/capture-approaches.

[46] D. Cebrucean and I. Ionel, "5.15 - biomass co-firing with carbon capture," in *Comprehensive Renewable Energy (Second Edition)*, T. M. Letcher, Ed., Second Edition, Oxford: Elsevier, 2022, pp. 330–347, ISBN: 978-0-12-819734-9. DOI: https://doi.org/10.1016/B978-0-12-819727-1.00044-3. URL: https://www.sciencedirect.com/science/article/pii/B9780128197271000443.

[47] Y. Zhu and H. Frey, "3 - integrated gasification combined cycle (igcc) power plant design and technology," in *Advanced Power Plant Materials, Design and Technology*, ser. Woodhead Publishing Series in Energy, D. Roddy, Ed., Woodhead Publishing, 2010, pp. 54–88, ISBN: 978-1-84569-515-6. DOI: https://doi.org/10.1533/9781845699468.1.54. URL: https://www.sciencedirect.com/science/article/pii/B978184569515600030.

[48] NETL, *8.4. IGCC Efficiency / Performance — netl.doe.gov*, 2022. URL: https://netl.doe.gov/research/Coal/energy-systems/gasification/gasifipedia/igcc-efficiency.

[49] Z. Zhang, D. N. Vo, J. Kum, S. H. Hong, and C. H. Lee, "Enhancing energy efficiency of chemical absorption-based co2 capture process with advanced waste-heat recovery modules at a high capture rate," *Chemical Engineering Journal*, vol. 472, p. 144 918, 2023, ISSN: 1385-8947. DOI: https://doi.org/10.1016/j.cej.2023.144918. URL: https://www.sciencedirect.com/science/article/pii/S1385894723036495.

[50] S. Vasudevan, S. Farooq, I. A. Karimi, M. Saeys, M. C. Quah, and R. Agrawal, "Energy penalty estimates for co2 capture: Comparison between fuel types and capture-combustion modes," *Energy*, vol. 103, pp. 709–714, 2016, ISSN: 0360-5442. DOI: https://doi.org/10.1016/j.energy.2016.02.154. URL: https://www.sciencedirect.com/science/article/pii/S036054421630216X.

[51] D. L. Pinti, "Composition of the earth's atmosphere," in *Encyclopedia of Geology (Second Edition)*, D. Alderton and S. A. Elias, Eds., Second Edition, Oxford: Academic Press, 2021, pp. 187–197, ISBN: 978-0-08-102909-1. DOI: https://doi.org/10.1016/B978-0-08-102908-4.00054-0. URL: https://www.sciencedirect.com/science/article/pii/B9780081029084000540.

[52] C. Scholes, M. Ho, and D. Wiley, "Membrane-cryogenic post-combustion carbon capture of flue gases from ngcc," *Technologies*, vol. 4, p. 14, Apr. 2016. DOI: 10.3390/technologies4020014.

[53] NETL, *Oxy-Combustion — netl.doe.gov*. URL: https://netl.doe.gov/node/7477.

[54] L. Zheng, "1 - overview of oxy-fuel combustion technology for carbon dioxide (co2) capture," in *Oxy-Fuel Combustion for Power Generation and Carbon Dioxide (CO2) Capture*, ser. Woodhead Publishing Series in Energy, L. Zheng, Ed., Woodhead Publishing, 2011, pp. 1–13, ISBN: 978-1-84569-671-9. DOI: https://doi.org/10.1533/9780857090980.1.

[55] T. Wall, Y. Liu, C. Spero, *et al.*, "An overview on oxyfuel coal combustion—state of the art research and technology development," *Chemical Engineering Research and Design*, vol. 87, no. 8, pp. 1003–1016, 2009, ISSN: 0263-8762. DOI: https://doi.org/10.1016/j.cherd.2009.02.005. URL: https://www.sciencedirect.com/science/article/pii/S0263876209000598.

[56] S. Talei, D. Fozer, P. S. Varbanov, A. Szanyi, and P. Mizsey, "Oxyfuel combustion makes carbon capture more efficient," *ACS Omega*, vol. 9, no. 3, pp. 3250–3261, 2024. DOI: 10.1021/acsomega.3c05034. URL: https://doi.org/10.1021/acsomega.3c05034.

[57] T. Ochs, D. Oryshchyn, J. Ciferno, and C. Summers, *Ranking of enabling technologies for oxy-fuel based carbon capture (Conference) | OSTI.GOV — osti.gov*, 2007. URL: https://www.osti.gov/servlets/purl/915510#page=2.26.

[58] D. Kearns, H. Liu, and C. Consoli, *TECHNOLOGY READINESS AND COSTS OF CCS*, 2021. URL: https://www.globalccsinstitute.com/wp-content/uploads/2021/03/Technology-Readiness-and-Costs-for-CCS-2021-1.pdf.

[59] X. Y. D. Soo, J. J. C. Lee, W. Y. Wu, L. Tao, C. Wang, Q. Zhu, and J. Bu, "Advancements in co2 capture by absorption and adsorption: A comprehensive review," *Journal of CO2 Utilization*, vol. 81, p. 102 727, 2024, ISSN: 2212-9820. DOI: https://doi.org/10.1016/j.jcou.2024.102727. URL: https://www.sciencedirect.com/science/article/pii/S2212982024000623.

[60] M. C. Duke, B. Ladewig, S. Smart, V. Rudolph, and J. C. Diniz da Costa, "Assessment of postcombustion carbon capture technologies for power generation," *Frontiers of Chemical Engineering in China*, vol. 4, no. 2, pp. 184–195, Sep. 2009, ISSN: 1673-7474. DOI: 10.1007/s11705-009-0234-1. URL: http://dx.doi.org/10.1007/s11705-009-0234-1.

[61] D. Berstad, A. Arasto, K. Jordal, and G. Haugen, "Parametric study and benchmarking of ngcc, coal and biomass power cycles integrated with mea-based post-combustion co2 capture," *Energy Procedia*, vol. 4, pp. 1737–1744, 2011, 10th International Conference on Greenhouse Gas Control Technologies, ISSN: 1876-6102. DOI: https://doi.org/10.1016/j.egypro.2011.02.048. URL: https://www.sciencedirect.com/science/article/pii/S1876610211002451.

[62] P. Lang, F. Denes, and L. Hegely, "Comparison of different amine solvents for the absorption of co2," *Chemical Engineering Transactions*, vol. 61, pp. 1105–1110, Oct. 2017. DOI: 10.3303/CET1761182. URL: https://doi.org/10.3303/CET1761182.

[63] *Amine | Organic Chemistry, Structure & Uses — britannica.com*, [Accessed 15-08-2024]. URL: https://www.britannica.com/science/amine.

[64] A. Benamor, M. K. Aroua, and A. Aroussi, "Kinetics of co2 absorption into aqueous blends of diethanolamine and methyldiethanolamine," in *Proceedings of the 3rd Gas Processing Symposium*, ser. Advances in Gas Processing, A. Aroussi and F. Benyahia, Eds., vol. 3, Oxford: Elsevier, 2012, pp. 64–70. DOI: https://doi.org/10.1016/B978-0-444-59496-9.50010-2. URL: https://www.sciencedirect.com/science/article/pii/B9780444594969500102.

[65] A. A. Olajire, "Co2 capture and separation technologies for end-of-pipe applications – a review," *Energy*, vol. 35, no. 6, pp. 2610–2628, 2010, 7th International Conference on Sustainable Energy Technologies, ISSN: 0360-5442. DOI: https://doi.org/10.1016/j.energy.2010.02.030. URL: https://www.sciencedirect.com/science/article/pii/S0360544210000848.

[66] M. K. Mondal, H. K. Balsora, and P. Varshney, "Progress and trends in co2 capture/separation technologies: A review," *Energy*, vol. 46, no. 1, pp. 431–441, 2012, Energy and Exergy Modelling of Advance Energy Systems, ISSN: 0360-5442. DOI: https://doi.org/10.1016/j.energy.2012.08.006. URL: https://www.sciencedirect.com/science/article/pii/S0360544212006184.

[67] B. R. Strazisar, R. R. Anderson, and C. M. White, "Degradation pathways for monoethanolamine in a co2 capture facility," *Energy Fuels*, vol. 17, no. 4, pp. 1034–1039, 2003. DOI: 10.1021/ef020272i. URL: https://doi.org/10.1021/ef020272i.

[68] X. Li, X. Zhou, J. Wei, Y. Fan, L. Liao, and H. Wang, "Reducing the energy penalty and corrosion of carbon dioxide capture using a novel nonaqueous monoethanolamine-based biphasic solvent," *Separation and Purification Technology*, vol. 265, p. 118 481, 2021, ISSN: 1383-5866. DOI: https://doi.org/10.1016/j.seppur.2021.118481. URL: https://www.sciencedirect.com/science/article/pii/S1383586621001830.

[69] *Boundary Dam Carbon Capture Project — saskpower.com*, [Accessed 02-06-2024]. URL: https://www.saskpower.com/our-power-future/infrastructure-projects/carbon-capture-and-storage/boundary-dam-carbon-capture-project.

[70] Reuters, *Emerging carbon capture projects at U.S. power plants*, 2023. URL: https://www.reuters.com/sustainability/emerging-carbon-capture-projects-us-power-plants-2023-05-12/#:~:text=Duke%20Energy%20Indiana%2C%20LLC's%20(DUKIN,2.4%20million%20tonnes%20per%20year..

[71] Energy.Gov, *Carbon Capture Opportunities for Natural Gas Fired Power Systems*. URL: https://www.energy.gov/fecm/articles/carbon-capture-opportunities-natural-gas-fired-power-systems.

[72] IEAGHG, *Start-up and shutdown protocol for natural gas-fired power stations with CO2 capture*, Technical Report, 2022.

[73] "Chapter 11 - co2 adsorption by swing technologies and challenges on industrialization," in *Advances in Carbon Capture*, M. R. Rahimpour, M. Farsi, and M. A. Makarem, Eds., Woodhead Publishing, 2020, pp. 241–267, ISBN: 978-0-12-819657-1. DOI: https://doi.org/10.1016/B978-0-12-819657-1.00011-6. URL: https://www.sciencedirect.com/science/article/pii/B9780128196571000116.

[74] C. H. Yu, C. H. Huang, and C. S. Tan, "A review of co2 capture by absorption and adsorption," *Aerosol and Air Quality Research*, vol. 12, no. 5, pp. 745–769, 2012, ISSN: 2071-1409. DOI: 10.4209/aaqr.2012.05.0132. URL: http://dx.doi.org/10.4209/aaqr.2012.05.0132.

[75] F. Deng, X. B. Luo, L. Ding, and S. L. Luo, "5 - application of nanomaterials and nanotechnology in the reutilization of metal ion from wastewater," in *Nanomaterials for the Removal of Pollutants and Resource Reutilization*, ser. Micro and Nano Technologies, X. Luo and F. Deng, Eds., Elsevier, 2019, pp. 149–178, ISBN: 978-0-12-814837-2. DOI: https://doi.org/10.1016/B978-0-12-814837-2.00005-6. URL: https://www.sciencedirect.com/science/article/pii/B9780128148372000056.

[76] M. Pardakhti, T. Jafari, Z. Tobin, B. Dutta, E. Moharreri, N. S. Shemshaki, S. Suib, and R. Srivastava, "Trends in solid adsorbent materials development for co2 capture," *ACS Applied Materials Interfaces*, vol. 11, no. 38, pp. 34 533–34 559, 2019, PMID: 31437393. DOI: 10.1021/acsami.9b08487. URL: https://doi.org/10.1021/acsami.9b08487.

[77] T. A. Saleh, "Chapter 2 - adsorption technology and surface science," in *Surface Science of Adsorbents and Nanoadsorbents*, ser. Interface Science and Technology, T. A. Saleh, Ed., vol. 34, Elsevier, 2022, pp. 39–64. DOI: https://doi.org/10.1016/B978-0-12-849876-7.00006-3. URL: https://www.sciencedirect.com/science/article/pii/B9780128498767000063.

[78] A. Bakhtyari, M. Mofarahi, and C.-H. Lee, "Chapter 9 - co2 adsorption by conventional and nanosized zeolites," in *Advances in Carbon Capture*, M. R. Rahimpour, M. Farsi, and M. A. Makarem, Eds., Woodhead Publishing, 2020, pp. 193–228, ISBN: 978-0-12-819657-1. DOI: https://doi.org/10.1016/B978-0-12-819657-1.00009-8. URL: https://www.sciencedirect.com/science/article/pii/B9780128196571000098.

[79] J. Hack, N. Maeda, and D. M. Meier, "Review on co2 capture using amine-functionalized materials," *ACS Omega*, vol. 7, no. 44, pp. 39 520–39 530, 2022. DOI: 10.1021/acsomega.2c03385. URL: https://doi.org/10.1021/acsomega.2c03385.

[80] F. Raganati, F. Miccio, and P. Ammendola, "Adsorption of carbon dioxide for post-combustion capture: A review," *Energy Fuels*, vol. 35, no. 16, pp. 12 845–12 868, 2021. DOI: 10.1021/acs.energyfuels.1c01618. URL: https://doi.org/10.1021/acs.energyfuels.1c01618.

[81] Y. Belmabkhout, Z. Zhang, K. Adil, P. M. Bhatt, A. Cadiau, V. Solovyeva, H. Xing, and M. Eddaoudi, "Hydrocarbon recovery using ultra-microporous fluorinated mof platform with and without uncoordinated metal sites: I- structure properties relationships for c2h2/c2h4 and co2/c2h2 separation," *Chemical Engineering Journal*, vol. 359, pp. 32–36, 2019, ISSN: 1385-8947. DOI: https://doi.org/10.1016/j.cej.2018.11.113. URL: https://www.sciencedirect.com/science/article/pii/S1385894718323477.

[82] S. Y. W. Chai, L. H. Ngu, and B. S. How, "Review of carbon capture absorbents for co2 utilization," *Greenhouse Gases: Science and Technology*, vol. 12, no. 3, pp. 394–427, 2022. DOI: https://doi.org/10.1002/ghg.2151. URL: https://onlinelibrary.wiley.com/doi/abs/10.1002/ghg.2151.

[83] G. Mondino, C. A. Grande, R. Blom, and L. O. Nord, "Moving bed temperature swing adsorption for co2 capture from a natural gas combined cycle power plant," *International Journal of Greenhouse Gas Control*, vol. 85, pp. 58–70, 2019, ISSN: 1750-5836. DOI: https://doi.org/10.1016/j.ijggc.2019.03.021. URL: https://www.sciencedirect.com/science/article/pii/S1750583618306868.

[84] A. Qader, B. Hooper, T. Innocenzi, G. Stevens, S. Kentish, C. Scholes, K. Mumford, K. Smith, P. A. Webley, and J. Zhang, "Novel post-combustion capture technologies on a lignite fired power plant - results of the co2crc/h3 capture project," *Energy Procedia*, vol. 4, pp. 1668–1675, 2011, 10th International Conference on Greenhouse Gas Control Technologies, ISSN: 1876-6102. DOI: https://doi.org/10.1016/j.egypro.2011.02.039. URL: https://www.sciencedirect.com/science/article/pii/S1876610211002360.

[85] L. Riboldi and O. Bolland, "Overview on pressure swing adsorption (psa) as co2 capture technology: State-of-the-art, limits and potentials," *Energy Procedia*, vol. 114, pp. 2390–2400, 2017, 13th International Conference on Greenhouse Gas Control Technologies, GHGT-13, 14-18 November 2016, Lausanne, Switzerland, ISSN: 1876-6102. DOI: https://doi.org/10.1016/j.egypro.2017.03.1385. URL: https://www.sciencedirect.com/science/article/pii/S1876610217315709.

[86] N. Tlili, G. Grévillot, and C. Vallières, "Carbon dioxide capture and recovery by means of tsa and/or vsa," *International Journal of Greenhouse Gas Control*, vol. 3, no. 5, pp. 519–527, 2009, ISSN: 1750-5836. DOI: https://doi.org/10.1016/j.ijggc.2009.04.005. URL: https://www.sciencedirect.com/science/article/pii/S1750583609000437.

[87] T. Merkel, W. Salim, C. Casillas, A. Borsaly, J. Kniep, E. Westling, T. Hofmann, and Z. Sun, "Scale-up testing of advanced polaris membrane in co2 capture technology," Aug. 2023. DOI: 10.2172/1995006. URL: https://www.osti.gov/biblio/1995006.

[88] H. Strathmann, "Membranes and membrane separation processes," in *Ullmann's Encyclopedia of Industrial Chemistry*. John Wiley Sons, Ltd, 2005, ISBN: 9783527306732. DOI: https://doi.org/10.1002/14356007.a16_187.pub2. URL: https://onlinelibrary.wiley.com/doi/abs/10.1002/14356007.a16_187.pub2.

[89] S. Elhenawy, M. Khraisheh, F. Almomani, and M. Hassan, "Key applications and potential limitations of ionic liquid membranes in the gas separation process of co2, ch4, n2, h2 or mixtures of these gases from various gas streams," *Molecules (Basel, Switzerland)*, vol. 25, Sep. 2020. DOI: 10.3390/molecules25184274.

[90] H. B. Park, J. Kamcev, L. M. Robeson, M. Elimelech, and B. D. Freeman, "Maximizing the right stuff: The trade-off between membrane permeability and selectivity," *Science*, vol. 356, no. 6343, eaab0530, 2017. DOI: 10.1126/science.aab0530. URL: https://www.science.org/doi/abs/10.1126/science.aab0530.

[91] B. D. Freeman, "Basis of permeability/selectivity tradeoff relations in polymeric gas separation membranes," *Macromolecules*, vol. 32, no. 2, pp. 375–380, 1999. DOI: 10.1021/ma9814548. URL: https://doi.org/10.1021/ma9814548.

[92] W. Norharyati, A. Ismail, T. Matsuura, and M. Abdullah, "Precursor selection and process conditions in the preparation of carbon membrane for gas separation: A review," *Separation Purification Reviews*, vol. 40, pp. 261–311, Oct. 2011. DOI: 10.1080/15422119.2011.555648.

[93] B. Dziejarski, R. Krzyżyńska, and K. Andersson, "Current status of carbon capture, utilization, and storage technologies in the global economy: A survey of technical assessment," *Fuel*, vol. 342, p. 127 776, 2023, ISSN: 0016-2361. DOI: https://doi.org/10.1016/j.fuel.2023.127776. URL: https://www.sciencedirect.com/science/article/pii/S0016236123003897.

[94] A. Kayvani Fard, G. McKay, A. Buekenhoudt, H. Al Sulaiti, F. Motmans, M. Khraisheh, and M. Atieh, "Inorganic membranes: Preparation and application for water treatment and desalination," *Materials*, vol. 11, no. 1, p. 74, 2018, ISSN: 1996-1944. DOI: 10.3390/ma11010074. URL: http://dx.doi.org/10.3390/ma11010074.

[95] M. Momeni, M. Mesbah, E. Soroush, and S. Shahsavari, "Hybrid membranes for carbon capture," in *Sustainable Agriculture Reviews 38: Carbon Sequestration Vol. 2 Materials and Chemical Methods*, Inamuddin, A. M. Asiri, and E. Lichtfouse, Eds. Cham: Springer International Publishing, 2019, pp. 85–120, ISBN: 978-3-030-29337-6. DOI: 10.1007/978-3-030-29337-6_4. URL: https://doi.org/10.1007/978-3-030-29337-6_4.

[96] M. Vinoba, M. Bhagiyalakshmi, Y. Alqaheem, A. A. Alomair, A. Pérez, and M. S. Rana, "Recent progress of fillers in mixed matrix membranes for co2 separation: A review," *Separation and Purification Technology*, vol. 188, pp. 431–450, 2017, ISSN: 1383-5866. DOI: https://doi.org/10.1016/j.seppur.2017.07.051. URL: https://www.sciencedirect.com/science/article/pii/S1383586617315964.

[97] N. Jusoh, Y. F. Yeong, T. Chew, K. K. Lau, and D. Mohd Shariff, "Current development and challenges of mixed matrix membranes for co 2 /ch 4 separation," *Separation Purification Reviews*, vol. 45, Jan. 2016. DOI: 10.1080/15422119.2016.1146149.

[98] E. Favre, "Membrane separation processes and post-combustion carbon capture: State of the art and prospects," *Membranes*, vol. 12, no. 9, 2022, ISSN: 2077-0375. URL: https://www.mdpi.com/2077-0375/12/9/884.

[99] D. Turi, M. Ho, M. Ferrari, P. Chiesa, D. Wiley, and M. Romano, "Co2 capture from natural gas combined cycles by co2 selective membranes," *International Journal of Greenhouse Gas Control*, vol. 61, pp. 168–183, 2017, ISSN: 1750-5836. DOI: https://doi.org/10.1016/j.ijggc.2017.03.022. URL: https://www.sciencedirect.com/science/article/pii/S1750583616308805.

[100] *Carbon Dioxide - Thermophysical Properties — engineeringtoolbox.com*. URL: https://www.engineeringtoolbox.com/CO2-carbon-dioxide-properties-d_2017.html.

[101] N. C. for Biotechnology Information, *Nitrogen — pubchem.ncbi.nlm.nih.gov*, [Accessed 06-06-2024], 2024. URL: https://pubchem.ncbi.nlm.nih.gov/compound/Nitrogen.

[102] D. Bell, *Oxygen*, 2019. DOI: 10.53347/rid-69541. URL: http://dx.doi.org/10.53347/rID-69541.

[103] N. Ghasem, "Chapter 21 - co2 removal from natural gas," in *Advances in Carbon Capture*, M. R. Rahimpour, M. Farsi, and M. A. Makarem, Eds., Woodhead Publishing, 2020, pp. 479–501, ISBN: 978-0-12-819657-1. DOI: https://doi.org/10.1016/B978-0-12-819657-1.00021-9. URL: https://www.sciencedirect.com/science/article/pii/B9780128196571000219.

[104] M. T. Ravanchi and S. Sahebdelfar, "Carbon dioxide capture and utilization in petrochemical industry: Potentials and challenges," *Applied Petrochemical Research*, vol. 4, no. 1, pp. 63–77, 2014, ISSN: 2190-5533. DOI: 10.1007/s13203-014-0050-5. URL: http://dx.doi.org/10.1007/s13203-014-0050-5.

[105] C. Hoeger, S. Burt, and L. Baxter, "Cryogenic carbon capture™ technoeconomic analysis," *SSRN Electronic Journal*, 2021, ISSN: 1556-5068. DOI: 10.2139/ssrn.3820158. URL: http://dx.doi.org/10.2139/ssrn.3820158.

[106] M. Abu-Zahra, A. Sodiq, and P. Feron, "29 - commercial liquid absorbent-based pcc processes," in *Absorption-Based Post-combustion Capture of Carbon Dioxide*, P. H. Feron, Ed., Woodhead Publishing, 2016, pp. 757–778, ISBN: 978-0-08-100514-9. DOI: https://doi.org/10.1016/B978-0-08-100514-9.00029-9. URL: https://www.sciencedirect.com/science/article/pii/B9780081005149000299.

[107] C. Song, Q. Liu, S. Deng, H. Li, and Y. Kitamura, "Cryogenic-based co2 capture technologies: State-of-the-art developments and current challenges," *Renewable and Sustainable Energy Reviews*, vol. 101, pp. 265–278, 2019, ISSN: 1364-0321. DOI: https://doi.org/10.1016/j.rser.2018.11.018. URL: https://www.sciencedirect.com/science/article/pii/S1364032118307731.

[108] L. Zhang, K. Ye, Y. Wang, W. Han, M. Xie, and L. Chen, "Performance analysis of a hybrid system combining cryogenic separation carbon capture and liquid air energy storage (cs-laes)," *Energy*, vol. 290, p. 129 867, 2024, ISSN: 0360-5442. DOI: https://doi.org/10.1016/j.energy.2023.129867. URL: https://www.sciencedirect.com/science/article/pii/S0360544223032619.

[109] P. Tilak and M. M. El-Halwagi, "Process integration of calcium looping with industrial plants for monetizing co2 into value-added products," *Carbon Resources Conversion*, vol. 1, no. 2, pp. 191–199, 2018, ISSN: 2588-9133. DOI: https://doi.org/10.1016/j.crcon.2018.07.004. URL: https://www.sciencedirect.com/science/article/pii/S2588913318300152.

[110] A. Perejón, L. M. Romeo, Y. Lara, P. Lisbona, A. Martínez, and J. M. Valverde, "The calcium-looping technology for co2 capture: On the important roles of energy integration and sorbent behavior," *Applied Energy*, vol. 162, pp. 787–807, 2016, ISSN: 0306-2619. DOI: https://doi.org/10.1016/j.apenergy.2015.10.121. URL: https://www.sciencedirect.com/science/article/pii/S0306261915013616.

[111] H. Dieter, M. Beirow, D. Schweitzer, C. Hawthorne, and G. Scheffknecht, "Efficiency and flexibility potential of calcium looping co2 capture," *Energy Procedia*, vol. 63, pp. 2129–2137, 2014, 12th International Conference on Greenhouse Gas Control Technologies, GHGT-12, ISSN: 1876-6102. DOI: https://doi.org/10.1016/j.egypro.2014.11.230. URL: https://www.sciencedirect.com/science/article/pii/S1876610214020451.

[112] Y. Hu and H. Ahn, "Process integration of a calcium-looping process with a natural gas combined cycle power plant for co2 capture and its improvement by exhaust gas recirculation," *Applied Energy*, vol. 187, pp. 480–488, 2017, ISSN: 0306-2619. DOI: https://doi.org/10.1016/j.apenergy.2016.11.014. URL: https://www.sciencedirect.com/science/article/pii/S0306261916315999.

[113] M. Strojny, P. Gładysz, D. P. Hanak, and W. Nowak, "Comparative analysis of co2 capture technologies using amine absorption and calcium looping integrated with natural gas combined cycle power plant," *Energy*, vol. 284, p. 128 599, 2023, ISSN: 0360-5442. DOI: https://doi.org/10.1016/j.energy.2023.128599. URL: https://www.sciencedirect.com/science/article/pii/S036054422301993X.

[114] J. Chen, L. Duan, Y. Ma, *et al.*, "Recent progress in calcium looping integrated with chemical looping combustion (cal-clc) using bifunctional cao/cuo composites for co2 capture: A state-of-the-art review," *Fuel*, vol. 334, p. 126 630, 2023, ISSN: 0016-2361. DOI: https://doi.org/10.1016/j.fuel.2022.126630. URL: https://www.sciencedirect.com/science/article/pii/S0016236122034548.

[115] S. He, Y. Zheng, X. Zeng, J. Wang, L. Gao, and D. Yang, "Proposal and thermodynamic investigation of pressurized calcium looping integrated with chemical looping combustion for tail-end co2 capture in a retrofitted natural gas combined cycle power plant," *Separation and Purification Technology*, vol. 346, p. 127 464, 2024, ISSN: 1383-5866. DOI: https://doi.org/10.1016/j.seppur.2024.127464. URL: https://www.sciencedirect.com/science/article/pii/S1383586624012036.

[116] D. Berstad, R. Anantharaman, R. Blom, K. Jordal, and B. Arstad, "Ngcc post-combustion co2 capture with ca/carbonate looping: Efficiency dependency on sorbent properties, capture unit performance and process configuration," *International Journal of Greenhouse Gas Control*, vol. 24, pp. 43–53, 2014, ISSN: 1750-5836. DOI: https://doi.org/10.1016/j.ijggc.2014.02.015. URL: https://www.sciencedirect.com/science/article/pii/S175058361400053X.

[117] U. S. G. A. Office, *Gao.gov*, [Accessed 24-06-2024], 2022. URL: https://www.gao.gov/assets/730/723198.pdf#page=3.21.

[118] T. Schmitt, S. Leptinsky, M. Turner, A. Zoelle, M. Woods, T. Schultz, and R. James, *Energy baseline revision 4a," national energy technology laboratory*, 2022. URL: https://netl.doe.gov/projects/files/CostAndPerformanceBaselineForFossilEnergyPlants_Volume1BituminousCoalAndNaturalGasToElectricity_101422.pdf#page=705.30.

[119] M. T. Ho, G. W. Allinson, and D. E. Wiley, "Reducing the cost of co2 capture from flue gases using pressure swing adsorption," *Industrial & Engineering Chemistry Research*, vol. 47, no. 14, pp. 4883–4890, 2008. DOI: 10.1021/ie070831e. URL: https://doi.org/10.1021/ie070831e.

[120] C. A. Scholes, M. T. Ho, and D. E. Wiley, "Membrane-cryogenic post-combustion carbon capture of flue gases from ngcc," *Technologies*, vol. 4, no. 2, 2016. DOI: 10.3390/technologies4020014. URL: https://www.mdpi.com/2227-7080/4/2/14.

[121] M. Tuinier, H. Hamers, and M. van Sint Annaland, "Techno-economic evaluation of cryogenic co2 capture—a comparison with absorption and membrane technology," *International Journal of Greenhouse Gas Control*, vol. 5, no. 6, pp. 1559–1565, 2011, ISSN: 1750-5836. DOI: https://doi.org/10.1016/j.ijggc.2011.08.013. URL: https://www.sciencedirect.com/science/article/pii/S1750583611001691.

[122] D. Berstad, R. Anantharaman, and K. Jordal, "Post-combustion co2 capture from a natural gas combined cycle by cao/caco3 looping," *International Journal of Greenhouse Gas Control*, vol. 11, pp. 25–33, 2012, ISSN: 1750-5836. DOI: https://doi.org/10.1016/j.ijggc.2012.07.021. URL: https://www.sciencedirect.com/science/article/pii/S1750583612001788.

[123] C. Fu, S. Roussanaly, K. Jordal, and R. Anantharaman, "Techno-economic analyses of the cao/caco3 post-combustion co2 capture from ngcc power plants," *Frontiers in Chemical Engineering*, vol. 2, p. 596 417, Jan. 2021. DOI: 10.3389/fceng.2020.596417.

[124] D. S. Mallapragada, D. J. Papageorgiou, A. Venkatesh, C. L. Lara, and I. E. Grossmann, "Impact of model resolution on scenario outcomes for electricity sector system expansion," *Energy*, vol. 163, pp. 1231–1244, 2018, ISSN: 0360-5442. DOI: https://doi.org/10.1016/j.energy.2018.08.015. URL: https://www.sciencedirect.com/science/article/pii/S0360544218315238.

[125] E. Zhou and T. Mai, "Electrification futures study: Operational analysis of u.s. power systems with increased electrification and demand-side flexibility," May 2021. DOI: 10.2172/1785329. URL: https://www.osti.gov/biblio/1785329.

[126] R. Valdmanis, *Quebec key to cutting new england power costs: Maine governor | reuters*, 2015. URL: https://www.reuters.com/article/us-usa-canada-energy/quebec-key-to-cutting-new-england-power-costs-maine-governor-idUSKCN0T21SR20151113.

[127] R. Macdonald, N. Bhatt, J. Parsons, D. Mallapraganda, and T. Schittekatte, *Input parameters for the iso-ne model*, PowerPoint presentation, 2023.

[128] E. Dimanchev, J. Hodge, and J. Parsons, *Two-way trade in green electrons: Deep decarbonization of the northeastern u.s. and the role of canadian hydropower*, Feb. 2020.

[129] R. Khorramfar, M. Santoni-Colvin, S. Amin, L. K. Norford, A. Botterud, and D. Mallapragada, *Cost-effective planning of decarbonized power-gas infrastructure to meet the challenges of heating electrification*, 2024. arXiv: 2308.16814 [eess.SY]. URL: https://arxiv.org/abs/2308.16814.

[130] Energy, I. (Environmental Economics, and E. F. I. (EFI), *New england reliability under deep decarbonization*, Accessed: 2024-07-27, 2020. URL: https://www.ethree.com/wp-content/uploads/2020/11/E3-EFI_Report-New-England-Reliability-Under-Deep-Decarbonization_Full-Report_November_2020.pdf.

[131] M. D. of Energy Resources, *Technical potential of solar in massachusetts*, Accessed: 2024-07-27, 2020. URL: https://www.mass.gov/doc/technical-potential-of-solar-in-massachusetts-report/download.

[132] P. Gagnon, R. Margolis, J. Melius, C. Phillips, and R. Elmore, "Estimating rooftop solar technical potential across the us using a combination of gis-based methods, lidar data, and statistical modeling," *Environmental Research Letters*, vol. 13, no. 2, p. 024 027, 2018, ISSN: 1748-9326. DOI: 10.1088/1748-9326/aaa554. URL: http://dx.doi.org/10.1088/1748-9326/aaa554.

[133] N. R. E. L. (NREL), *2023 annual technology baseline (atb) electricity data*, Accessed: 2024-07-27, 2023. URL: https://atb.nrel.gov/electricity/2023/data.

Appendix A

Model Repository

The Zenodo repository below contains relevant GenX modeling files and inputs used in this modeling work. The model and data can be accessed via the DOI reference below or from the following link: Model Repository

Knight, C., & MacDonald, R. (2024). GenX Optimization Model Incorporating Advanced CCS Penalties During Start-Up Operations. Zenodo. https://doi.org/10.5281/zenodo.13324278